(9) FINAL TECHNICAL REPORT.

(6) INVESTIGATION OF IGNITION/COMBUSTION PHENOMENA IN A 30MM LIQUID MONOPROPELLANT GUN.

(Covering Period 15 April 1975 to 15 October 1976)

(11) December 1976

(12) 113 p

ARPA Order No. 2945
Program Code No. 5G10
Contractor: Calspan Corporation
Effective Date of Contract: 1 June 1975
Contract Expiration Date: 15 October 1976
Telephone No. 716/632-7500 Ext. 722

Amount of Contract: $265,180
Contract No.: N00123-75-C-1520
Principal Investigator: G.A. Sterbutzel
Telephone No. 716/632-7500 Ext. 8175
Project Engineer: E.B. Fisher

(10)

(15) N00123-75-C-1520, ARPA Order No. 2945

Sponsored by
Advanced Research Projects Agency

This research was supported by the Advanced Research Projects Agency of the Department of Defense and was monitored by the Naval Weapons Center under Contract No. N00123-75-C-1520.

Prepared by
Calspan Corporation
Report No. KB-6002-X-1

(11) CALSPAN

Form Approved, Budget Bureau – No. 22-R-293

4C11-1

FOREWORD

This report is the culmination of a program designed to generate experimental data of a diagnostic nature to help identify and understand phenomena involved with ignition and combustion in liquid propellant guns (LPG) and to apply this understanding to LPG design. This effort was sponsored by Defense Advanced Research Projects Agency (DARPA) and monitored by the Naval Weapons Center (NWC), China Lake, California.

The program generated many important results, and, in several instances, shed new light on significant phenomenological aspects of the ignition/combustion cycle. The most important of these new findings and observations are stated briefly in the following section called "Index of Phenomenological Facts and Observations." The program approach and results are described briefly in the Summary while the body of this report gives substantial detail and interpretation on all aspects of the program.

The authors appreciate the contributions of many people during this program. These include Calspan personnel such as K.W. Graves, who designed the LPG fixture; Jim Weibel, who made it fire; Herb Thompson who designed the optical instrumentation network; and the Technical Services Group who performed tasks related to photography. Special thanks go to Mr. Don Armstrong and Argonne National Laboratory for loaning their Cordin 375 camera for use on this program. The consultation with others working in this area of LPG combustion is deeply appreciated by the authors. These include Dr. E. Fishman and Dr. J. Broadwell of TRW's Defense and Space Systems Group, Mr. R. Comer and Dr. N. Klein of the Army's Ballistic Research Laboratories, Dr. A. Charters and L. Liedtke of the Naval Weapons Center, China Lake, and Mr. L. Elmore of Pulsepower Systems Inc.

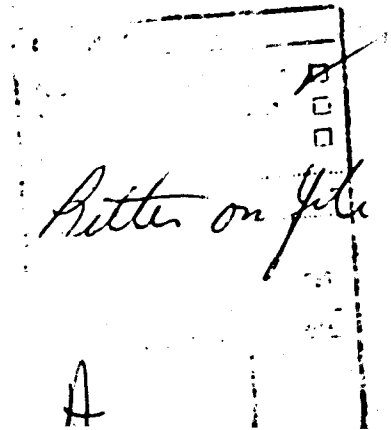

INDEX OF PHENOMENOLOGICAL FACTS AND OBSERVATIONS

The Calspan diagnostic experimentation program generated a wealth of new information for application to the LPG design. In fact, we believe that the catastrophe experienced at Pulsepower Systems Inc. (PSI) in August 1976 may have been averted had this information been available for incorporation in the PSI LPG design.* Some of the more significant observations and deductions of this program are listed in this index along with the section number in the report where more detail can be found.

1. A test involving static propellant loading was conducted at Calspan that was similar to the dynamically loaded explosion-like mishap at PSI in that the pressure-time curve in both cases exhibited an initial pressure pulse followed by a delay period at very low pressure and, then a nearly instantaneous rise to excessively high pressure (Section 3.3.2.2).

2. We believe that the original PSI 3-step precombustion chamber configuration was at least partially responsible for high overpressures in the Calspan fixture by failing to provide adequate control over mixing prior to ignition and flame front growth (Sections 3.3.2 and 3.3.4).

3. The precombustion chamber and its exit (intermediate chamber) can be configured to produce a relatively flat front separating the cool propellant and the ignition medium which promises to control the rate of combustion, thereby diminishing instantaneous pressure excursions (Section 3.3.3.2).

4. Control of ullage can be extremely important in controlling the initial pressure spike from both combustion delay and hydrodynamic standpoints (Sections 3.3.2.2 and 3.3.4).

*This is a strong statement by normal-scientific reporting standards in that too few tests have been run for confirmation. However, we have observed conditions similar to those of the PSI fixture in our test fixture and have demonstrated on a limited basis, the ability to rectify those conditions.

5. It was demonstrated that breech geometry changes make it possible to control the magnitude of the initial pressure spike in an electrically ignited LPG when firing NOS365, even after a potentially dangerous combustion delay (Section 3.3.4).

6. From the heat meters, it can be surmised that about 1/3 of the breech end of the chamber will dry during the rise to the first pressure peak but is wet between the first and second peaks, as indicated by presence or absence of heat flux (Section 3.4.1.2).

7. The major pressure waves in the chamber can logically be charted based on the results of the pressure sensors and the liquid acoustic velocity (Section 3.4.1.2).

8. Rise in pressure to the second peak appears to be due to velocity-augmented combustion in the Taylor cavity. Hydrodynamic-augmented combustion may be important in the rise to the first peak (Section 3.4.1.2).

9. The presence of and the mechanisms by which the Taylor cavity is formed can be postulated from the heat data (Section 3.4.1.2).

10. The second pressure peak appears to occur when the breech end of the chamber becomes dry (Section 3.4.1.2).

11. In our 30mm fixture, the front half of the chamber still had wet walls when the projectile left the barrel at 5650 ft/sec (Section 3.4.1.2).

12. Chamber heating in an LPG is somewhat less than that of a comparable caseless round of equal performance (Section 3.4.1.3).

13. The mode of combustion (delay or immediate) appears to be strongly tied to the length of the formative phase and the electrical energy transmitted during this period for a given precombustion chamber geometry (Section 3.3.1).

TABLE OF CONTENTS

TABLE OF CONTENTS (CONT'D.)

TABLE OF CONTENTS (CONT'D.)

FIGURE INDEX

FIGURE INDEX (CONT'D.)

FIGURE INDEX

TABLE INDEX

1.0 SUMMARY

1.1 TECHNICAL PROBLEM

This research program is part of the DARPA-sponsored Liquid Propellant Gun Phenomenology Program to provide technical support for the development of a "High Performance, Medium Caliber, Liquid Propellant, Anti-Armor Gun System." The gun system, using an electrically-ignited liquid monopropellant, is currently being developed by Pulsepower Systems Inc. (PSI). The liquid monopropellant for the system, designated NOS365, was recently developed by the Naval Ordnance Station at Indian Head, Maryland.

Liquid propellant guns have been characterized by erratic performance. Large variations in muzzle velocity and peak pressure were observed in the initial feasibility studies of the current PSI effort. The phenomenology program represents an attempt to conduct a coordinated analytical/experimental research effort aimed at understanding the causes of the observed performance variability. The output from this program is expected to provide an expanded technological base for the gun system design. Calspan was selected to perform the diagnostic experimentation phase of the phenomenology program.

1.2 GENERAL METHODOLOGY

The program was intended to provide direct support for the gun system development program currently being conducted at PSI and, therefore, the fixture and an electrical discharge unit were patterned after the 30mm single-shot gun system used by PSI during their feasibility investigation (Ref. 1). The final gun system will fire a 75mm projectile but the Calspan fixture bore was selected to be 30mm. This permitted the fixture to be relatively close in size to the 75mm system currently being developed, while being small enough to facilitate fabrication and handling of hardware as well as economical with respect to hardware and propellant costs.

Diagnostic instrumentation and test techniques used by Calspan for several years on solid propellant systems were incorporated in this fixture and used to help define and understand phenomena that occur during the firing of a liquid propellant gun. These techniques included simultaneous measurement of pressure and heat flux along the gun chamber in order to define the time of flame arrival at the chamber wall in relation to peak pressure. The most unique aspect of the Calspan task was the use of sapphire viewing ports in order to visually characterize ignition and combustion phenomena. Data were generated from these diagnostics to help elevate the technological basis for subsequent system analysis and design.

1.3 TECHNICAL RESULTS

Significant advances in the understanding of liquid propellant gun ignition and combustion phenomena were made during this program. The topics of electrical discharge, propellant ignition, and combustion phenomenology were addressed. The diagnostic techniques incorporated during this program have resulted in generation of data not available previously. When coupled with previous and current LPG research, we believe that the technological understanding of LPG ignition and combustion phenomena required for design has been elevated.

High-speed motion pictures were taken of an electrical discharge in the same configuration used to ignite the gun. A luminous volume was observed to grow around the tip of the center electrode during the formative phase of the discharge. The volume increased in size until it touched the edge of the precombustion chamber, at which time the arc was initiated. Intense light was given off during the early portion of the arc phase but this was eventually obscured by the growth of an opaque layer. A similar layer was observed during a discharge in nitric acid but not in distilled water. Therefore, it is presumed that the layer consists of products of propellant decomposition, such as NO_2.

High-speed motion pictures taken of the breech region adjacent to the precombustion chamber contributed much to the understanding of ignition phenomena. Several different forms of ignition were observed and appear to correlate with formative energy. Ignition by formative energy below a certain threshold value is characterized by emergence of what appears to be a brilliant arc-light scattering medium from the precombustion chamber. It is postulated that this medium mixes with cool liquid propellant in the breech end of the gun chamber. If the energy content of the medium is quite low, as correlated with a low value of formative energy, the resultant mixture does not achieve the conditions necessary for ignition and a misfire results. Higher energy levels will create mixture conditions that cause propellant ignition, but with ignition delays ranging from nearly zero to several milliseconds and experiencing peak pressures from below 10,000 psi to well in excess of 100,000 psi. In many instances, this delay type of ignition has resulted in nearly instantaneous rise to these excessive pressures, a potentially damaging occurrence which is to be avoided.

If the formative energy is above the threshold level for a given precombustor geometry, the flame front was observed to be established within the precombustion chamber. Pressures can still exceed 100,000 psi but the rise rate is somewhat less and it is believed that the consistency of the combustion process is far greater when initiated by this more energetic ignition. The problem remains to achieve the proper combination of parameters, including the precombustor geometry, in order to control the magnitude of the initial spike. A limited number of tests conducted at Calspan have demonstrated that addition of an intermediate combustion chamber between the precombustor and the chamber, in some cases with a crushable, shock-absorbing foam liner, can reduce the magnitude of the initial pressure spike substantially.

Some technical progress was made with respect to overall combustion phenomenology. Data were obtained from heat sensors that indicate the existence of a dry wall at the breech end of the chamber during the rise to the first pressure peak. The sensors measured zero heat input between the first and second pressure peaks which suggests that the breech region was re-wetted during this period.

Finally, chamber heating was re-initiated at the breech very close to the time of the second pressure peak. This onset of heating progressed forward in the chamber in nearly linear fashion. These data indicate the existence of a Taylor cavity in the combustion cycle and also that the middle region of the chamber was still wet at the time the projectile passed from the barrel.

The presence of hydrodynamic phenomena was observed beginning with the pressure wave generated by the arc. The existence of a strong hydrodynamic and velocity-augmented combustion rate was also noted. This was amply demonstrated by the rapid increase in breech pressure at times correlating with arrival of reflected pressure waves. Pressure was also observed to rise after the projectile had passed from the short barrel, indicating a substantial increase in combustion rate. These coupled hydrodynamic and velocity-related combustion phenomena appear to be dominant characteristics of the combustion process.

1.4 IMPLICATIONS FOR FURTHER RESEARCH

The primary problems that currently plague liquid propellant guns are performance variability and the frequent occurrence of high overpressures. Performance variability is related to many parameters but perhaps the most important one is the ignition pulse consistency. Research should be directed toward design considerations for an electrical ignition system that will provide a repeatible pulse with the characteristics required to ignite the propellant properly. Electrode configuration (center electrode and ignition chamber) and surface preparation as well as electrical discharge circuitry are the primary elements to be included in the research.

Calspan experiments have shown that the initial pressure spike can be reduced significantly through precombustion chamber design and possibly through introduction of ullage in the region of the precombustion chamber. It appears that much benefit can result through research aimed at control of flame front initiation and growth. Hydrodynamic and velocity-coupled combustion phenomena are also thought to be major contributors to high overpressures and research should be directed toward controlling these mechanisms.

2.0 EXPERIMENTAL EQUIPMENT

2.1 TEST FIXTURE AND APPARATUS

2.1.1 Basic Fixture

2.1.1.1 Fixture Configuration

A liquid propellant single-shot test fixture was designed and fabricated by Calspan for use during the subject investigation. It was designed to fire a 30mm projectile at velocities in excess of 5000 ft/sec and incorporate an electrical ignition system. The nominal propellant charge weight to projectile mass ratio for this gun is 1.25. The gun fixture was designed for simplicity and easy access for instrumentation and photography. It consists of three major components; a chamber block, short and long barrels, and a three-piece frame. Auxiliary devices and components include a breech plug, a spark plug, an electrical discharge system and the plumbing for propellant loading. A photograph of the gun fixture, complete with final photographic instrumentation, is shown in Figure 1.

The chamber block is a hollow cylinder having thick walls (5.65 inches O.D.) to permit a multiplicity of instrumentation and viewing port penetrations. The overall length of the block is 21 5/8 inches, and it is internally threaded for a breech plug with a 1 7/8 inch-8 UNC thread which is 1 3/4 inches long. A 1.562 inch diameter bore for accepting the spark plug extends beyond these threads at the breech end of the chamber block to a depth of 4 1/4 inches. Sealing of the breech end is provided by a bulky teflon ring having a truncated wedge-shaped cross section that fits around a neck of the spark plug housing. It is backed up by a slender beryllium-copper ring to prevent extrusion. The chamber section is 1.24 inches in diameter and 8 inches long, followed by a 5.9 inch long section of smooth-bore 30mm barrel. A 15 degree transition section connects the chamber and barrel. The forward end of the chamber block contains internal threads for barrel attachment. The chamber bore is machined to a 32 microinch finish.

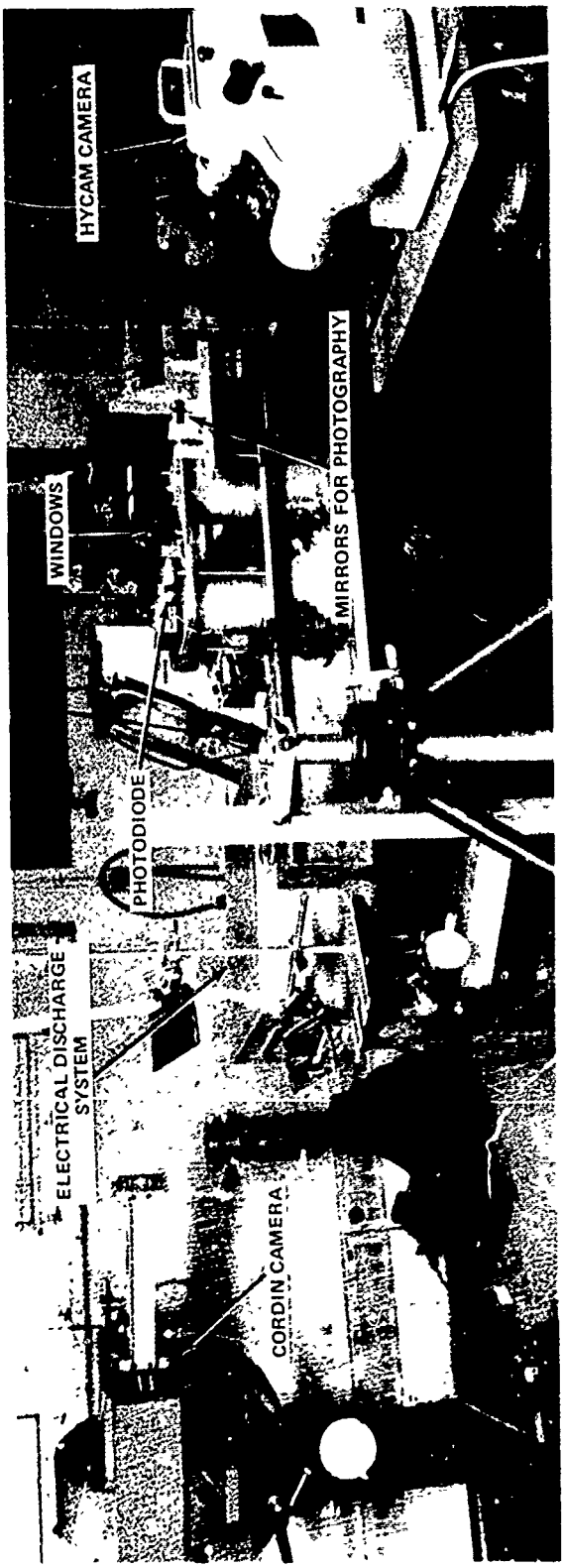

Figure 1 CALSPAN LIQUID PROPELLANT GUN AND ASSOCIATED HARDWARE

Two chamber blocks were machined during this program. The first block was used as a test bed to evaluate instrumentation and sapphire window designs and mounting techniques. This block was machined from vacuum melted stainless steel, type 15-5PH, and was hardened to condition H1025. A pair of diametrically opposed windows was installed in the breech end of this chamber block. The location of the windows and other instrumentation ports is shown in Figure 2. The second block was made from type 13-8PH stainless steel, and hardened to condition H1025. This chamber was equipped with three diametrically opposed window pairs, three transducer and six heat sensor ports as shown in Figure 3.

The chamber block is supported in the frame at its two ends between massive steel bulkheads. The breech-end bulkhead is integral with the base plate of the frame and is counterbored to accept the end of the chamber block. The other bulkhead is a separate piece and has a circular opening. During assembly it slides over the end of the chamber block, which is slightly reduced in diameter, until it seats. Then the bulkhead is bolted down by a clamping plate to a raised pad on the main frame piece so that the chamber block is restrained snugly.

The barrel piece adds 87.5 inches of barrel length to the fixture for a total of 93 1/4 inches. Its bore has the smooth, 32 microinch finish, also. The wall is approximately 1.6 inches thick to provide ample depth for thermal, pressure and erosion sensors. A short barrel piece was also fabricated. The total barrel length with this piece installed is 8.9 inches.

Sealing at the joint between barrel and chamber is provided by an "O" ring. This installation is known as the captured "O" ring type inasmuch as it is confined completely in its groove by a projection of the mating metal surface that matches the groove and extends partly into it. In this gun fixture the "O" ring groove is in the end face of the barrel and the matching projection is at the seat in the chamber block.

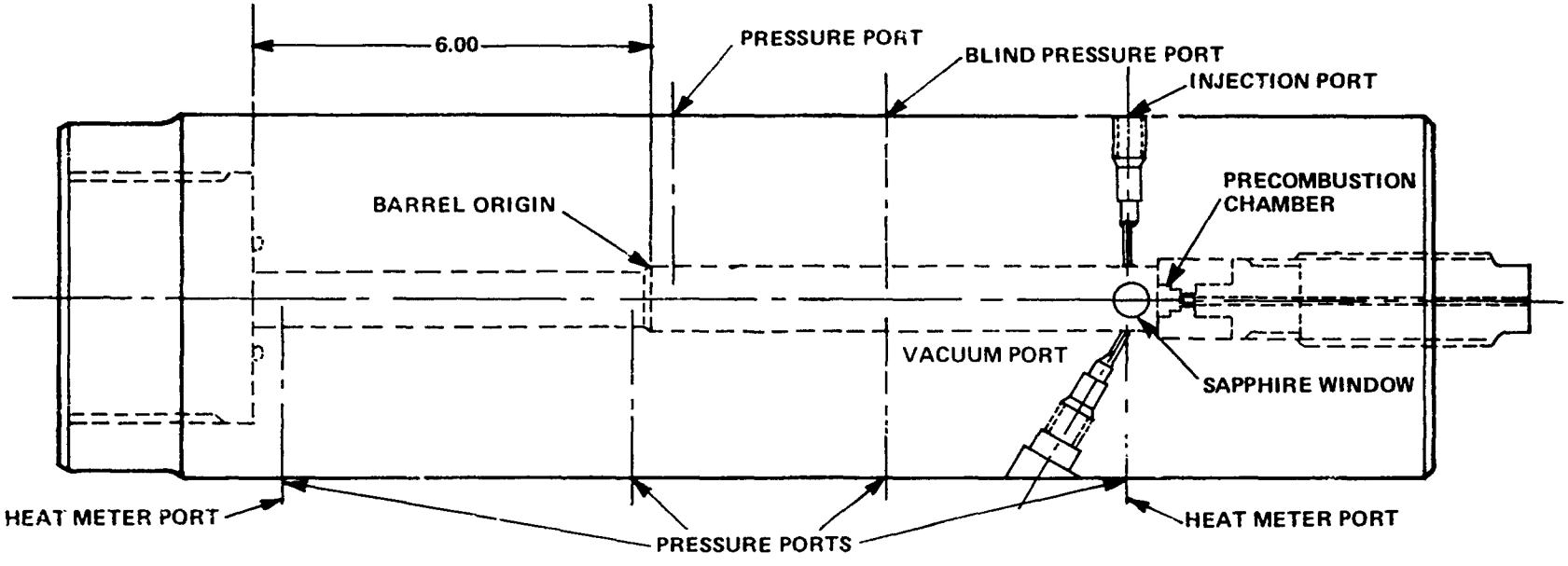

Figure 2 INITIAL LPG CHAMBER BLOCK WITH BREECH WINDOW

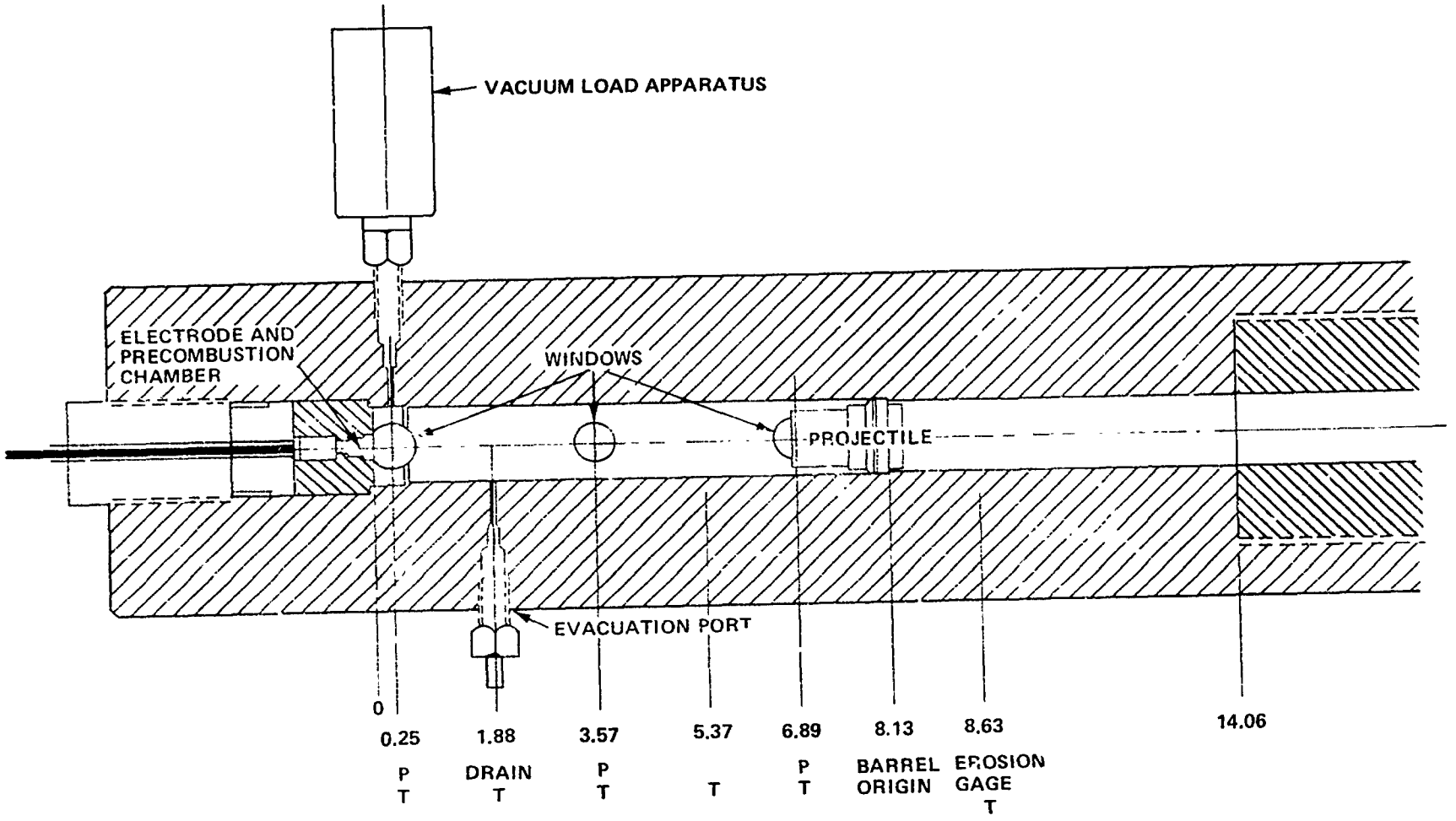

Figure 3 FINAL LPG CHAMBER WITH INSTRUMENTATION LAYOUT

2.1.1.2 Propellant Loading Procedure

The LPG fixture is equipped with two needle valves that are used in the propellant loading procedure. One valve, located in the bottom of the chamber, is connected to a vacuum pump and is used to evacuate the chamber prior to loading. Once the chamber is evacuated, this valve is closed prior to initiation of loading.

A second valve is located at the top of the chamber. A translucent Nylon tube and an open-ended container equipped with a stopper are attached to this valve with vacuum-tight fittings. The charge of propellant to be loaded is placed in the container. The chamber is evacuated with the loading valve open, (the stopper prevents propellant from flowing into the chamber at this point) the vacuum valve is closed, and the stopper is pulled which permits flow of propellant into the chamber.

The loading technique begins by manually seating the projectile by tapping it in place with a hammer and brass rod. A measurement of projectile position is made to verify that the shot-start band is truly seated at the barrel origin. The barrel is evacuated to assure that the projectile remains seated during the subsequent chamber evacuation. When the loading container stopper is lifted, propellant rushes into the chamber. This loading procedure allows some of the air dissolved in the propellant to boil off and remain as ullage, normally a small fraction of a percent.

When propellant stops flowing into the chamber, the loading container is removed and some of the propellant is removed so that the propellant level in the Nylon tube is clearly visible. A house air line is connected to the tube and the amount of ullage in the system is determined by measuring the change in liquid level in the tube as pressure is applied. The equation used to calculate ullage is

$$V_u = 0.1772 \left(\frac{p_a}{\Delta p} + 1\right)(\Delta X - 0.0108 \Delta p)$$

where V_u is the ullage in cm^3

p_a is the ambient atmospheric pressure, psi

ΔP is the increment in applied pressure, psi

and ΔX is the change in liquid level due to the increment in applied pressure, cm.

This ullage determination technique takes advantage of the fact that the volume a perfect gas occupies is inversely proportional to its pressure and that the process is performed slowly enough to allow the assumption of an isothermal process. The term subtracted from ΔX accounts for the expansion of the Nylon tube.

After the ullage is determined, the Nylon tube and loading valve are removed and excess propellant removed from the valve cavity. The valve is replaced and tightened to a torque of about 30 foot-pounds. This is sufficient for the valve to seal against a pressure of 200,000 psi. A water line is attached to the loading valve and a water driven aspirator is attached to the vacuum valve in order to flush the system in case of a misfire. At this point, the electrode is connected electrically, the capacitors are charged and the system is ready to fire.

The values of ullage for this loading procedure typically range from a low value of 0.05% to a high value of 0.5%. The average value is 0.15%, which represents an absolute ullage of approximately 0.25cc.

2.1.2 Electrode/Precombustion Chamber

The precombustion chamber is defined as the small volume adjacent to the breech end of the main chamber, and the electrode is a rod that protrudes into this volume. Together they form the "spark plug" that is the source of ignition for the Calspan liquid propellant gun. The configurations of the electrode and precombustion chamber are critical to the performance of the gun. They govern many of the characteristics of the electrical discharge and subsequent ignition of the propellant.

The electrode/precombustion chamber configuration used during most of this program is similar to that used during the Pulsepower Systems Inc. 30mm LPG test program described in Reference 1 and is shown in Figure 4. The electrode was a 1/16 inch diameter 304 stainless steel rod. The surface was either polished or sand blasted and the tip was either hemispherical or flat. These characteristics are significant parameters that influence electrode performance. The dimensions on this figure apply to the precombustion chamber used during Runs 52 to 57, discussed at length later in this report. Other precombustion chamber geometries involved in the research will be identified in Section 3.0. The electrode is connected electrically to the "hot" terminal of the discharge system and is insulated from the main body of the fixture. The precombustion chamber is made from a 15-5 PH stainless steel and is at ground potential.

2.1.3 Electrical Discharge System

The electrical discharge system provides the source of energy required to ignite the propellant. The ignition energy is generated by the discharge of capacitors. The system currently incorporates two 60-microfarad capacitors, each rated for 6000 volts. These capacitors can be connected in parallel, series, or individually as desired. They are charged to the desired voltage with a power supply that is capable of providing voltages up to a maximum of 3000 volts in increments of ten. The circuit connecting the capacitors with the electrode, includes an inductance coil of No. 10 copper wire to retard the rate of discharge. The circuit is closed by a remotely actuated mercury relay. The system is safeguarded by a normally closed relay which causes the capacitors to be completely discharged when the system is not in use. A circuit diagram of the electrical discharge system is shown in Figure 5.

2.1.4 Chamber-Wall Window Design

A variety of window designs were investigated for their feasibility of application to photography of the interior of the LPG chamber. These designs involved the use of sapphire crystal for windows, which material exhibits very good optical quality, and a very high strength when loaded in pure compression, but is relatively weak in bending and is especially sensitive

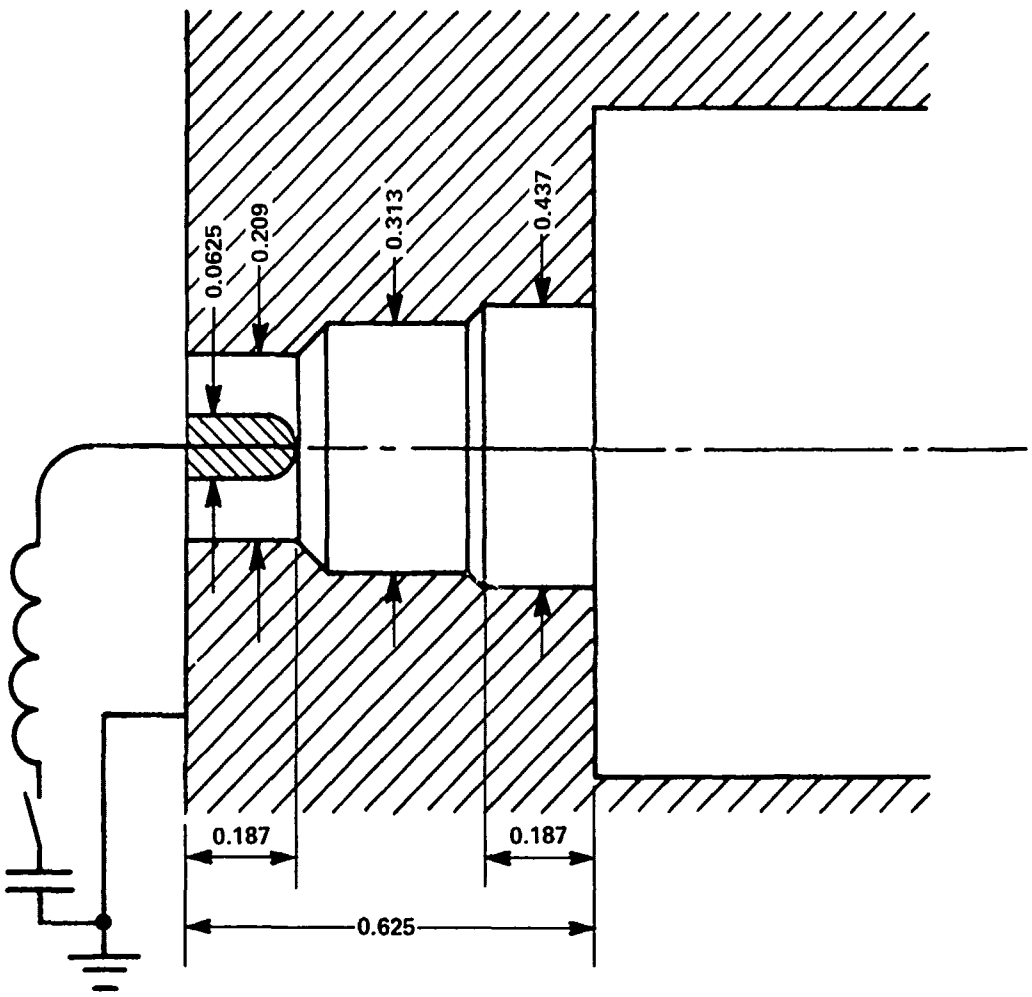

Figure 4 PRECOMBUSTION CHAMBER/ELECTRODE CONFIGURATION

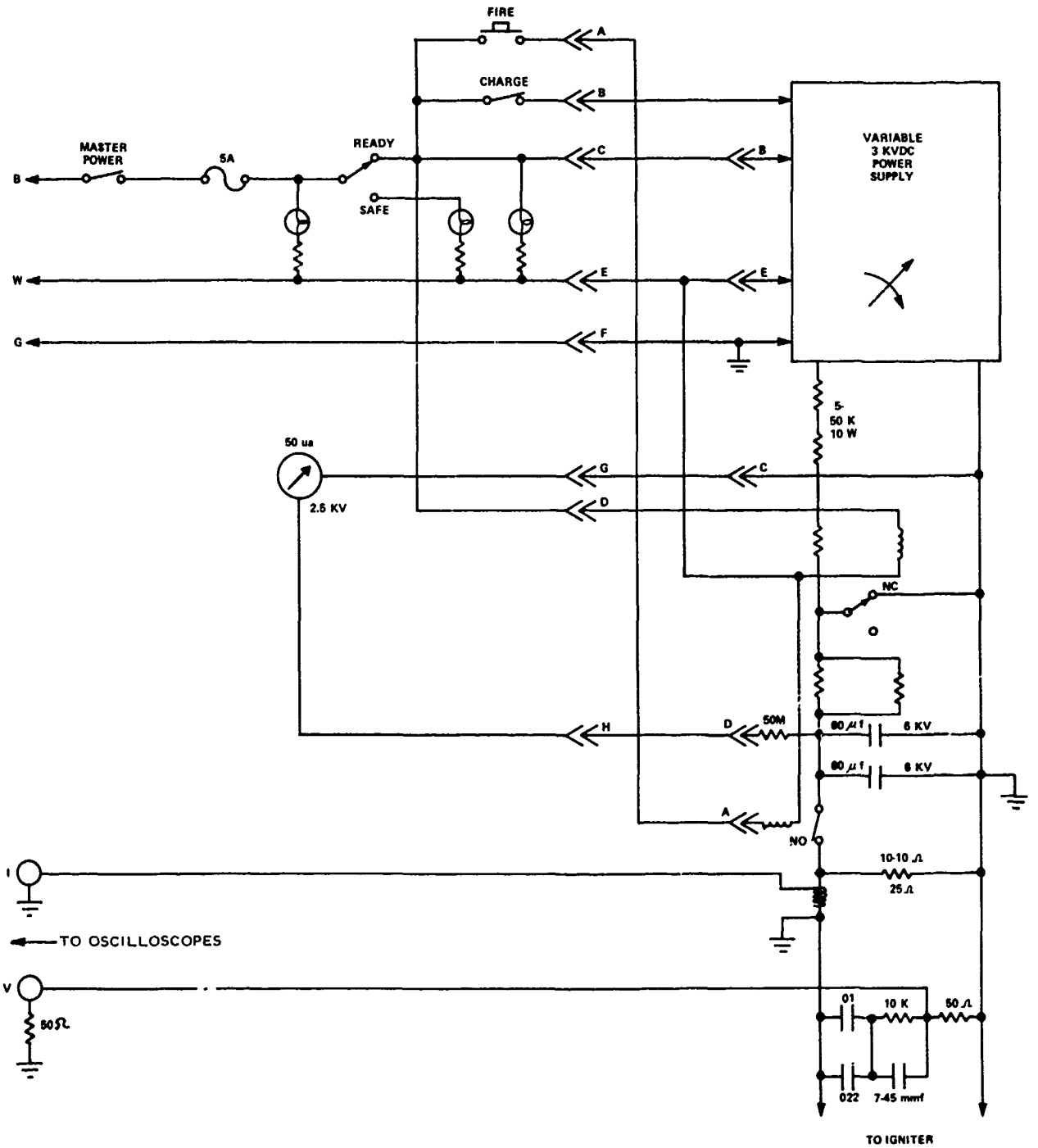

Figure 5 LPG ELECTRICAL DISCHARGE SYSTEM

to concentrated loading. Consequently, window design is an exercise in devising practical methods for securing the sapphire so that the stress at the pressurized surface is transmitted uniformly to the resisting surface by compression, insofar as is possible.

The design finally adopted was found to withstand firing conditions reasonably well and was among the simpler and least expensive of the designs evaluated. This design incorporates a cylindrical sapphire window element as shown in Figure 6. It makes use of a dynamic seal that was developed at Calspan for gun chamber work, specifically to seal one end of each of the chambers in the revolving cylinder of the M39 gun. This seal is exposed to the pressure and bears against the flat surface of the window at its pressurized end. The seal also has another surface that fits snugly in the window bore. When suddenly exposed to high pressure gases, leakage occurs between these adjoining surfaces and the leakage flow occurs at high velocity with a Venturi effect. This causes a force unbalance on the seal so that it bears tightly against restraining surfaces, thereby producing a sealing effect. A soft copper washer is provided at the outer end of the sapphire window element so that it will distribute the reaction force uniformly around the window.

The window and its seals fit into a counterbore in the chamber that is 1 inch in diameter (1.25 inch diameter for 1.25 inch diameter windows) by 1.313 inches deep, relative to a milled face. This face is large enough to accept 10 tapped holes for capscrews that are used to bolt down the window holder. The window element and seals occupy the counterbore to a depth slightly in excess of that available (up to .002 inch) so that the dynamic seal crushes slightly upon assembly.

Experience with the windows has shown that this design for holding the sapphire will allow it to survive pressures up to 100,000 psi. Many windows subjected to pressures in excess of this pressure suffered structural failure that destroyed them optically, but they did not blow out of their port. However, during three instances, windows at the projectile base or breech location actually blew out.

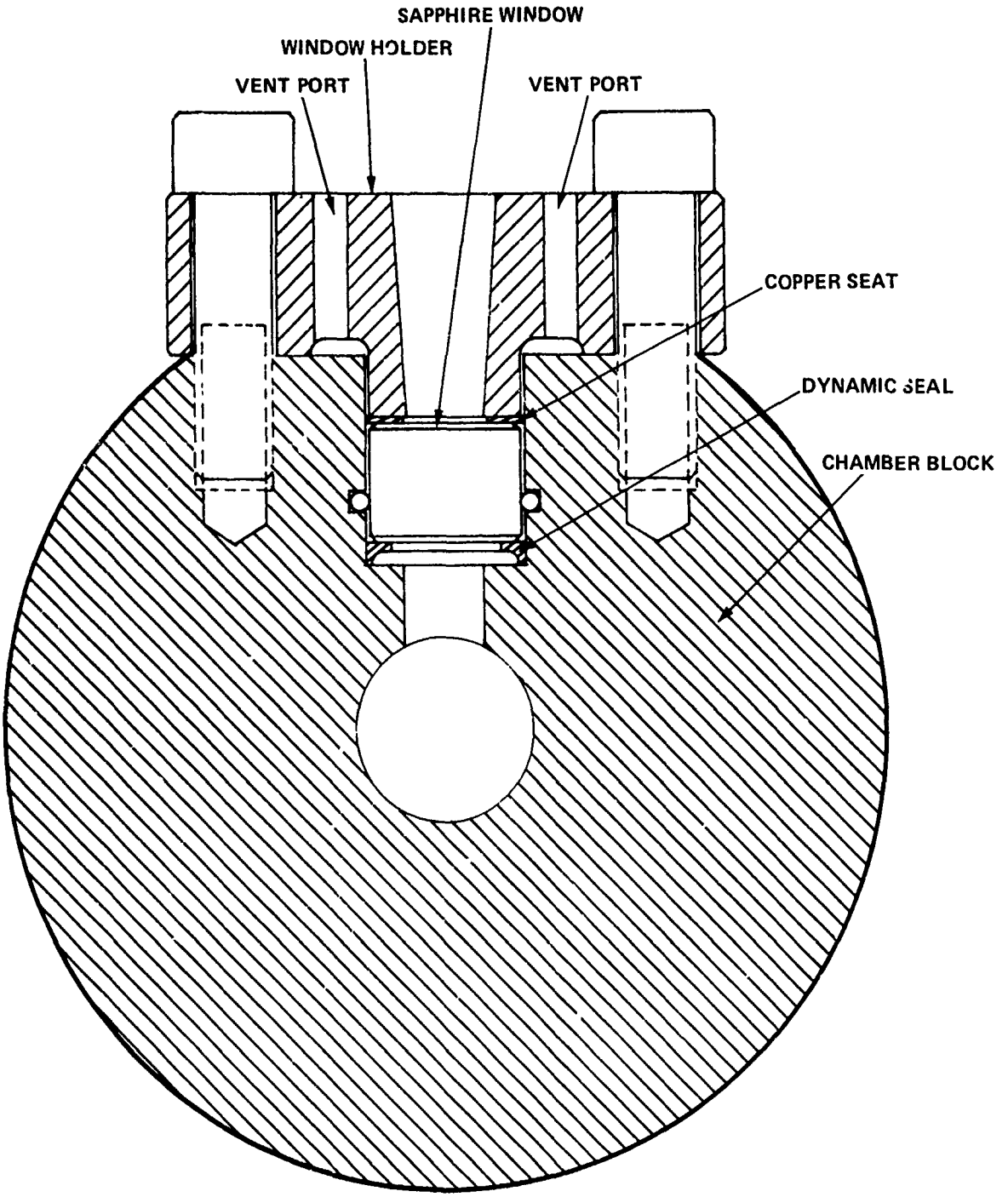

Figure 6 CYLINDRICAL WINDOW INSTALLATION

2.1.5 Projectile Design

Two projectile configurations were used during this program. Both configurations used a brass slug body with an afterbody; the only basic difference being the afterbody material as shown in Figures 7, 8, and 9. Rigid urethane foam was used for one configuration and aluminum for the other. The foam-afterbody design was that used by Pulsepower Systems (PSI) during runs 8.267 and 8.276 of their 30mm program (Ref. 1). The projectile body is made from annealed Naval brass. The hardness of this material was measured to be 59 on the Rockwell "B" scale, which corresponds to a strength of 51,000 psi. The shot start of a projectile was measured by pressing it through the area reduction at the barrel origin of the test fixture with Calspan's tensile tester. This device pushed the projectile at a constant rate and recorded the force of resistance. Changes in shot start band thickness from 0.030 to 0.060 cause the peak resistance pressure to change from 5000 to 9500 psi.

The urethane foam used as projectile afterbody is a rigid, closed-cell material with a nominal bulk density of 20 pounds per cubic foot. The foam material is made at Calspan from a kit supplied by Polymir Industries of Oakland, California.

A stress-strain test was performed on a sample of the polyurethane foam used for projectile afterbodies. A piece of foam 3 7/16 inches long was cut from a bar of material and machined to a diameter of one inch. The foam sample was placed in a 4-inch long piece of one-inch pipe and pressed with a steel rod slightly less than one-inch in diameter. Calspan's tensile tester machine was used to press the foam and provide a continuous measurement of the force exerted during the test. Values of force were recorded at 1/16 inch deflection intervals. These data were normalized to show strain in inches per initial inch of foam length and stress in terms of psi and are presented in Figure 10. The data show that general compressive failure occurs in the 800-1500 psi range when the sample length was decreased by nearly 50%. As pressure is increased, the foam deflection approaches 80% asymptotically. The material density at this level of compression is very close to that of the materials used to make the foam.

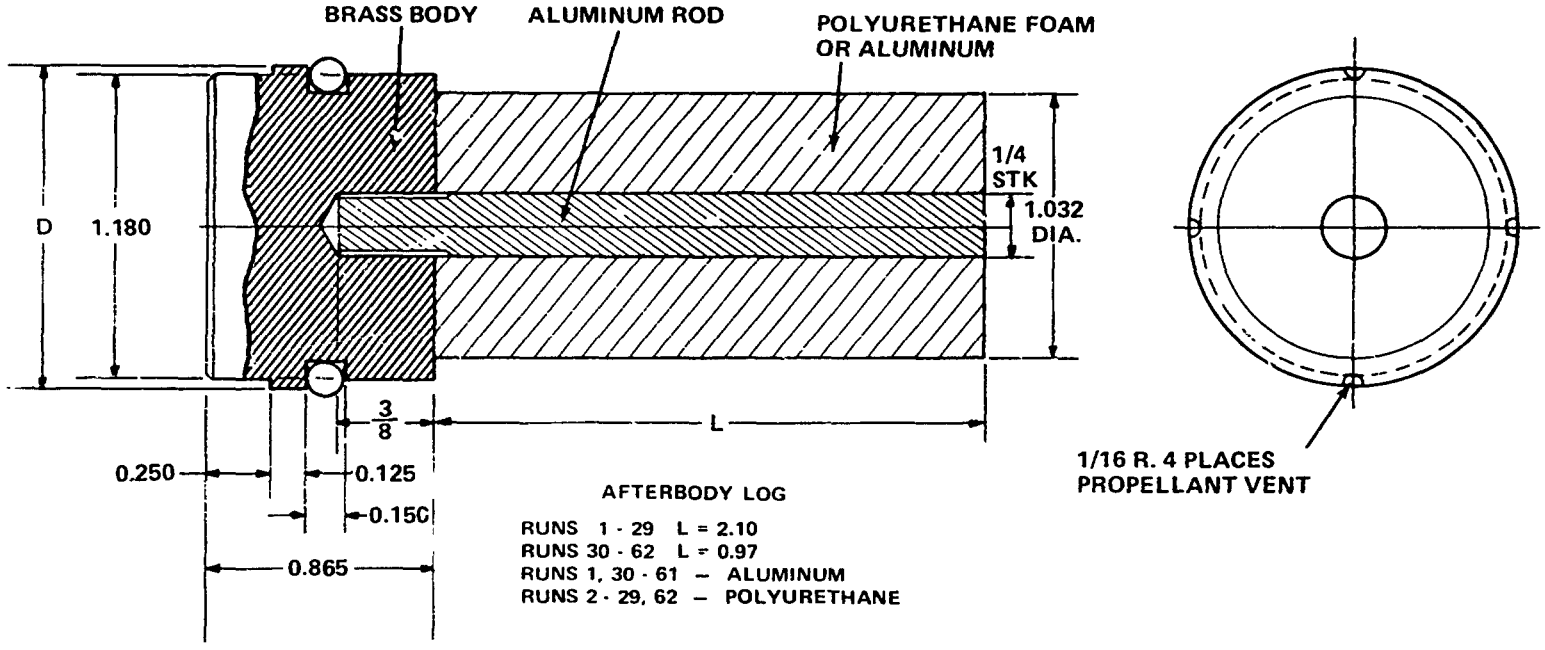

Figure 7 30mm SLUG PROJECTILE

Figure 8 30 mm PROJECTILE WITH ALUMINUM AFTERBODY

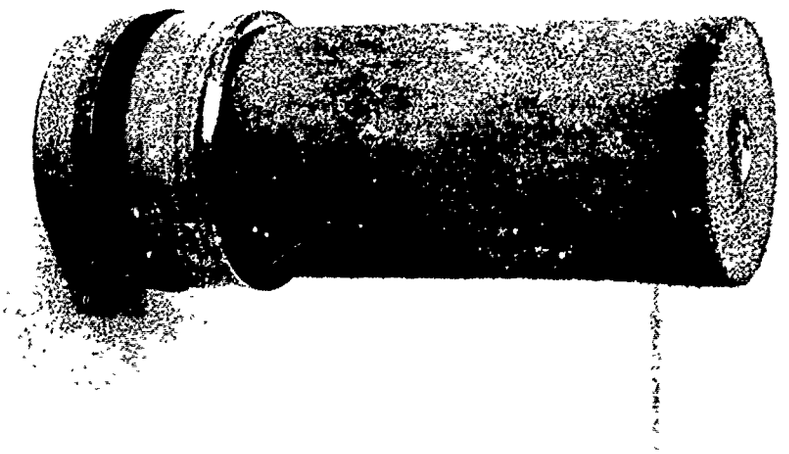

Figure 9 30mm PROJECTILE WITH POLYURETHANE FOAM AFTERBODY

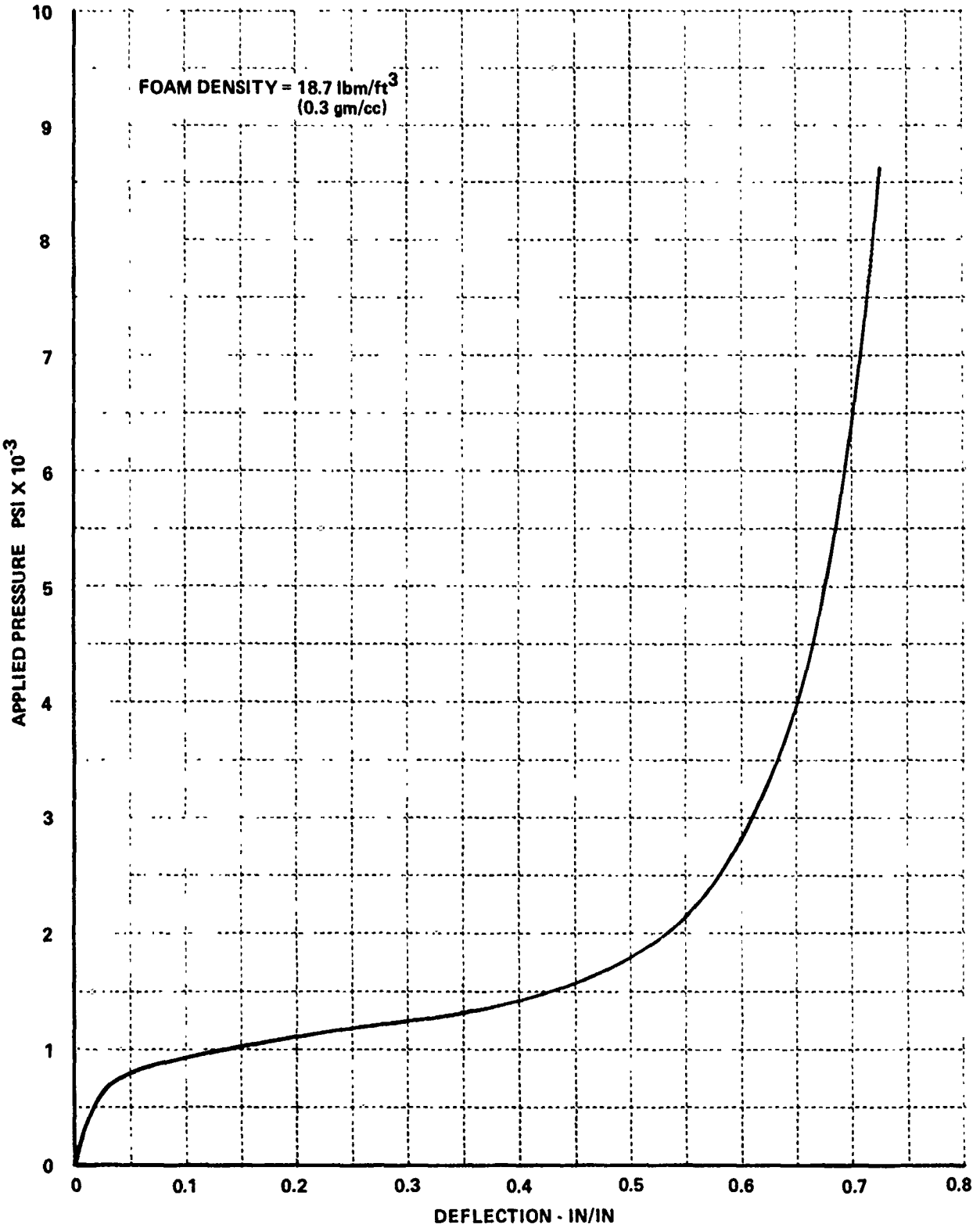

Figure 10 STRESS-STRAIN CHARACTERISTICS OF HIGH DENSITY, RIGID URETHANE FOAM

2.2 INSTRUMENTATION AND DATA ACQUISITION

2.2.1 Pressure Measurement

Each of the gun chambers used during this program contained ports for mounting pressure transducers at several locations as shown in Figures 2 and 3. The transducers used during the program are manufactured by PCB Piezotronics, Inc. They are of the 118-119 series and are statically calibrated to 120,000 psi.

Considerable difficulty in measuring pressure was encountered as a result of the severe environment created when the gun was fired. Much was learned as these problems were overcome and solutions to specific problems are recorded here for posterity.

The first transducers that were used contained built-in signal amplifiers. The severe vibration experienced during a firing caused the electronics to become open-circuited. This was cured by removing the built-in amplifier and by either using a separate amplifier mounted on a surface unaffected by the gun or mount or by using a charge amplifier. The former technique has the advantage of reduced noise because of the low impedance voltage output, but both are acceptable.

In gun research, the orifice and cavity adjacent to the diaphragm of an installed pressure transducer are sometimes filled with silicone grease or RTV silicone rubber to act as a thermal barrier and to improve response. It was discovered that this practice contributed to a diaphragm failure problem. It is surmised that hydrodynamic wave transmission through this material and reflection at the diaphragm surface momentarily caused the pressure to exceed the chamber pressure substantially, which caused the diaphragm failure. The transducers currently used have ceramic-coated diaphragms for thermal protection. A thin coating of silicone grease is rubbed on the diaphragm but the cavity and orifice are left empty, except for the propellant that enters when the gun is loaded.

Gun vibrations as well as high pressures resulted in failure of the tiny charge pickoff wire at the crystal. This failure renders the transducer inoperative and it cannot be repaired. PCB revised the design of the charge pickoff wire attachment and the transducers are more durable than before. The new designation is 119M08 for a positive signal and 119M09 for a negative signal.

Finally, the threaded-signal lead attachment became loose during most high pressure tests as a result of the severe vibrations. Upon recommendation from NWC, the fitting was attached to the transducer with epoxy. It is important for the epoxy to be applied to the threads for this technique to work. Normally, the epoxy will be cracked after a test and must be re-attached for each subsequent test.

2.2.2 Heat Sensors

Heat flux has become a routine measurement in gun and ammunition research at Calspan. These measurements have been directed toward gun heating as related to ammunition cookoff, chamber and barrel optimum design, and barrel erosion in solid propellant systems. The heat sensors used in this research were developed by Calspan and exhibit the important qualities of structural integrity in the high pressure gun environment, fast response, relative ease of fabrication, and ability to readily convert the output of the sensor to heat flux.

The current application of these heat sensors is to signal the arrival of the flame front at a given position in the chamber in addition to measuring the heat flux. Unlike a pressure transducer, the heat sensor will not generate a signal as long as it is immersed in the room-temperature liquid, but will respond when it is exposed to the gaseous products of combustion. Therefore, this piece of instrumentation appears to be an ideal complement to pressure measurement to help characterize ignition and flame spread in a liquid propellant gun in a manner that can reveal the mechanisms responsible for erratic pressures.

The basic heat meter design is shown in Figure 11 and photographs of a meter specially fabricated for the LPG program are shown in Figure 12. The sensing element is made of silver and its thickness is a parameter that can be adjusted for a specific test. A thick sensor provides the greatest heat content while a thin sensor gives the most rapid response. A requirement of this program is to time correlate the onset of local heating with pressure. Therefore, the fastest response consistent with structural durability is desired. A 0.020 inch thick sensor element has demonstrated the ability to withstand the high LPG pressures long enough to generate the desired information and with sufficient response, about 20 Kh, to correlate with pressure.

2.2.3 Spark Plug Voltage and Current

The electrical ignition system is instrumented to measure the current flowing through the spark plug and the voltage drop across the spark plug gap simultaneously. The current is measured by passing the electrode lead through a Model 110 Pearson Electronics, Inc., current transformer. The signal generated by the transformer is recorded on an oscilloscope. The voltage is provided by conventional voltage divider circuitry as shown in Figure 5 and is recorded on an oscilloscope.

2.2.4 High Speed Photography

2.2.4.1 Equipment

A Hycam camera was used to take high-speed motion pictures of LPG ignition and combustion. A split frame prism was used for the initial work where pictures were taken through the breech window. Pictures were taken at a rate of 18000 pps with the split prism. Resolution with this setup is at least 35 line pairs per millimeter. The camera was equipped with a quarter-frame prism when three chamber windows were used. This increased the picture rate to a nominal value of 36000 pps. The resolution with this camera configuration is at least 20 line pairs per millimeter. Sixteen millimeter Ektachrome EF film was used with this camera.

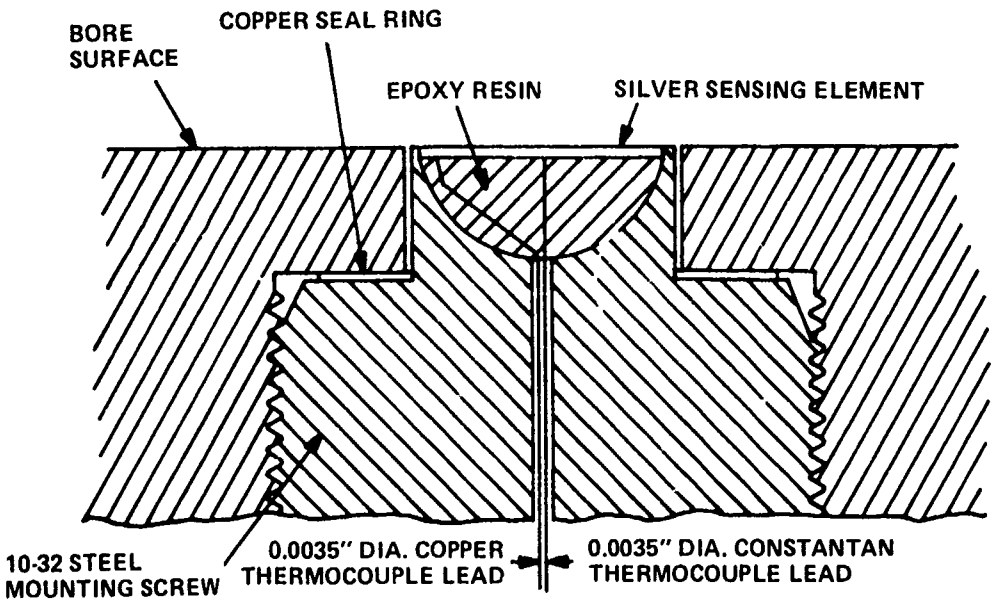

Figure 11 SKETCH OF HEAT FLUX METER

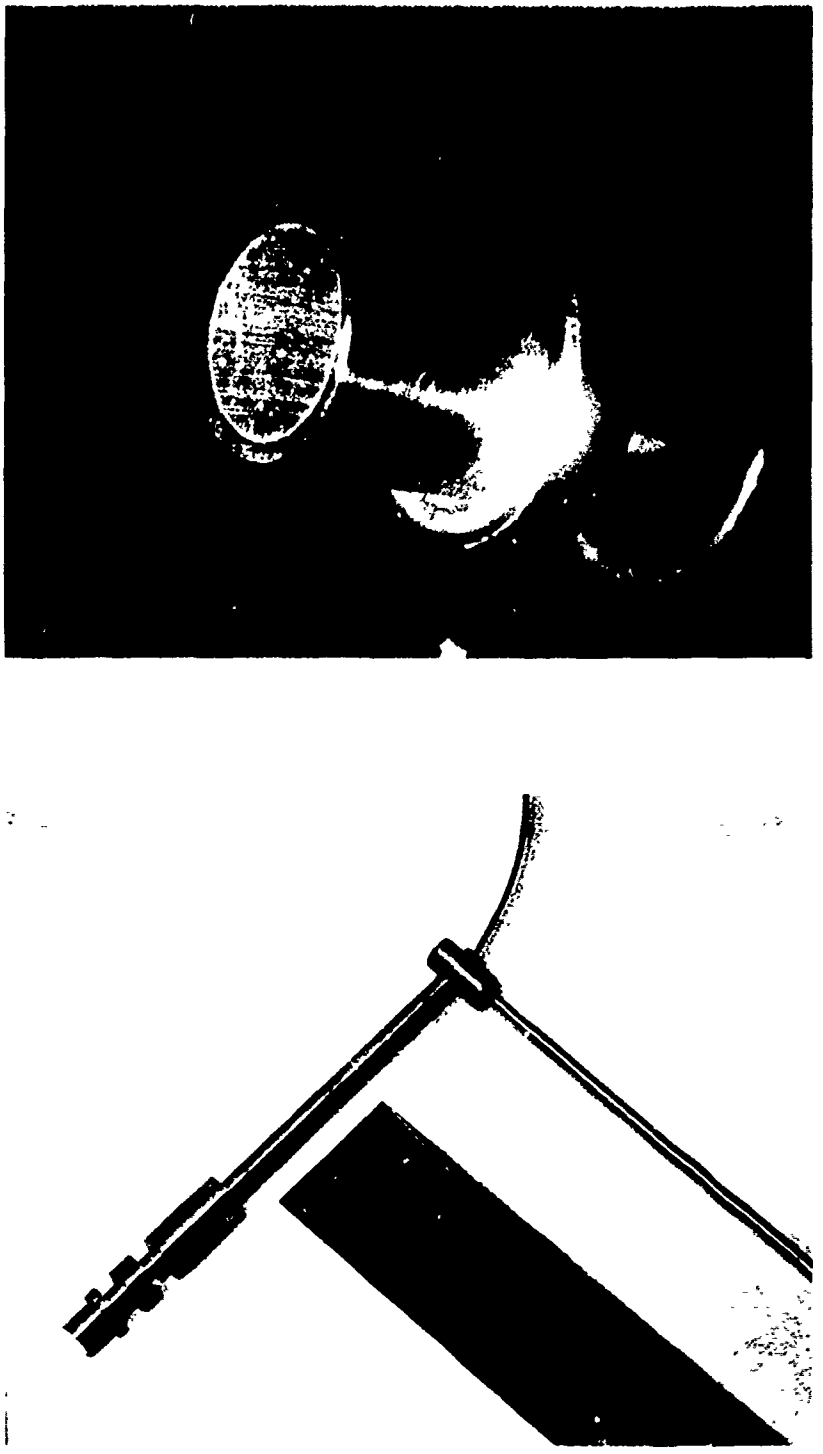

Figure 12 CALSPAN CONTOURED HEAT METERS

A Cordin 375 camera was loaned to Calspan by Argonne National Laboratory for use on this program. This camera has the ability to take up to 500 pictures at speeds up to 200,000 pps. This camera features a rotating drum and prism system which allow film exposure over the entire circumference of the drum with continuous access. The camera was operated by manually opening the shutter prior to the event and by allowing the light from the event to expose the film. This camera was especially well suited to photographing such events as spark discharges during open cup tests. Seventy millimeter high-speed Ektachrome color film and Tri-x black and white film were used during this program.

2.2.4.2 Optical Setup

Two optical setups were used during this program. One incorporated the gun chamber with a single pair of windows at the breech. The optical train for this chamber is shown in Figure 13. The Hycam camera was installed to observe optical events through one window while the other diametrically opposed window was used either to allow motion picture backlighting or as a viewing port for a spectrograph or for radiometers.

The second setup incorporated the gun chamber with three window pairs as shown in Figure 14. An optical train, consisting of a network of mirrors, was designed to allow the events from the three window ports to be photographed simultaneously within each frame. The quarter frame format of the camera was well suited to this purpose. The mirrors were mounted on a platform with the Hycam camera to minimize camera alignment problems from test to test. The three pairs of diametrically opposed windows allow backlighting for each axial window position. However, the Cordin camera was used to view events at the breech window during some tests, as shown in Figure 14, and this prevented use of backlight at the middle and breech window positions for those tests.

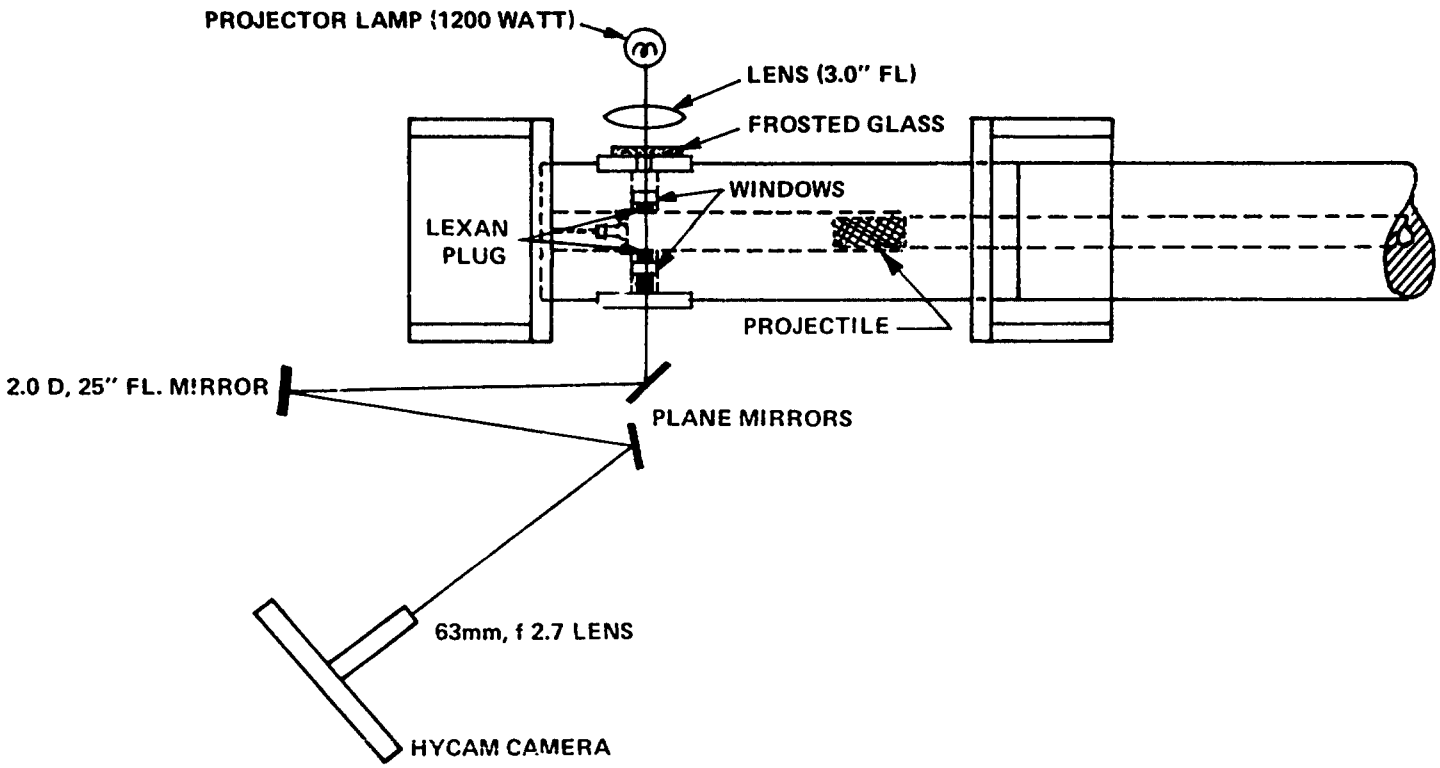

Figure 13 OPTICAL TRAIN FOR MOTION PICTURES THROUGH SAPPHIRE WINDOWS OF INITIAL CHAMBER

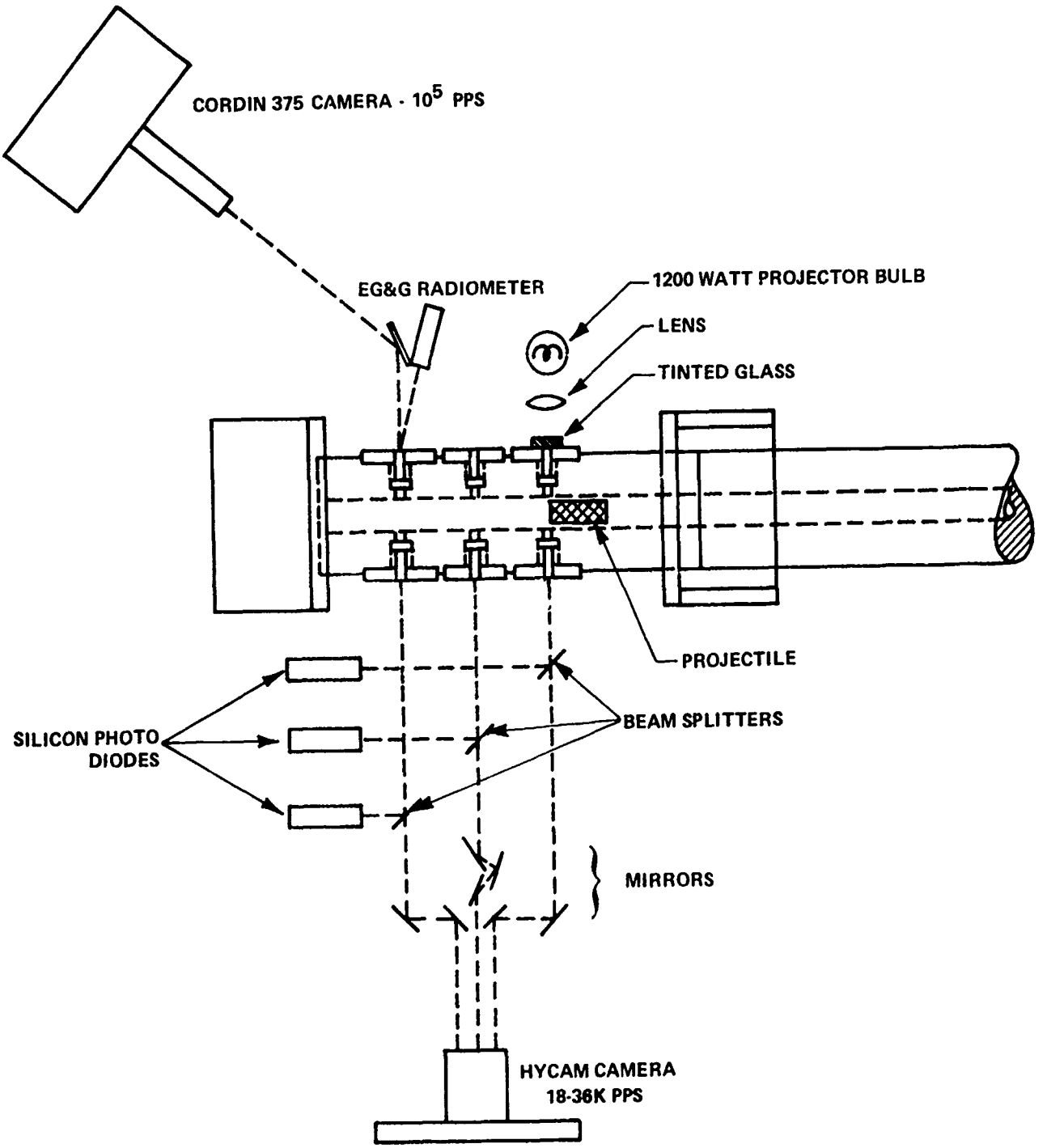

Figure 14 FINAL INSTRUMENTATION SETUP FOR LPG TESTS

2.2.5 Radiation Instrumentation

The sapphire windows afford an opportunity to obtain optical and radiative-type data continuously. Two types of radiometers were used during this program. One was a Fairchild FPT110 phototransistor wired as a photodiode that had a wavelength response of 3500 A to 1.1 microns. The photodiodes were installed in a holder and used to view a spot in the center of the window. An EG&G SDG 100 photomultiplier with S-11 response (3000A-5000A) was installed to permit a view of the entire window area. Both instruments are capable of responding to a radiation signal within a few microseconds, well within the time scale of the data records. The installation of these radiometers is shown in Figure 14. The use of a beam splitter in the optical train for the photodiodes permits them to provide a continuous record of the same optical events recorded by the camera.

An f6.3, 3/4m focal length Czerny-Turner grating spectrograph with a dispersion of 20 A/mm was also used during the program. This device was used to provide a time-integrated record of the spectra generated during the ignition phase over the range from 3000 A to 9000 A. The effort expended on this task was minimal and it represents only a first attempt to investigate the chemistry of the ignition process. The spectrograph was used during open cup as well as actual gun tests.

2.2.6 Muzzle Velocity

Muzzle velocity is a routine ballistic test measurement at Calspan. The technique used during these tests incorporates two silvered electrical grid paper targets placed ten feet apart, a Calspan designed and fabricated pulse generator, and an Atec Model 2000 Universal Digital Electronic Counter. When a projectile passes through the first piece of grid paper, an electrical circuit is broken and a pulse is generated that initiates the time counter. A second pulse is generated when the projectile passes through the second target and this stops the counter. The muzzle velocity is simply the distance of 10 feet divided by the elapsed time given by the counter. The velocity can be resolved to within $\pm$ 3 feet per second

2.2.7 Projectile Position

Projectile position can be measured as a function of time with the short barrel (8.9 inches long) gun configuration. This short barrel length makes it possible to attach a sting to the front of the projectile so that the tip of the sting protrudes from the barrel before the gun is fired. Projectile motion is recorded by using a high-speed motion picture camera to photograph sting movement. Time correlation with other events is provided by initiation of a timing light when the electrical system begins to discharge. The initial sting, shown in Figure 15 was made from aluminum rod and was tapered from 0.25 inch diameter at the point of attachment to the projectile, to 1/16 inch diameter at the tip. Bright orange and black bands, each 1/2 inch long were painted on the sting to provide the scale factor and to facilitate position measurement. This design proved unsatisfactory because of inability to withstand the large acceleration forces. A second design shown in Figure 16, has been recommended and successfully tested by NWC/China Lake.

Other techniques were found to be more easily incorporated and correlated. These included use of break wires to signal the time of projectile exit from the barrel and use of a wire probe mounted inside the barrel to signal the time the projectile had moved a given distance. In addition, the projectile base is positioned near the midpoint of the forward window. Thus, initial projectile motion can be recorded in relation to combustion events.

2.2.8 Data Acquisition

All pressure, heat transfer, and radiometer data were recorded on Tektronic 502 oscilloscopes and current and voltage data were recorded on Tektronic 585 oscilloscopes. Permanent records of these data were taken with Polaroid oscilloscope cameras. The trigger pulse was generated by the voltage discharge pulse.

The use of electrical discharge as the ignition source caused data acquisition problems. In particular, the discharge current pulse became superimposed on all other oscilloscope-recorded data. This problem of ground

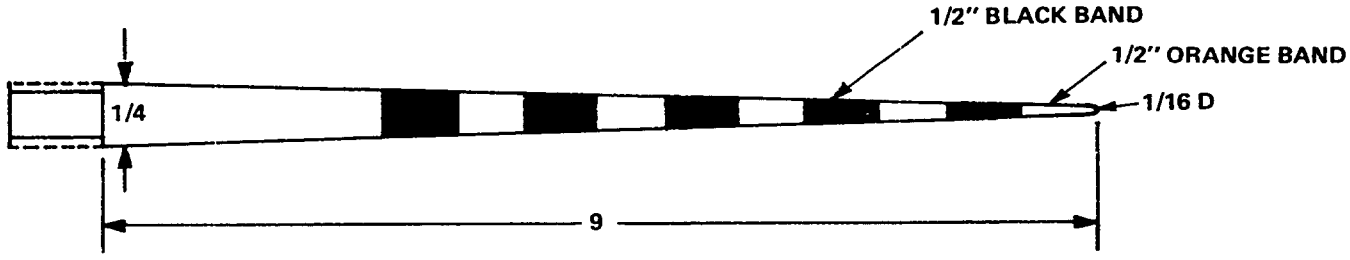

Figure 15 TAPERED PROJECTILE STING

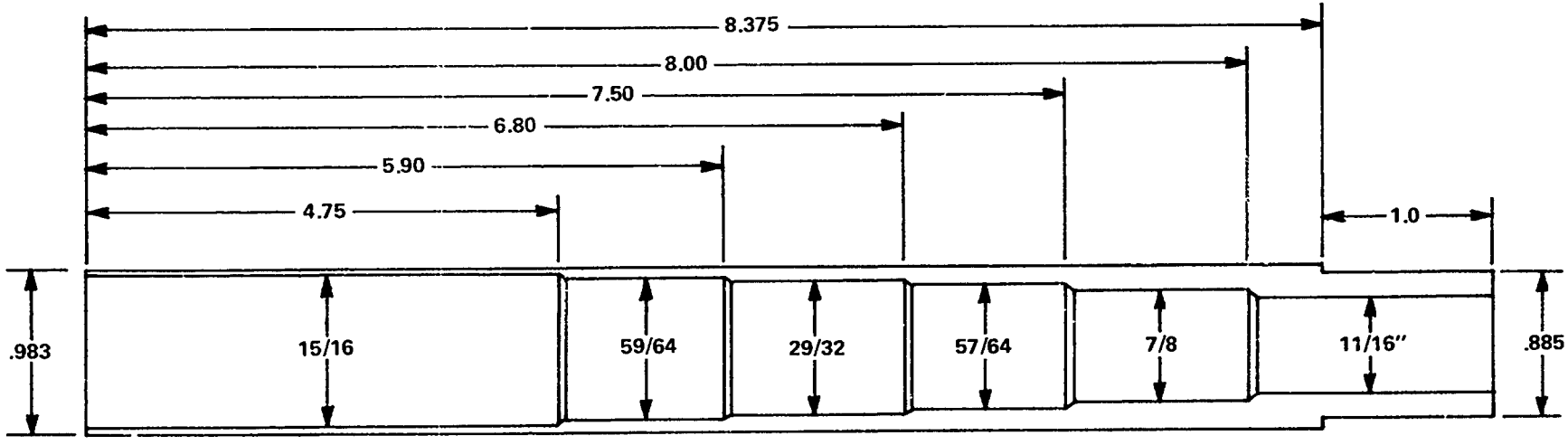

Figure 16 STEPPED SHELL PROJECTILE EXTENSION

loops was reduced to an acceptable level by paying strict attention to ground circuitry. In particular, a special ground junction for instrumentation was established on the chamber wall near the instrumentation. All oscilloscopes were grounded to this point, which is also the instrumentation ground. A separate ground circuit was provided for the discharge ground. This action essentially eliminated discharge-related noise on other data.

3.0 DISCUSSION OF SIGNIFICANT EXPERIMENTS AND RESULTS

3.1 OVERVIEW

The objective of the DARPA Liquid Propellant Gun Phenomenology Program was to provide a technological base for the development of a liquid propellant gun system as stated in Section 1.1 of this report. This program was to provide a coordinated analytical/experimental attack to understand and resolve the problems of LPG performance variability and overpressurization. Calspan was to perform diagnostic experiments in order to provide hard data and other information of an experimental nature, not normally obtained by LPG gun developers, to support the phenomenology and gun development programs.

The approach to the diagnostic experimentation phase was to transfer technology from the gun developer to Calspan. This technology was in the form of a tested design of a gun and electrical discharge system. Calspan was to build such a fixture and then launch into an experimental test program that was primarily concerned with taking high-speed motion pictures through sapphire windows and use of diagnostics to characterize the combustion process. The first phase of the experimental program was an attempt to duplicate the results of a 30mm test program conducted at PSI, described in Reference 1. The PSI results could not be duplicated in the Calspan fixture. The electrical power settings used by PSI resulted in a high frequency of misfires. High overpressures were experienced during most tests where ignition was achieved. Apparently, inconsistency among propellant batches and perhaps subtle differences between test fixtures and firing techniques caused large performance differences. The details of this effort are described in Reference 2. .

Subsequently, the three-step precombustion chamber-spherical tipped electrode design used by PSI was abandoned in favor of a two-step precombustor, flat-tipped electrode design used by NWC on their bipropellant systems. Inductance was added to the circuitry at this time to control the rate of discharge. This firing configuration never produced a misfire but

a low pressure combustion phenomenon with peak pressures below 10,000 psi, was observed. After two inductance reductions to a final value of 28 μh and several power increases to a peak value of 540 joules, high pressure combustion characterized by high overpressures after a short delay following the discharge, was obtained. This result was not consistent as low pressure combustion tests were also experienced during this period. The results of tests using the NWC precombustion chamber/electrode configuration are discussed in Reference 3.

The performance problems were further complicated by instrumentation difficulties, most of which were related to the excessive pressures that were experienced. Increases in projectile shot start pressure to 9500 psi and use of an enlarged PSI-type precombustion chamber seemed to improve gun performance. At this point the instrumentation problems were resolved and the primary diagnostic investigation was begun. Subsequently, much new information has been generated at Calspan that has provided new insight into the phenomenology of ignition and combustion in liquid propellant guns.

The purpose of this section is to discuss and concentrate the results of the diagnostic test program into a form useful to the LPG community. Results of individual tests are presented in a chronological fashion in the semi-annual and monthly reports (Ref. 2 through 7). Not all of the data presented in those reports will be repeated here; instead an attempt will be made to select meaningful data to describe specific phenomena. The three areas to be addressed in this manner are: (1) electrical discharge, (2) ignition and combustion, and (3) the total combustion cycle. The topic of electrical discharge is concerned with what actually occurs during a discharge and factors that appear to govern discharge consistency. The topic of ignition and combustion is concerned with the mechanisms that lead to full scale combustion after an electrical discharge. The third topic is concerned with mechanisms that influence combustion and gun performance.

The results of this report represent an important step in LPG research and development. While the knowledge of the processes of LPG combustion is still in the formative stage, significant advances were made as a result of the total ARPA program. The results of this work have led the authors of this report to make certain hypothesis about the processes of ignition and combustion. These are considered as tentative because clearly they are substantiated by too few experimental tests. On the other hand, they can be valuable as a focus for further discussion and design of tests.

3.2 ELECTRICAL DISCHARGE PHENOMENOLOGY

3.2.1 Discharge Characterization

The electrical discharge network used during this research program is described in detail in Sections 2.1.2 and 2.1.3. To recap briefly, the discharge takes place in a volume called the precombustion chamber. The walls of the chamber form the ground electrode and a rod in the center of this chamber is the hot electrode. For tests of this program, the rod was always the cathode. The center electrode received a negative potential supplied by a capacitor bank after a mercury switch was closed, which initiated the electrical discharge.

Open cup tests provide a convenient and inexpensive method for investigating electrical discharges. The elements of this test consist of the electrode/precombustion chamber assembly actually used in the test fixture, and the discharge system. This assembly is mounted vertically so that the precombustion chamber can be entirely filled with propellant or other liquid. The early features of the electrical discharges obtained with this test setup have been observed to be quite similar to those obtained during a firing test.

High framing rate pictures were taken of electrical discharges during several open cup tests. One set of these pictures taken during a test involving a discharge into NOS365 propellant is shown in Figure 17. These

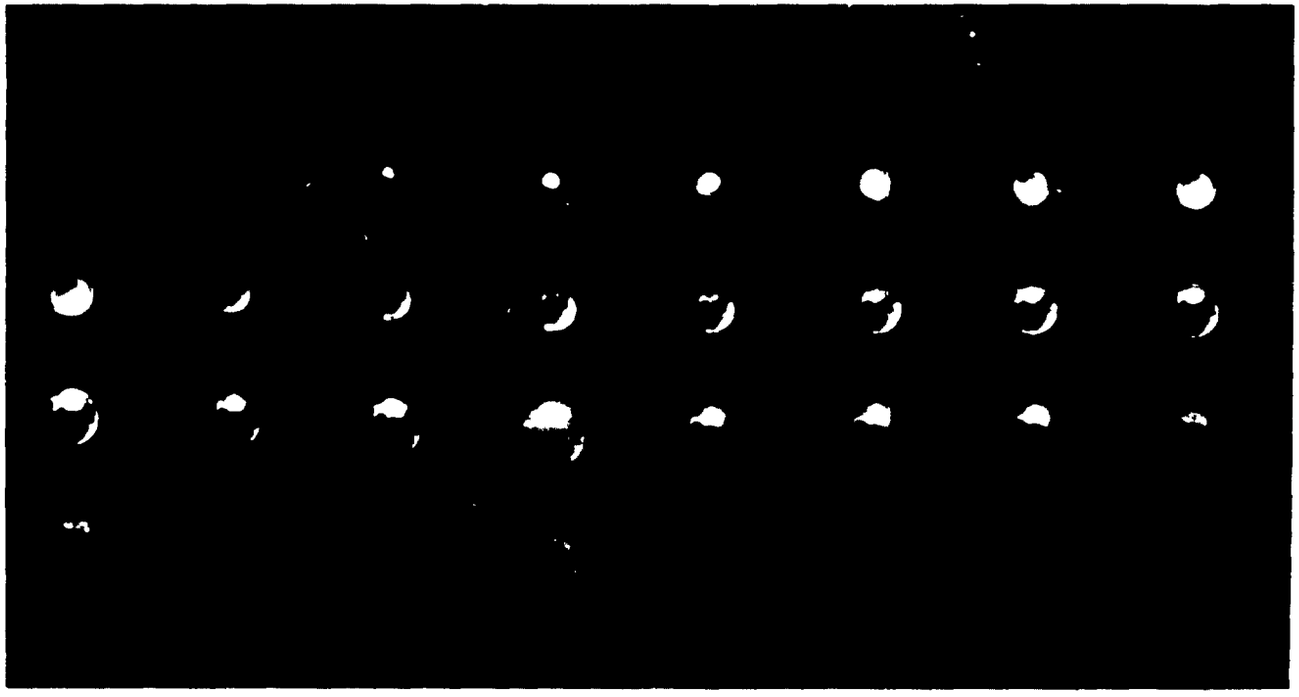

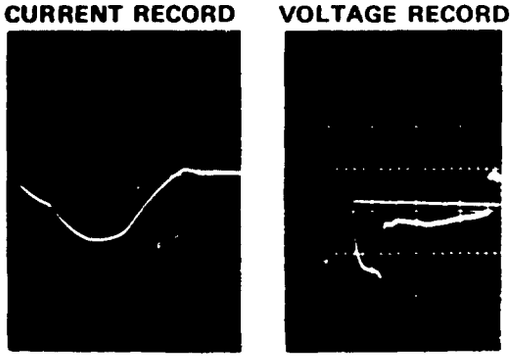

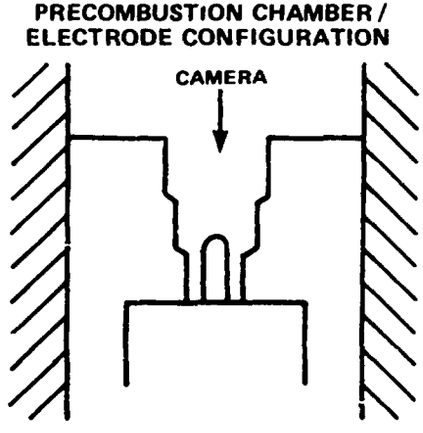

Figure 17 HIGH SPEED PHOTOGRAPHS OF THE ELECTRICAL DISCHARGE DURING AN OPEN CUP TEST

pictures were taken at a rate of 200,000 pps, so that the interval between pictures is 5 microseconds. The electrode/precombustion chamber configuration for this particular test is shown on the figure, along with the current and voltage record obtained during the test. Several obvious observable effects and events may be distinguished:

1. growth of a luminous, somewhat irregular, ball at the center electrode which appears to touch the wall of the chamber at the sixth picture;
2. occurrence of the arc as signified by a brilliant blue-white hue;
3. obscuring of bright areas by dark billows and streaks
4. growth of a light scattering medium and emergence of this medium from the cavity; and
5. persistence of light in direct correlation to the current.

The first six pictures, going from left to right in the top row, constitute what is called the formative phase of the discharge and is that portion of the current curve up to the cusp. This is a period during which electricity is conducted through the propellant at a rate governed by its ohmic resistance. A glowing yellow-white medium forms and grows around the tip of the center electrode, the region with the highest current density.

The seventh picture in this series shows an extremely bright blue-white light which correlates in time with the initiation of the arc phase, characterized by extremely high and localized current flow. The cusp in the current curve at about 40 microseconds marks the beginning of the arc discharge, since the violent resistance change is reflected in the value of the current. The inductance present in the circuit prevents the current from rising more rapidly. The sharp drop in voltage also marks the beginning of the arc discharge. The bright, white light was observed to persist as long as current flows. It is significant to note that most of the light is obscured by an opaque layer, at the interface between the gaseous products and the cool liquid, which will be discussed later.

The electric discharge step is closely related to a phenomena known as Glow-Discharge Electrolysis. Hickling (Reference 8 and 9) has described the process. The discharge begins with heating of the liquid followed by boiling at the center electrode. As the liquid boils, a corona discharge develops from the electrode and is visible in Figure 17 as a growing, luminous ball. The arc strikes when the corona reaches the wall. The current throughout the discharge is determined by the L-C-R parameters of the circuit.

The growth of the luminous medium or Corona during the formative phase, as represented by mean diameter, is shown as a function of time and compared with the corresponding current curve in Figure 18. The corona probably does not appear the instant current starts to flow so there is a time uncertainty of five to ten microseconds in the corona growth curve. The onset of the arc appears to occur when one part of the corona touches the chamber wall, which is observed to occur at the sixth picture. This event represents the final point on the corona growth curve of Figure 18 and further serves to illustrate the time uncertainty. The point to be made here is that very little if any corona exists before the current has flowed for about ten microseconds.

Corona growth does not appear to be entirely uniform over the tip of the electrode. It is noted in the third picture that the ball is nearly egg-shaped whereas it appears to be nearly spherical by the fifth picture. Apparently, nonuniformities in the electrode surface cause locally high electrical fields which accelerate vaporization in the region of the nonuniformity. However, these initial effects appear to be smoothed out by the continuing addition of vaporized propellant bubbles which tend to reduce the influence of these surface effects as the ball grows. If the nonuniformity is rather extreme, the asymmetry may persist, and the corona may touch the wall sooner, leading to a shorter formative phase. Of particular interest is the appearance of streamers in the fifth picture as the ball approaches the chamber wall and the conditions become favorable for the arc formation.

CORONA GROWTH; d / d_{max} where $d_{max} = 0.25''$

CURRENT; I/I_{fmax} where $I_{fmax} = 630$ amps

SET VOLTAGE; 2500 volts

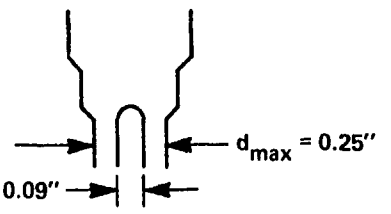

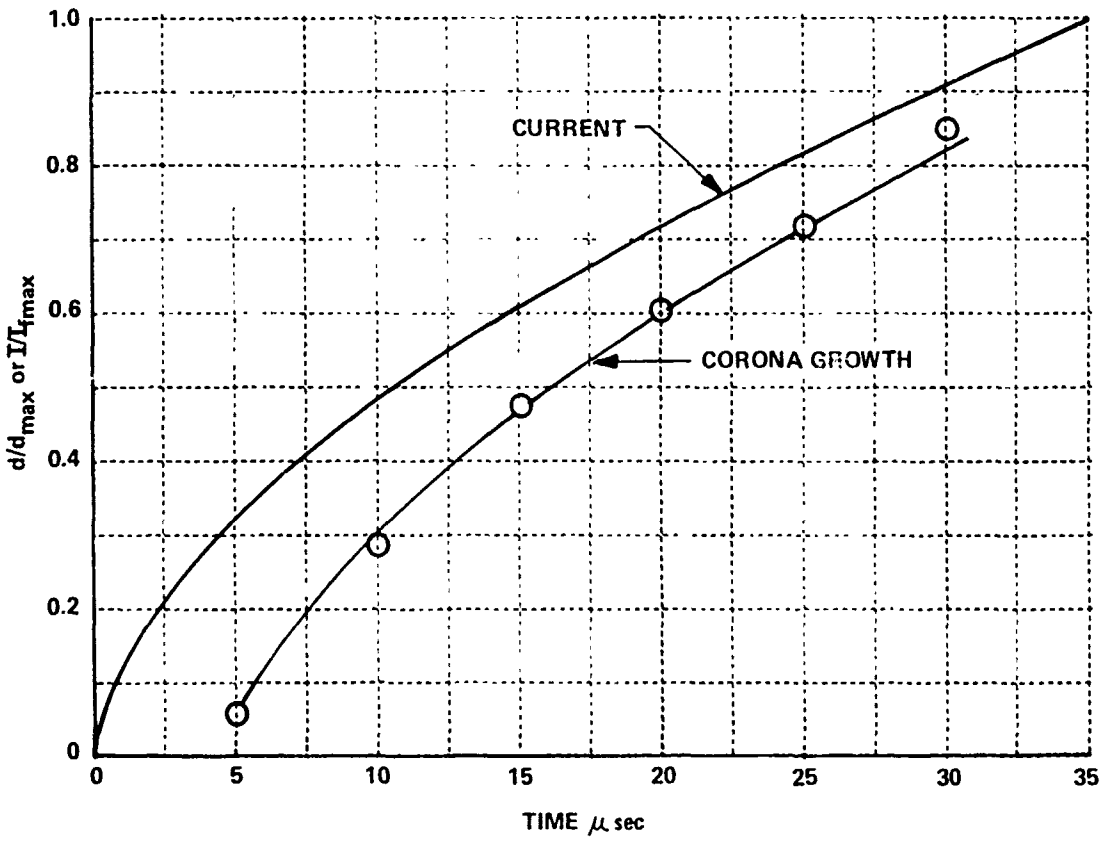

Figure 18 CORONA GROWTH AND CURRENT DURING THE FORMATIVE PHASE OF AN OPEN CUP TEST

An open cup test was also conducted with a solution of 20 percent nitric acid and 80 percent water as the liquid constituents; and another test was conducted using deionized water. Pictures taken during these tests, along with the respective current curves and a sketch of the test setup are shown on Figure 19. It is noted that the test with nitric acid is quite similar to the test with NOS365 with regard to the corona growth, subsequent expulsion after the arc, and formation of the opaque layer. In contrast, the test with deionized water, exhibited a very short formative phase and a strong arc. The pictures presented here were of the second discharge into the water, the first discharge creating a formative phase of 150 μsec duration with a current level so low it appeared to be zero on the scale of 1000 amps/cm. The discharge into water caused a less energetic expulsion from the precombustion chamber and no corona development during the very short formative phase. In addition, the dark opaque layer was absent.

Current flow during the formative phase is generally considered to be quite uniform over the electrode surface in contrast to the locally high current during the arc phase. Most of the formative energy is left in the propellant by virtue of the short, multiple paths of the discharges inside the corona and the inherent internal resistive heating elsewhere. However, the arc is considered to be a short circuit between electrodes that allows large current flow with little resistance. Temperatures in the ionized path are measured in tens of thousands of degrees but radiation or conduction from this region to the liquid is probably not a primary source of energy required for ignition. This is proven by failure to ignite propellant with a strong arc after a short formative phase.

The pressure does appear to rise rapidly in the precombustion chamber at the time of the arc as indicated by the rapid growth of the medium after the arc onset in Figure 17. One viewpoint states that the arc ignites the propellant vaporized during the formative phase. However, rapid expulsion of the medium was also observed during the open cup test involving the nitric acid solution, where there was no combustion. Therefore, another viewpoint proposed for consideration is that the arc may have added the required energy to the medium constituting the corona to cause the observed pressure increase.

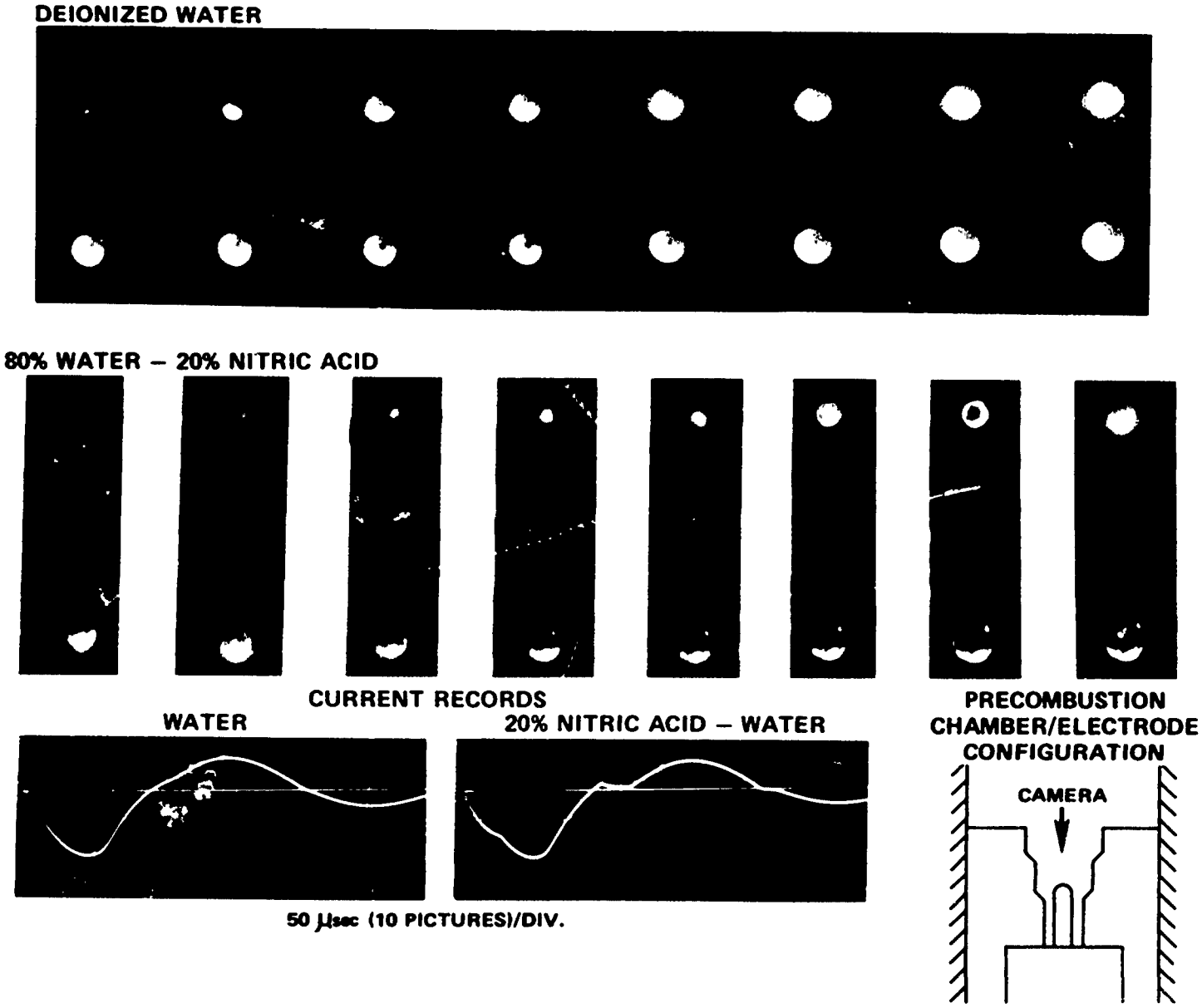

Figure 19 HIGH SPEED PHOTOGRAPHS OF ELECTRICAL DISCHARGES INTO DEIONIZED WATER AND A 20% NITRIC ACID SOLUTION

This viewpoint is supported by the observation that the electrode used during the deicnized water discharge experienced substantially greater and much more localized erosion than the electrode used in the nitric acid discharge, even though peak current during the arc was about the same in both cases. This greater symmetry in electrode wear of the nitric acid and propellant tests makes it appear as if most of the corona were the conductive medium through which the arc current passed. If this is true, then the corona ball would receive additional energy by virtue of this arc current flow in a mode similar to that of formative energy dissipation in the corona stated above. The primary difference between the formative and arc phases would then be the ionized path versus resistance controlled current flow through only the liquid. Energy addition during the arc phase is probably augmented by combustion of a small amount of propellant, most likely that propellant vaporized during the formative phase, adding to the energy available for the ignition process.

3.2.2 Discharge Parameters

Many parameters affect electrical discharge characteristics. Results of tests and observations during this program that pertain to electrode and discharge system design are given in this section.

3.2.2.1 Configuration

The main configurational changes that can have an influence on electrical discharge are center electrode diameter, its tip shape (hemispherical or flat), electrode gap and position. Precombustor geometry is also presumed to affect electrical discharge characteristics but the geometries used during this program were similar enough to make these effects quite small.

Electrode diameter has a significant effect on discharge characteristics. Typical current traces generated during open cup tests with diameters of 0.0625 and 0.090 are shown in Figure 20. The electrode position and gap were the same for both tests. The current level for each at corresponding times of the discharge is observed to be proportional to the electrode diameter,

1000 amps/div
50 μsec/div

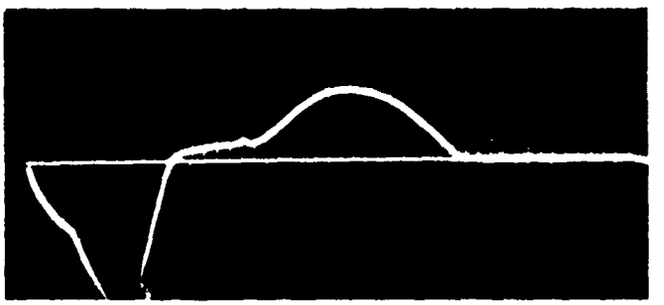

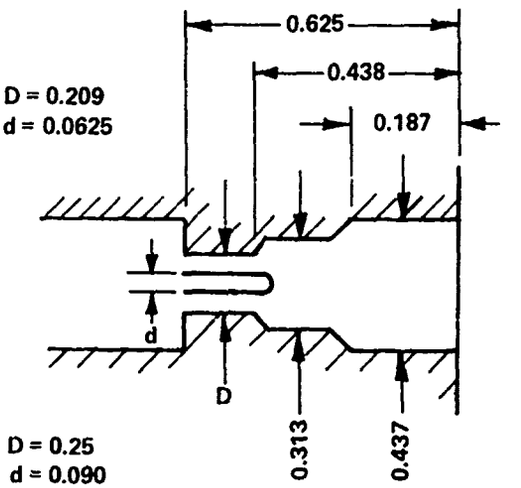

Figure 20 TYPICAL CURRENT WAVE FORMS MEASURED DURING OPEN CUP TESTS WITH 0.0625 AND 0.090-INCH DIAMETER CENTER ELECTRODES

which, except for the tip, is related to the surface area. In addition, the average formative phase duration was found to vary with diameter by about the same factor. As a result, the total formative energy is doubled by increasing the electrode diameter by 44% for the same gap. The tip area is roughly doubled by this increase in diameter causing a diminished field strength which means that the current density is reduced while more propellant must be vaporized to form the corona. This suggests that benefits of the larger electrode might be, improved consistency as a result of reduced field strength (although this has not been proven), and less tip erosion as a result of the lower current density. However, if a given field strength must be maintained for ignition, i.e., current density, the larger electrodes will require more energy.

Electrode gap is obviously an important parameter. During a series of carefully controlled transparent chamber tests (see Section 3.3.3), an increase in ignition chamber diameter from 0.21 to 0.25 inch, a 26% increase in gap, produced an increase in the average formative phase of the discharge from 27 to 37 μsec, or 37%. This increase is verified by the corona growth curve shown in Figure 18. This result can be explained by the fact that a larger gap provides additional space for a uniformly developing corona to occupy. The larger gap dimension also has a tendency to reduce the significance of electrode surface imperfections that might induce an arc prematurely.

The position of the electrode tip with respect to the precombustion chamber, which also infers electrode length, is also an important parameter. The formative phase current is strongly dependent on the exposed electrode length by virtue of surface area (see Table I of Section 3.3.3). As with larger diameter electrodes, however, the increased formative energy is distributed over more propellant. It was also observed that the formative phase duration decreases as the electrode is withdrawn into the inner chamber. This is probably due to a combination of effects. Current paths are increasingly confined to the small, inner segment of the precombustion chamber and the electrode tip is in closer proximity to the abrupt area changes between segments. Both parameters tend to increase the electrical field strength, which

decreases the formative phase duration as it increases the rate of corona growth. On the other hand, if the electrode is extended in the precombustion chamber so that it becomes long and the tip is in the large diameter portion of the precombustion chamber, the electrical field in the tip region may be reduced to the level of that at the cylindrical shank of the electrode in the small-diameter-chamber section. In this case, a slowly growing corona probably would form over the cylindrical section according to the distribution of field strength. Extremely long formative phases have been obtained by this procedure but the formative energy is distributed over a large amount of propellant in such cases, which is potentially unfavorable for ignition.

Electrode tip shape can be flat or spherical. It has been stated that the spherical tip provides better ignition (Ref. 10) but that the flat tip is more consistent (Ref. 11). The flat-tipped configuration is designed to attract an arc to the tip edge in the same manner each time. The sharp edge concentrates the electrical field thereby overshadowing the effects of surface imperfections. The strong localized field probably does not allow creation of as large a volume of corona as does the spherical configuration. However, the results shown in Table I of Section 3.3.3 indicate a higher formative energy for the flat tipped configuration.

3 2.2.2 Surface Preparations

During the course of this research program insight has been gained into the art of preparing an electrode. It was observed early in the program (Ref. 2) that much care is required to remove all random roughness such as machining marks and gouges. These create locally high electrical fields and induce an early arc of a random nature. If the electrode is polished so that the surface is shiny, the initial field will be uniform and predictable but the bubble formation process will be of a random nature. Bubbles of various sizes will develop over the surface because there are no localized "hot spots" as with a rough surface that encourage and position bubble formation (Ref. 4). Bubbles are essentially insulators and an uneven bubble pattern can severely distort the electrical field and initiate an early arc. Therefore, a uniform

roughness, as created by sandblasting, is required to provide order to the bubble formation process. A series of open cup discharges with sandblasted electrodes, described in Reference 5, showed remarkable discharge consistency.

All electrodes have a surface film of some type. A carefully polished electrode will begin to develop an oxide coating when the polishing is stopped. Factors such as humidity govern the rate of growth and thickness of this film. When the electrode is placed in propellant, a different film may be formed. Impurities that might come in contact with the surface can cause the properties of this film to vary. The point is that the film is an insulator with an exceedingly intense field across it when voltage is applied. Variations in the film can cause similar variations in the electrical field. This kind of variation could be reduced by taking special care to form the proper kind of surface film when the electrode is made. Late in the program, the practice of soaking the sandblasted electrode in propellant for about 1/2 hour was initiated and this seemed to improve discharge characteristics.

It has been observed during open cup tests that the formative phase of the first test of a series is usually not as long as that of subsequent tests, provided the surface was not severely eroded during the first test. Part of the reason may be due to minor surface imperfections that were removed during the discharge, but it is felt that formation of a uniform surface film during the arc process may also have contributed to the observed improvement.

3.2.2.3 Circuitry

A direct discharge across a gap in a circuit with line resistance and capacitance only, is extremely brief and current can be high. This creates a situation where corona growth is rapid but formative phase duration is quite sensitive to electrode imperfections. If inductance is added to the circuit, the current levels are reduced, the discharge is prolonged and it is not as readily influenced by minor surface characteristics. Examples of discharges for two values of inductance with all other parameters unchanged are shown in Figure 21.

148 μ h INDUCTANCE
(RUN 32, REF. 3)

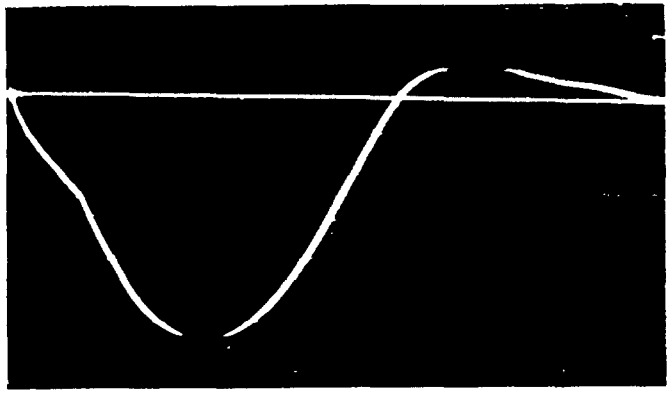

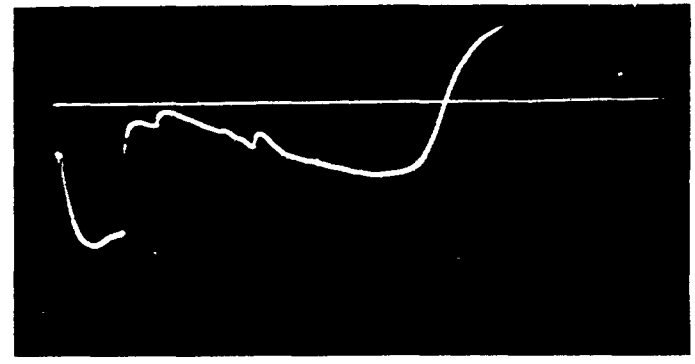

210 amps/div
CURRENT:
420 amps/div

500 volts/div
VOLTAGE:
800 volts/div

72 μ h INDUCTANCE
(RUN 34, REF. 3)

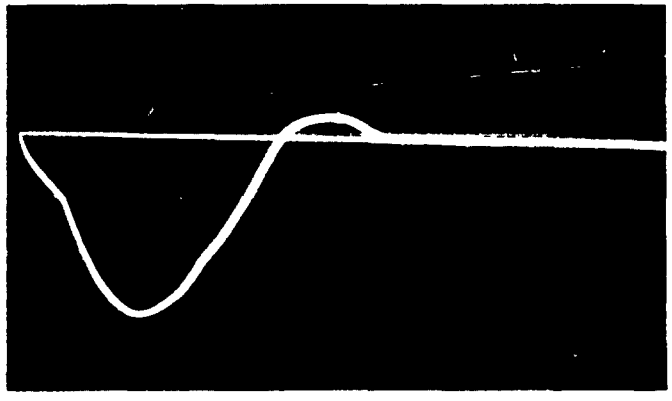

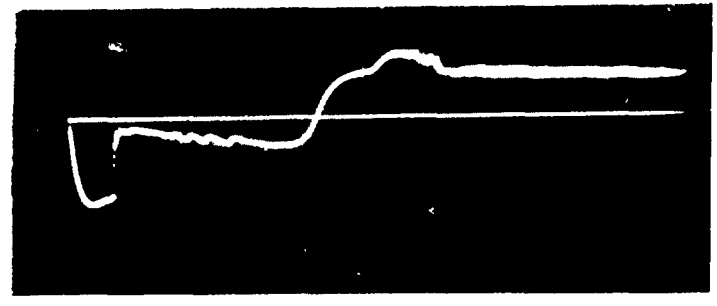

TIME: 50 μ sec/div

Figure 21 VOLTAGE AND CURRENT TRACES FROM TESTS USING 60 μ f CAPACITANCE AND 2000 VOLTS POTENTIAL WITH DIFFERENT INDUCTANCE

3.2.2.4 Polarity

The majority of firing and open cup tests were conducted with the center electrode as the cathode. A brief series of open cup tests was conducted with the center electrode as the anode (Ref. 2). Severe erosion of the electrode occurred during these tests; much more than was experienced when the center electrode was the cathode.

3.3 IGNITION AND COMBUSTION PHENOMENOLOGY

3.3.1 Aspects of Electrical Ignition

The most favorable type of electrical LPG ignition, as experienced during this research program and others, is initiated by an electrical discharge characterized as having a suitably long formative phase followed by a strong arc when the formative current is high. Good ignition was always obtained at Calspan with a formative phase duration of 30-40 μsec and a peak current level in excess of 600 amps. On the other hand, the gun consistently failed to ignite if the formative phase was less than 15 μsec or excessively long, say in excess of 60 μsec. As mentioned previously, the corona is very small for a short formative phase which means that only a small amount of propellant was vaporized prior to the arc. This appears to be an important criterion for ignition.

The opposite extreme of a long formative phase followed by a weak arc or no arc at all may or may not produce a misfire. Several successful firings were conducted at PSI (Ref. 12) where there was no arc at all; but, during the Calspan program, misfires resulted. The long formative phase is characterized by a rise in current followed by a decrease to a very low level. It is stated in Ref. 13 that the luminous corona exists only during the high current period and that this medium or matter in the region occupied by the corona, becomes dark when the current decreases. According to the reference, the dark medium is not likely to ignite or result in formation of an energetic arc and, therefore, sufficient energy must be deposited in the propellant during the period of high current flow to actually bring the required amount of propellant to ignition conditions. Evidently, the Calspan tests with long formative phases (Ref. 2) (>50 μsec with 75 joules formative

energy) did not contain sufficient formative energy to achieve ignition without an arc and misfires resulted.

This impact of the formative energy on gun performance is clearly illustrated in Figure 22. Here, a sampling of test results is presented with the only evident variable being the formative phase of the electrical discharge. The first example, identified as Run 53, is one in which the formative phase was short, approximately 10 μsec, and therefore, the energy imparted to the propellant during this phase was low, of the order of 5 joules. This pulse was not sufficient to sustain ignition and the test was a misfire.

Test Number 54 is characterized by a formative phase somewhat longer, about 20 μsec, with an associated energy of 15 joules. The results of this test belong to a class of tests experiencing combustion delay, but in addition, exhibit an incomplete combustion phenomenon. Much unburned propellant is usually expelled during this type of test. One viewpoint pertaining to this low pressure phenomenon states that the combustion of NOS365 propellant occurs in pressure-bounded stages so that complete combustion does not occur until pressure reaches a level in excess of 3000 psi (Ref. 14). Accordingly, it is hypothesized that this low pressure test is a result of failure to achieve the proper combination of pressure and thermal conditions required for the chemical reactions to proceed to completion. Another viewpoint, Ref. 15, states that once the propellant is ignited, combustion goes to completion but that physical mechanisms control the relationship between burn rate, burning surface, and projectile motion to produce low pressure.

Run 52 has discharge characteristics quite similar to those of Run 54. The initial portions of the two pressure curves are practically identical. However, at some point, the proper conditions were reached and a high pressure was obtained. The differences between Runs 52 and 54 are extremely subtle which infers unpredictability and the borderline nature of the combustion delay type of result.

RUN	FORMATIVE PHASE DURATION-μSEC	CURRENT AT END OF FORMATIVE PHASE-AMPS	AVERAGE VOLTAGE DURING FORMATIVE PHASE-VOLTS	OHMIC HEATING ENERGY-JOULES
(53)	10	365	1750	4.8
(52)	18	548	1925	12.6
(54)	22	694	1650	15.9
(55)	32	804	1575	24.8

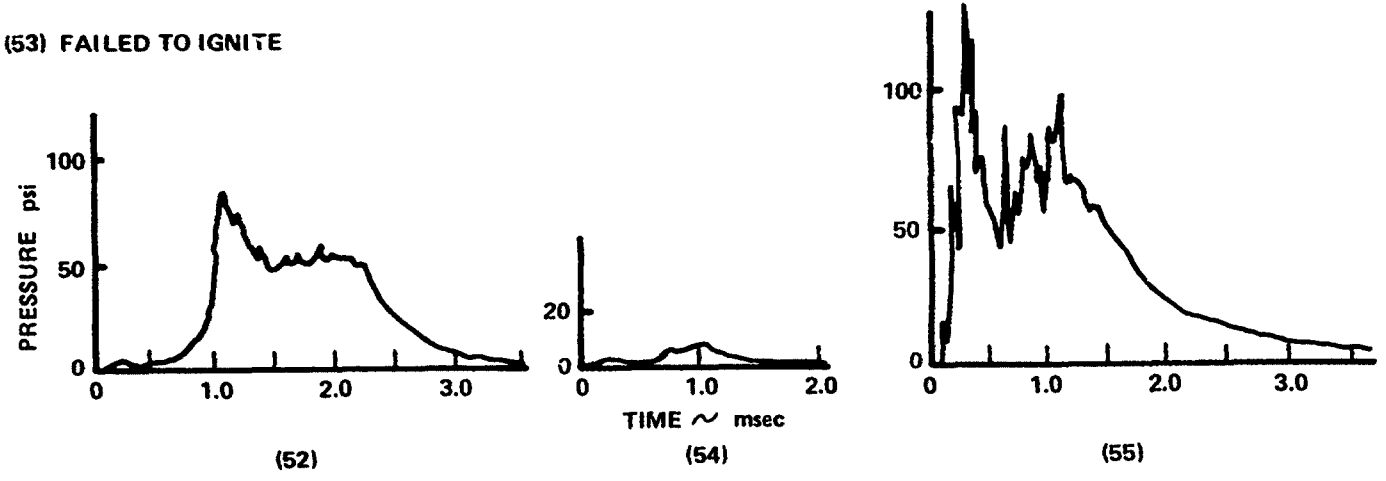

Figure 22 CORRELATION OF PRESSURE OUTPUT WITH ELECTRICAL DISCHARGE CHARACTERISTICS

Finally, Run 55 was initiated by a discharge formative phase duration of 32 μsec with an energy of 25 joules. This result is characterized by virtually no delay with the pressure level reaching a high peak value in about 300 μsec.

These results are representative of the experience gained during the Calspan research program and serve to verify the significance of the formative phase. The following sections will present photographic evidence that will help describe the sequence of events during the ignition process after an electrical discharge.

3.3.2 Breech Region Ignition Phenomena

3.3.2.1 Overview

A series of high-speed motion pictures were taken through sapphire windows at the breech end of the chamber. The windows were positioned to observe the characteristics of the effluent from the precombustion chamber as shown in Figures 2 and 13. The pictures and data presented here illustrate the many different mechanisms present during the ignition process and early stages of combustion. The nominal camera speed for the pictures to be presented in this section was 18,000 pps, representing an elapsed time of 55 μsec between pictures. The tests discussed here were conducted with the precombustion chamber/electrode assembly shown in Figure 4. In addition, each of these tests were fired with a discharge circuit capacitance of 120 μf and an inductance of 28 μh. The tests to be discussed in this section are Runs 52 to 56. The voltage for these tests was 2500 volts for Runs 52 to 54, 2400 volts for Run 55 and 2200 volts for Run 56. The test fixture used the short, 9-inch long barrel for each of the tests discussed in this section. The average propellant and projectile weights for these tests discussed in Section 3.3.2 were 208 gms. and 158 gms., respectively.

3.3.2.2 High Pressure Combustion After Delay

A general class of test results cited in the previous section is characterized by high pressure combustion after chemical incubation. This result has been observed to follow an electrical discharge characterized by a formative phase less than 25 μsec in duration.

A sequence of pictures taken during two tests experiencing this delay are shown in Figures 23 and 24. A brilliant white cloud can be seen emerging from the precombustion chamber in both figures. The brilliant hue gives way to orange and black regions, the orange being indicative of flame and the black regions probably signifying the presence of opaque products of decomposition. During Run 52 (Figure 23), the sequence of pictures from 10 to 14 are mottled in appearance and give the impression of turbulent mixing on a macroscopic level. The bright orange continuum of picture 18 signifies the event of high pressure combustion. The events of Run 56 (Figure 24) are obscured by an opaque sheath after the disappearance of the brilliant cloud until the occurrence of high pressure combustion signified by the sudden appearance of the single picture consisting of a bright orange continuum. It should be noted that the window port diameter was 7/16 inch for Run 52 and 0.6 inch for Run 56.

Thus, two mechanisms leading to high pressure combustion have been observed to exist during the delay period, one a macroscopic mixing process in the presence of visible combustion, followed by a relatively gradual rise in pressure, and the other an incubation process completely obscured by what is presumed to be opaque products of decomposition that is terminated by sudden explosion-like combustion. Others (Ref. 14 and 16) have observed pressure dependent combustion modes for NOS365 propellant and it is suspected that this pressure dependence may play an important role during this delay period.

In the previous discussion on the events concerning ignition, it was presumed that a small amount of propellant is vaporized in the vicinity of the center electrode tip. Combustion of this vaporized propellant is

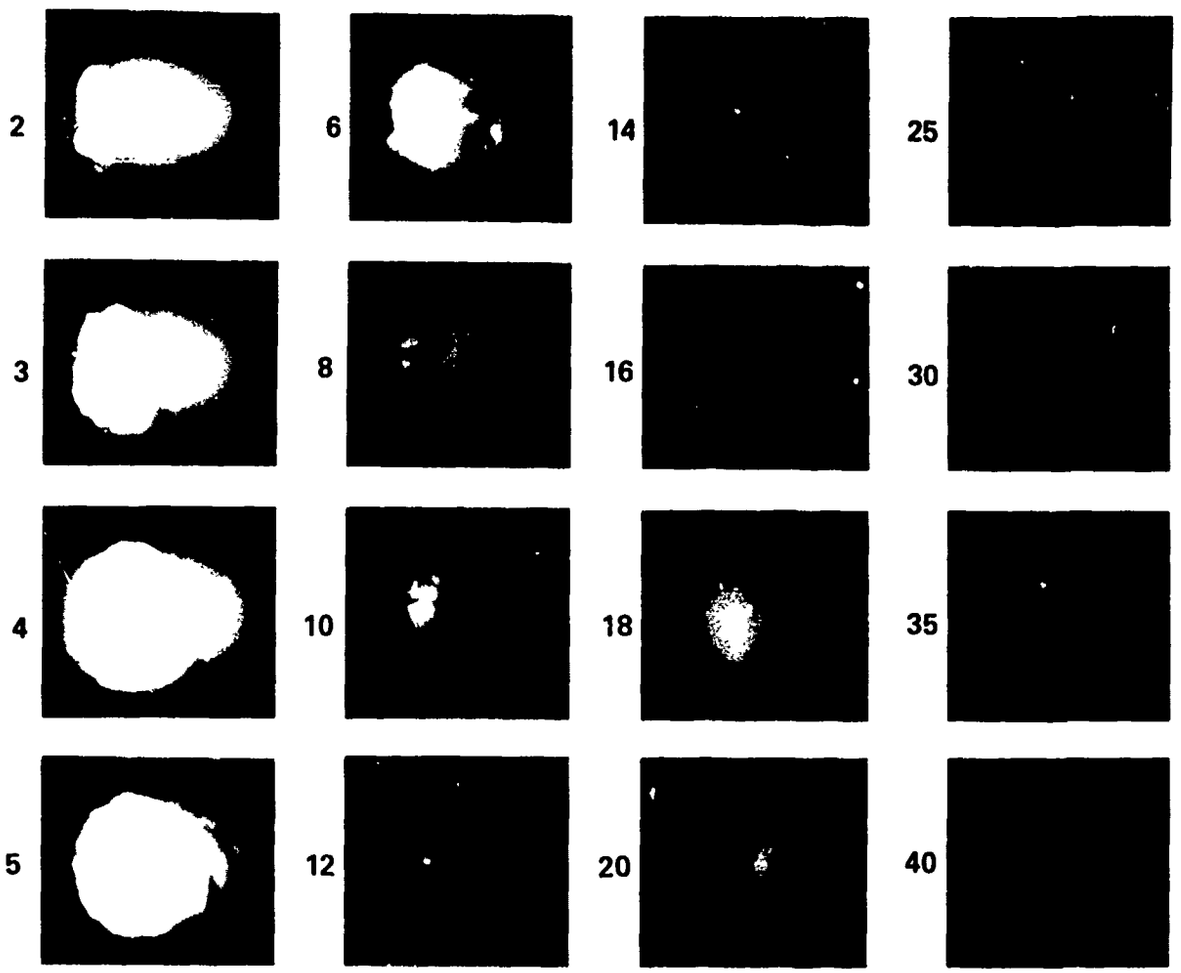

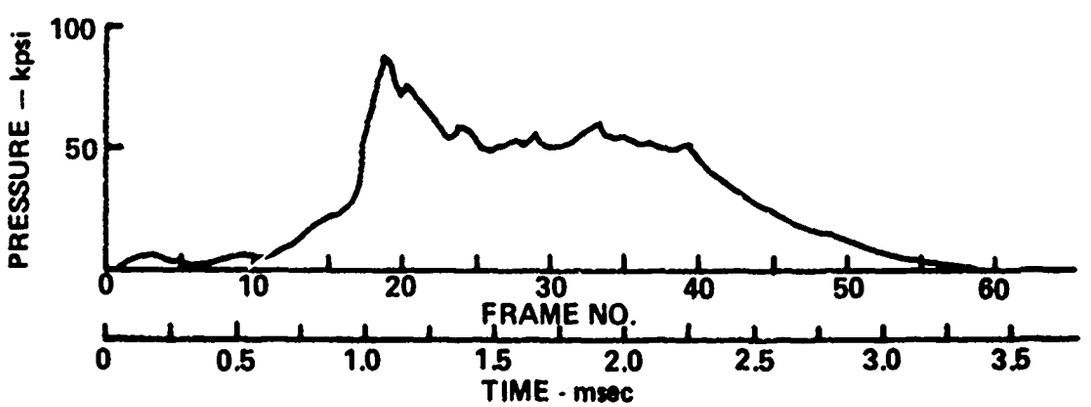

Figure 23 SELECTED MOTION PICTURE FRAMES FROM RUN 52

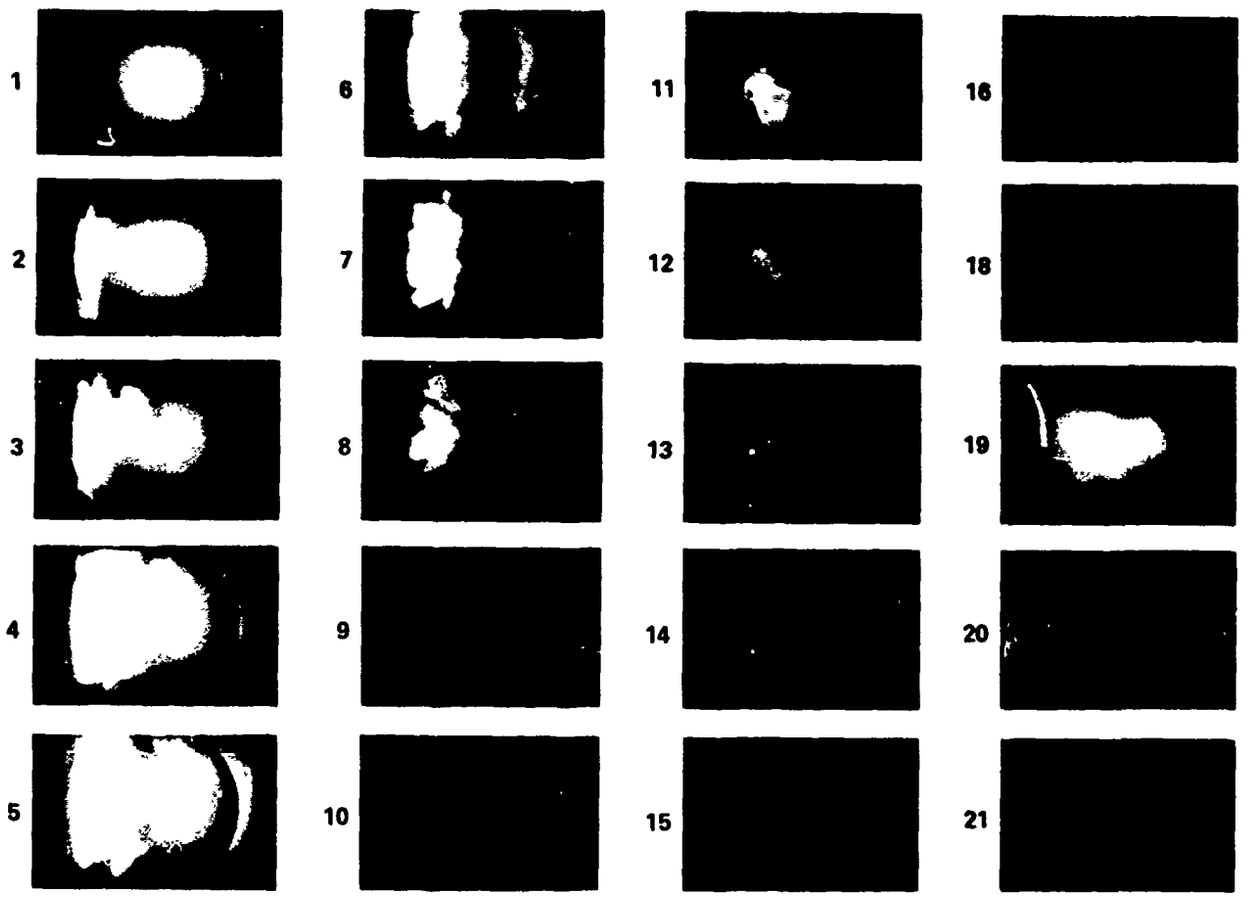

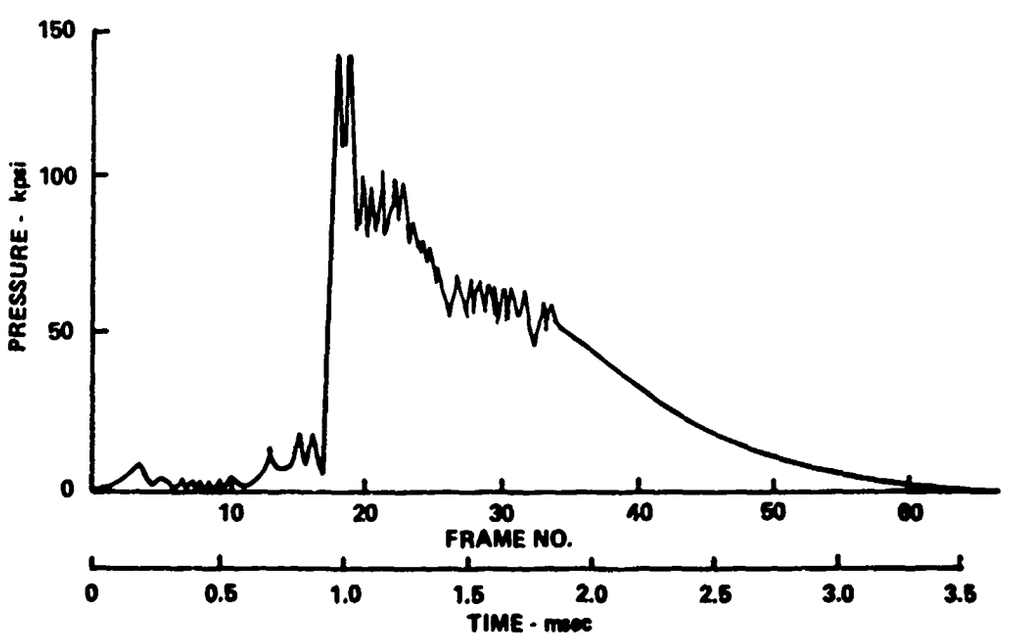

Figure 24 FRAMES FROM MOTION PICTURES TAKEN DURING RUN 56

believed to occur at the transition to the arc phase. The cloud that emerges from the discharge region is postulated to be an arc light scattering medium that consists of the combusted propellant gas and propellant droplets. The initial pressure of this medium is believed to be very high, of the order of 20-30,000 psi, and is strongly dependent on discharge characteristics. This sudden pressure rise creates a strong compression wave or waves that travel through the precombustion chamber and into the main chamber. This causes the liquid to flow in the same direction and the luminous medium expands as it occupies the volume behind it. Therefore, the boundary of the luminous cloud, by this description, represents the interface between the cool liquid propellant and the medium created during the discharge. The velocity of this medium as it leaves the precombustion chamber is approximately 200 ft/sec, as determined from the photographs. From the water-hammer equation, a liquid acceleration to a velocity of this magnitude would be created by a sudden pressure rise of the order of 20,000 psi. This result appears to be of the expected order of magnitude for pressure experienced in the precombustion chamber.

According to Ref. 15, vigorous mixing of this medium with the body of cool liquid propellant is initiated by the formation of vortices at geometrical area discontinuities, particularly at the precombustion chamber exit. This mixing is presumed to be the mechanism by which the energy of the white medium is transferred to the propellant, leading to ignition. The amount of propellant involved in the mixing process is governed to some degree by the contact surface area, which is related to the medium size. The size of the white medium was measured and found to be approximately equal to the sum of the initial ullage and the volume created by propellant compression. The incubation time, or the time required for ignition to occur after the onset of mixing, is a function of the energy density of the medium. Thus, for a given amount of initial energy deposited in the medium, the energy density of the medium will decrease, and more propellant will be involved in the mixing with increased expansion of the medium. The first factor tends to increase ignition delay while the second increases the amount of propellant that is gradually approaching ignition conditions. Therefore, increased medium size resulting from initial ullage or from early projectile motion would seem to have a strong

influence on ignition, early combustion characteristics, and variability in them. Of course, variation in electrical discharge affects the pressure in the precombustion chamber which also affects the ultimate size of the medium after it expands, creating additional variation in the mixing process.

The sequence of pictures in Figure 24 provides an especially vivid account of the ignition events. This sequence shows a distinct tuft protruding from the front of the luminous medium. This tuft is roughly the same diameter as the ignition chamber, the innermost segment of the precombustion chamber. The exit diameter of the precombustion chamber is the full width of the white cloud at the left side of picture number 5 of this figure. The presence of the tuft gives evidence that the arc originated in the innermost chamber. The pressure was apparently maximum there and waves generated in this region lost velocity and strength as they expanded to the outer segments. The tufted cloud appears to reflect this expansion in the precombustion chamber. Pictures taken during a subsequent test where the electrode extended from the inner chamber did not show this tuft. Beginning with Picture 5, both fronts appear to reverse direction as the cloud takes on a mushroom-shape. The initial pressure wave traveling at 5000 ft/sec would reflect at the projectile base and return to the breech between the 5th and 6th pictures and may be instrumental in causing the peculiar shape. The following incubation period, characterized by complex chemistry and mixing as described in the previous paragraph, culminates in an extremely sudden ignition and pressure rise at Picture 19. The sapphire window experienced failure at this point but it is interesting that the next picture is black. On several occasions, heat sensors located at the breech have indicated the presence of flames from the beginning of pressure rise to the time of peak pressure as shown in Figure 25. The instant the pressure began to decrease, the sensor indicated zero heating. It is surmised that this sudden loss of heating and the black picture after peak pressure result from hydrodynamic shifting of the liquid. This will be discussed in Section 3.4.

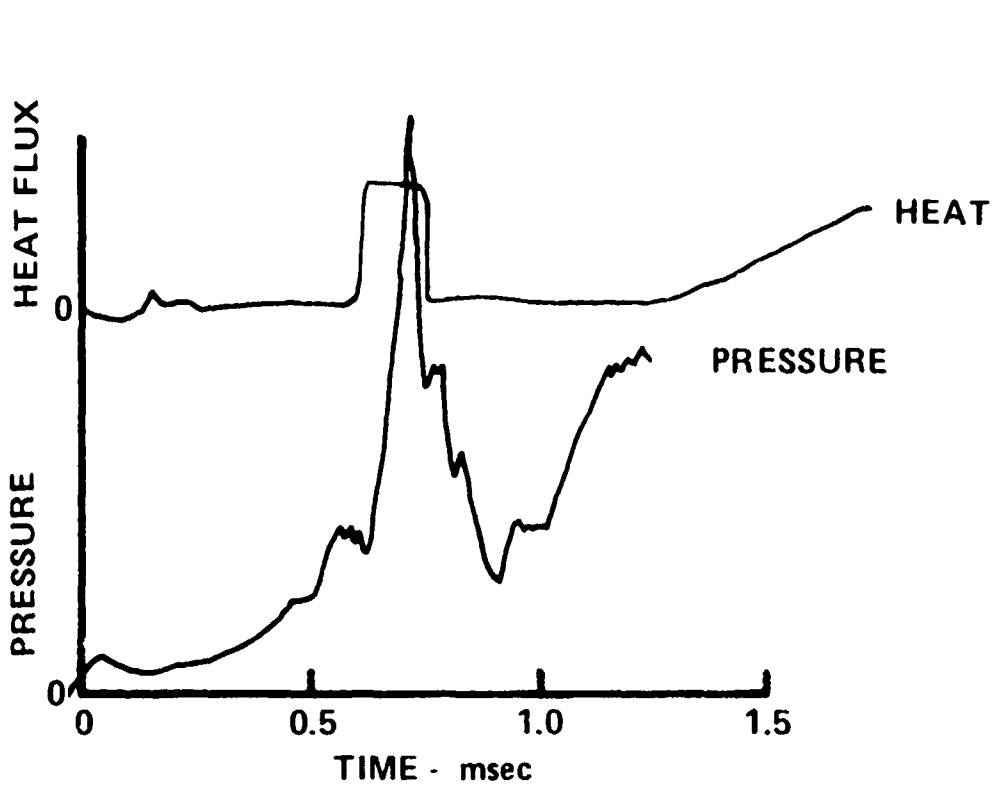

Figure 25 WALL HEATING DURING INITIAL PRESSURE SPIKE

3.3.2.3 Low Pressure Combustion

Low pressure combustion is defined to mean a firing result where the projectile passed from the gun but the peak pressure was less than 10,000 psi. This phenomenon was observed during several Calspan tests as reported in Reference 5. Much unburned propellant passed from the barrel during some, but not all of these tests. Pictures and the pressure time record from one of these tests, Run 54, are shown in Figure 26. The window port diameter for this test was 0.5 inch.

It is noted that the initial portion of this low pressure run is quite similar to that of Run 52, Figure 23. In fact, the formative phase and ignition energy for Run 54 were higher than for Run 52 (Figure 22). The mottled orange appearance of turbulent combustion and mixing is readily apparent during all of Run 54. Some event or stimulus must have been absent to prevent the occurrence of high pressure combustion during this run. The identity of this stimulus is not known but its reasonable candidates include pressure dependent combustion chemistry, projectile motion, and hydrodynamic interaction.

3.3.2.4 High Pressure Combustion Without Delay

Tests with no ignition delay are significantly different in that mixing during a distinct induction period does not occur. Run 55 is an excellent example of this. Pertinent ignition data are given in Figure 22 and high rate pictures of the ignition sequence are shown in Figure 27. The window diameter for this test was 0.5 inch. These pictures indicate that ignition occurred inside the precombustion chamber and that the bright medium was either not present at all or only for a short period between pictures. The first picture in this series shows the first light from the arc before any front has reached the window position. The second picture in this figure, 55 μsec later, gives the impression of the continuum radiation characteristic of high pressure combustion, but partially obscured by a dark opaque sheath. Evidently, the flame front is well established at this time and has passed the window port. The peak pressure condition is reached by the third picture

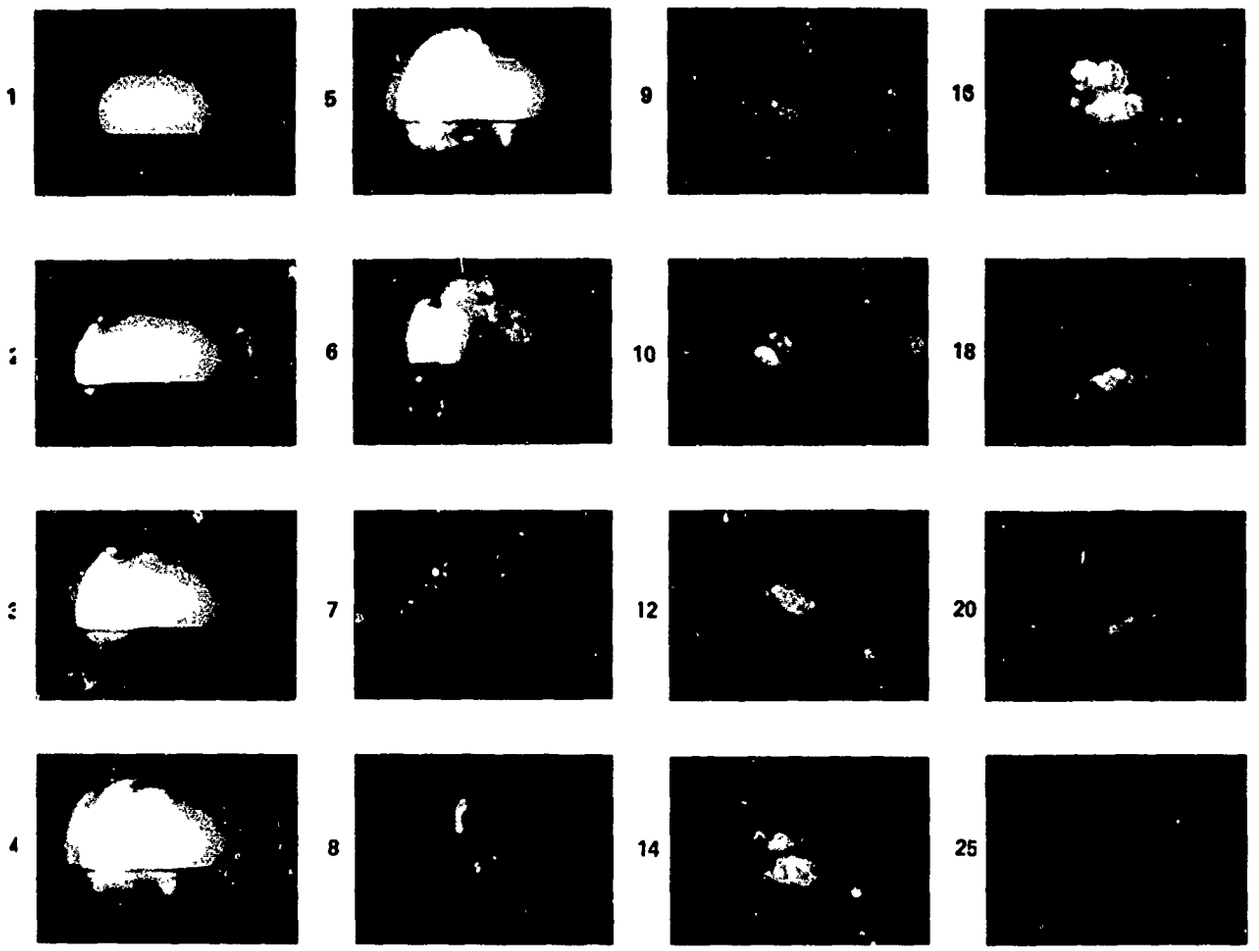

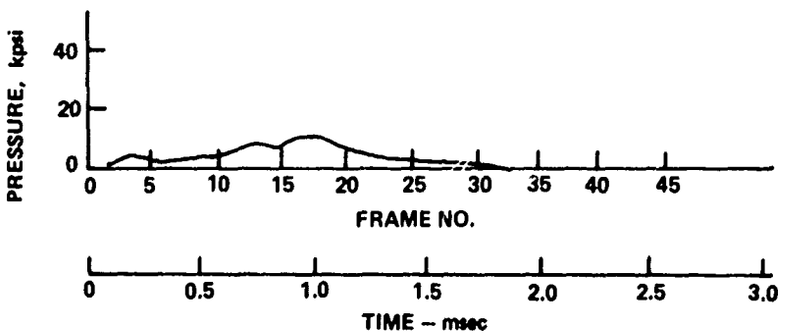

Figure 26 SELECTED MOTION PICTURE FRAMES FROM RUN 54

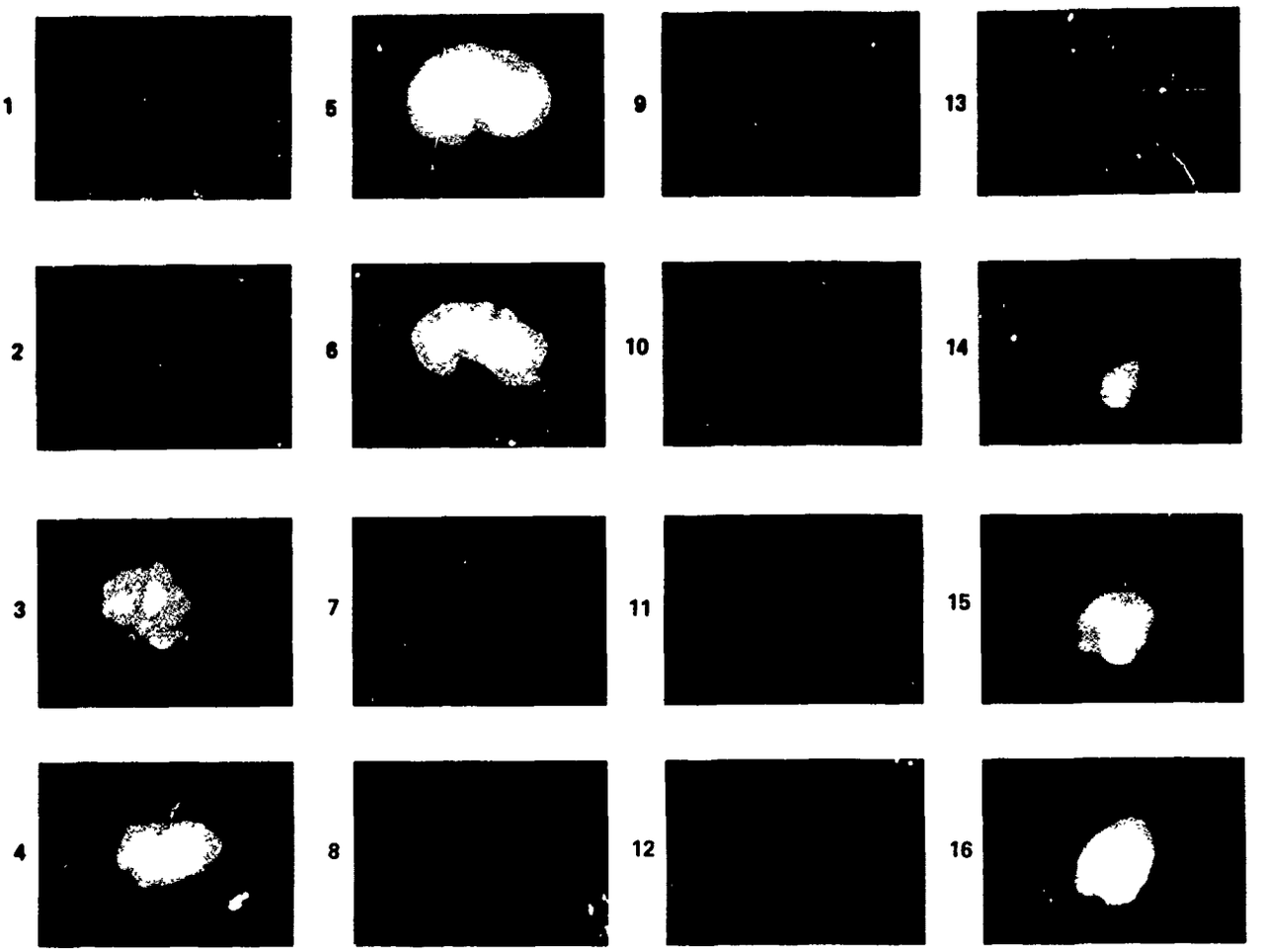

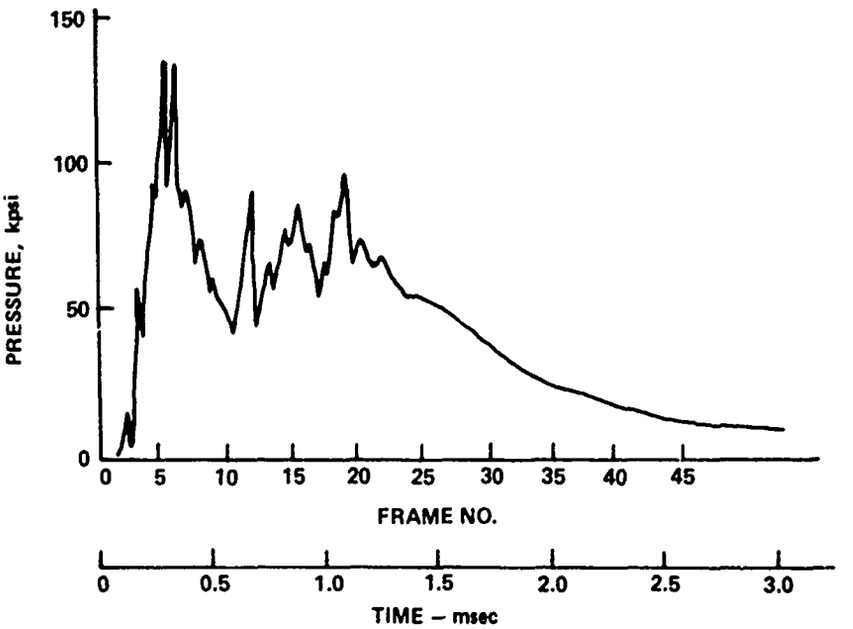

Figure 27 SELECTED MOTION PICTURE FRAMES FROM RUN 55

as indicated by the bright orange continuum. The formative phase for this test was 32 μsec (Figure 22), somewhat longer than that of tests experiencing high-pressure combustion after delay ($< 25\,\mu$sec). Thus, it is apparent that variation in formative phase, the primary variable in tests discussed in Section 3.3.2, creates drastic differences in the sequence of ignition events.

3.3.2.5 Discharge Into Dilute Nitric Acid

A control test was performed using dilute nitric acid instead of propellant in order to observe ignition mechanisms in the absence of combustion. This test was performed in the firing fixture with the same technique and procedures used in an actual firing test. The pictures from this test (0.5 inch window port diameter), shown in Figure 28, indicate a sequence of events similar to those observed during tests experiencing ignition delay. This is especially true with regard to Run 56, Figure 24. By comparison of the two, it can be surmised that little or no combustion occurred during Run 56 other than some decomposition yielding opaque products, until the occurrence of the bright orange continuum. The formative phase during the nitric acid test was similar to that of those tests with no combustion delay, about 25 μsec with a formative energy of 24 joules. A rough estimate was made of the gas phase internal energy of the white medium shown emerging from the precombustion chamber in Figure 28. The energy content of a given volume of gas is $E \approx \rho V c_v \Delta T$. When combined with the perfect gas equation of state, $E \approx PVc_v/R$. This assumes that ΔT and the gas temperature are approximately equal. The precombustion chamber pressure is assumed to be 20,000 psi on the basis of the exit velocity of the white medium, the precombustion chamber volume, V, is 0.8 cm^3, and c_v and R are assumed to be 0.2 Btu/lbm°R and 60 ft-lbf/lbm°R, respectively. The energy computed from these inputs is nearly 300 joules, far in excess of the formative energy. This estimate is supported by little experimental data and may be as much as 2-300% high, but this does not alter the conclusions based on it. Therefore, it appears that the formative energy by itself is not sufficient to cause the appearance of the white medium and that energy from some other source is required. Such a source may be arc energy addition to the gaseous medium generated during the formative

phase (see Section 3.2.1). Measurements of current and voltage drop across the electrode indicate that an upper limit of energy addition by this mode is about 100 joules. Fishman (Ref. 17) has also suggested that oxidation of metal removed from the center electrode during the arc phase may provide this additional energy.

The white cloud observed during firing tests with NOS365 seems to grow more rapidly and attains a larger volume than that of the nitric acid test (see Figures 24 and 28). This is another indication that propellant combustion does occur within the precombustion chamber and provides a source of energy. This source probably plays a significant role during tests characterized by high pressure combustion without delay.

3.3.3 Transparent Precombustion Chamber Tests

3.3.3.1 Test Setup

A special apparatus was set up for use in the investigation of the electrical ignition of NOS365 liquid monopropellant with a variety of precombustion chamber/electrode geometries. The gun chamber was simulated by a transparent polycarbonate tube, 1.24 inches inside diameter and 8 inches long, which provided the confinement of the gun chamber. Each precombustion chamber was machined into a slug of transparent acrylic that was shaped to fit tightly into one end of the polycarbonate tube. The acrylic slug in turn mated with a steel cylinder that housed the spark chamber, forming the outer electrode that enclosed it. The whole arrangement was clamped in an upright position with the open end of the polycarbonate tube up as shown by Figure 29. An insulated center electrode, made from stainless steel wire as used in the gun fixture, was mounted to extend along the central axis of the apparatus into the spark chamber and was connected at its other end by a cable to the high voltage supply of the liquid propellant gun fixture.

All joints were sealed by vacuum grease so that the vessel that was thereby formed could contain liquids. The precombustion chamber was filled with liquid gun propellant for each test and a polyethylene film was "cemented" over its end face by vacuum grease. Then the vessel was filled

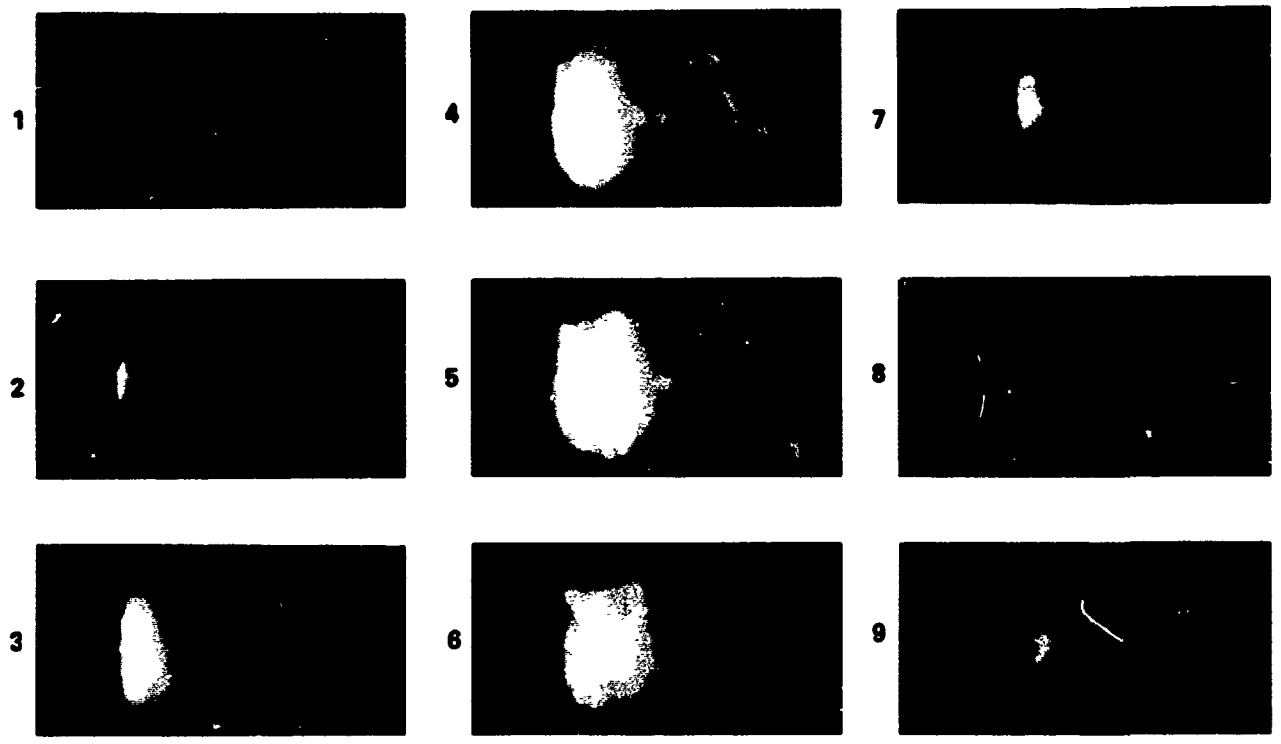

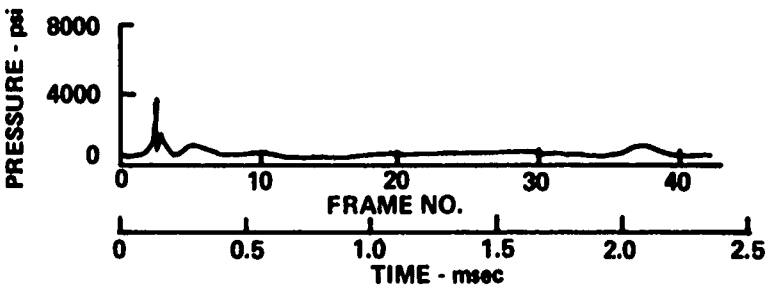

Figure 28 FRAMES FROM MOTION PICTURES TAKEN DURING A TEST USING A MIXTURE OF 20% NITRIC ACID AND WATER

with water to duplicate the hydraulic properties of a chamber completely filled with liquids up to the time a wave could travel the entire length of the chamber and back, about 200 μsec.

Three flat mirrors were mounted near the apparatus, as shown in Figure 29. One was placed directly overhead from the open end of the polycarbonate tube to direct axial rays from the precombustion chamber to the camera. Another was placed about 2 inches nearer the camera so that half the view from the first was blocked and it directed rays coming from a lower mirror that was oriented to obtain an image from the side of the precombustion chamber. In this way each camera frame was split to obtain both end and side views into the precombustion chamber.

The Cordin camera was used with color film at a framing rate of 200,000 pps. Voltage and current from the power supply were recorded by oscilloscopes.

The geometries of the precombustion chamber that were tested are shown by Figure 30. Configuration A is the basic shape (PSI configuration) and was used during four tests, each of which used a variation in center electrode design. Throat diameter of the spark chamber was 0.210 inch. Configuration B is the long cone (approximately 15 degree semi-vortex angle) with a single intermediate step from the 0.210 or 0.250 inch diameter throat as indicated in Table I to 0.313 inch diameter bore. Configuration C was a steep, 45° cone, without bore step. Configuration D was similar to Configuration C except that it incorporated a .187 long, .313 diameter bore step in the acrylic body. A spherical tipped, 1/16 inch diameter center electrode, ending at the metal acrylic interface (0.217 inch long) was used during these tests, unless otherwise specified in Table I.

In all cases the transition between bore steps was shaped by drill point (conical, with approximately 120° included angle). Power source voltage was 2400 for all tests. Pertinent details of the tests are presented in Table I.

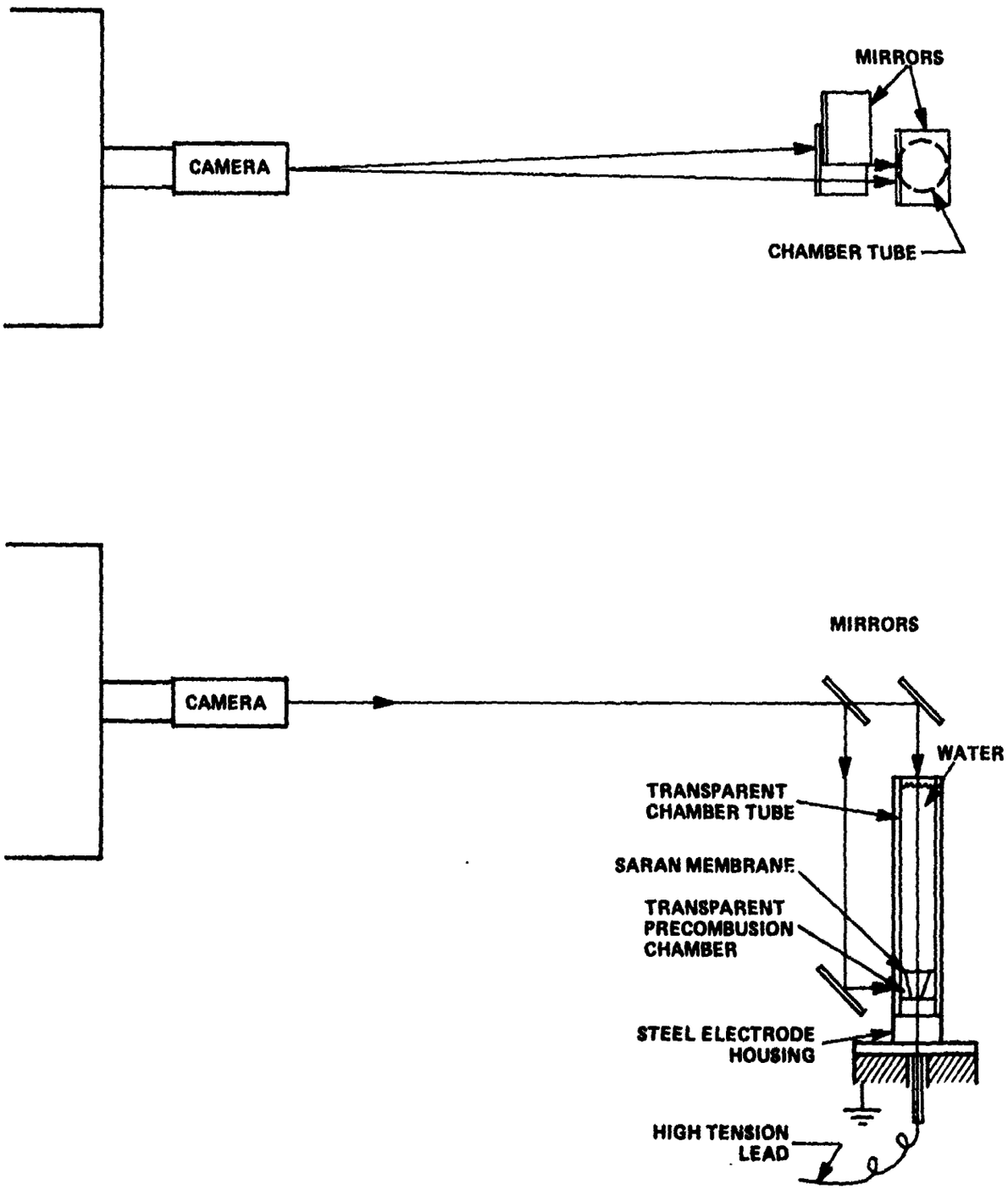

Figure 29 TRANSPARENT CHAMBER APPARATUS FOR FILMING IGNITION TEST

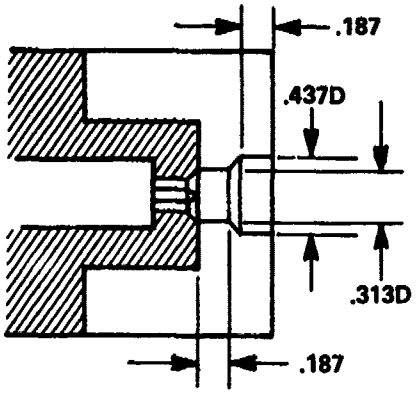

CONFIG. A

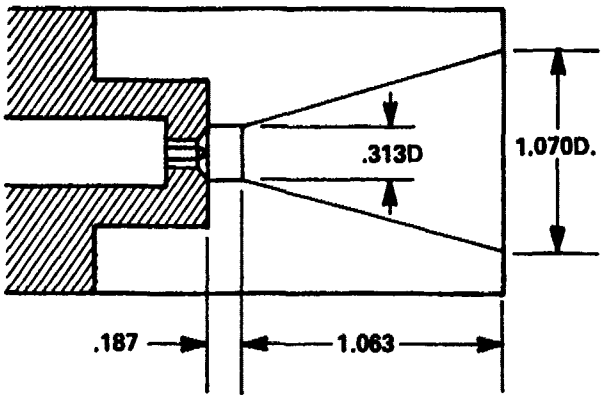

CONFIG. B

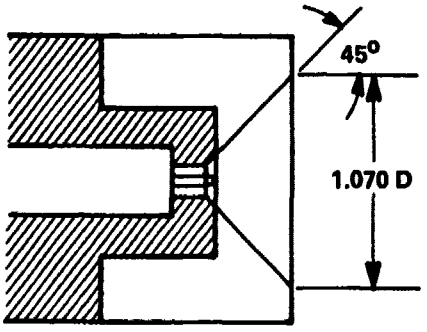

CONFIG. C

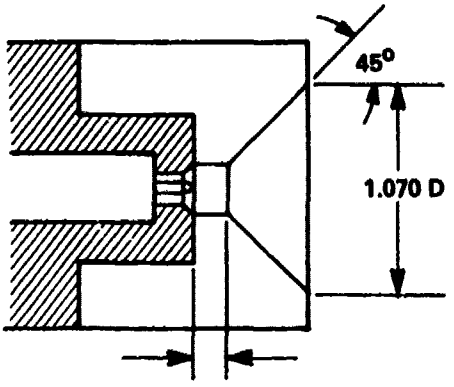

CONFIG. D

Figure 30 TRANSPARENT PRECOMBUSTION CHAMBER CONFIGURATIONS

TABLE I

DETAILS OF IGNITION TESTS

Test No.	Precombustion Chamber	Outer Electrode 1			Center Electrode 2			Formative Phase	
		Shape	Diameter -Inch	Length -Inch	Tip Shape	Length	Surface Condition	Duration μSec	Energy Joules
1	A	Annular	.210	.187	Spherical	.217	Sandblasted	27	16.2
2	A	"	↓	↓	↓	.187	"	20	9.2
3	A	"	↓	↓	↓	.145	"	20	9.2
4	A	"	↓	↓	↓	.217	Polished	25	---
5	A	"	↓	↓	Flat	↓	Sandblasted	30	18.9
6	C	"	↓	↓	Spherical	↓	"	27	14.9
7	D	"	↓	↓	↓	↓	"	25	12.5
8	B	"	↓	↓	↓	↓	"	17	9.0
9	B	"	.250	↓	↓	↓	"	37	14.4

NOTES: 1. Outer electrode surface was sandblasted for all tests

2. Center electrode was .063 inch diameter in all cases

3.3.3.2 Ignition Test Results

The film strip for test number 1, shown in Figure 31, exhibited 38 significant images set in a dark background and included a side and an end view. At the film speed of 200,000 pps, the time interval between them was 5 μsecs so the period spanned by them was 185 μsecs. The beginning events are revealed on the film by 8 end view images that appear as a dot of light that waxes and wanes, becoming very bright in its 2nd image and starting to dim by the fifth. The next 3 images (dots) can be barely discerned. The ninth image is faint but its highlights form the well defined shape of the annular electrode system. These highlights become brighter and at the 12th image the side view appears.

The 14th image shows the first signs of what appears to be a billowy cloud forming over the tip of the center electrode. The billowing is suggested by the extreme contrast shown by the boundaries of the cells that are pictured, compared to their bright centers. This is evident in the side view as well but for only several images as the glowing zone expands and moves along the precombustion chamber. The contrast is greater in the end view and the cell boundaries or creases are prominent almost to the end. Obviously, the glowing region contains heated vapor and the dark creases across the glowing image may well be caused by combustion products that exhibit rapid gradients in opacity where their depth changes. About 2/3 of the water was expelled during the test. The current level rose to 550 amps at the end of the formative phase (27 μsecs).

The film of test number 2 shows a similar sequence of events and images were spread over approximately the same period as test number 1. However, the billowy effect was limited in that a single dark streak appeared that seemed to lie across the tip of the center electrode and the electrode gap became dark after the arc subsided. This darkened annular region suggested the billowy effect by its irregularity in width that was manifested by cusp-like changes. Current reached about 430 amps at the end of the formative phase.

CURRENT RECORD

50 μsec (10 PICTURES) / DIV.

TEST CONFIGURATION

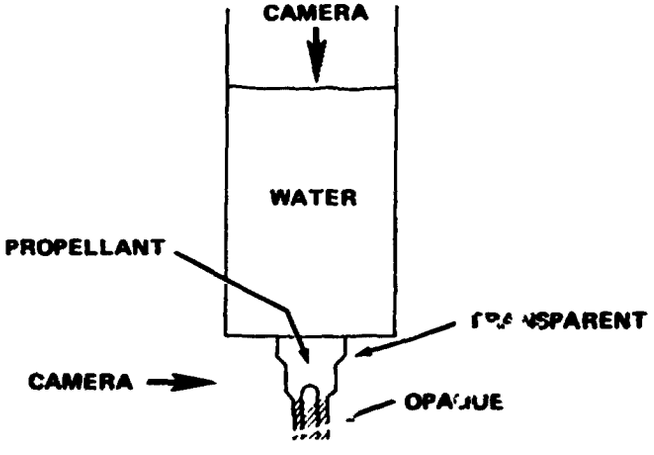

Figure 31 HIGH SPEED PHOTOGRAPHS OF IGNITION PHENOMENA IN A 3-STEP TRANSPARENT PRECOMBUSTION CHAMBER

Films from the third test were not as revealing as the previous films, and the flowing regions appeared to have a nearly uniform intensity. It was interesting also that the membrane was highlighted strongly and the changes in its profile could be seen vividly. It developed an extreme bulge that was still growing in the last image that was displayed. Current reached about 400 amps at the end of the formative phase.

The initial image on the film of test number 4 showed a reflection in the side view that was brighter than the dot in the end view. It exhibited slightly more billowing than test number 2 but less than test 1, with some of the cloud reaching the wall of the outermost step (.437 inch diameter bore). A portion of the membrane could be seen.

The formative phase for test number 5, which used the flat-tipped electrode, was longer than for the previous tests, and the current reached 600 amps at the end of the phase, the highest recorded for any of the tests. Total energy of the formative phase was a maximum also, with a value of 18.9 joules indicated. The film images showed effects very similar to those observed for test number 1 with the formation of a vapor cloud that exhibited strongly contrasted billows.

A total of 48 images could be detected on the film of test number 6. The chief feature of these was the glowing vapor cloud that grew out of the spark chamber. It was bright white and its billows appeared late in the test. Even then they were only faintly defined, in direct contrast to test number 1 for which they formed only a few intervals after the arc receded and were strongly creased. The vapor cloud did not reach a point beyond 2/3 the distance along the conical portion of the precombustion chamber and once there, it remained for many images as its glow faded.

The pictures from test number 7, shown in Figure 32, were much like those of test number 6 except that the vapor cloud actually came into contact with the membrane during the time it was still visible on the film, and before it had faded much in intensity. Again, it did not exhibit the

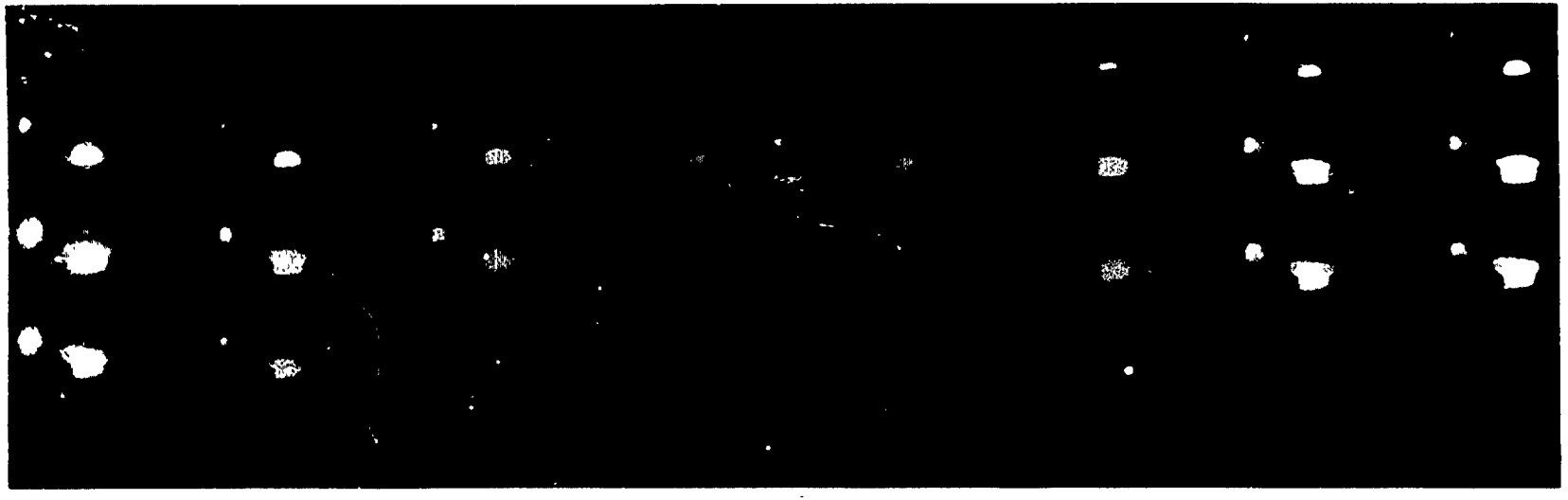

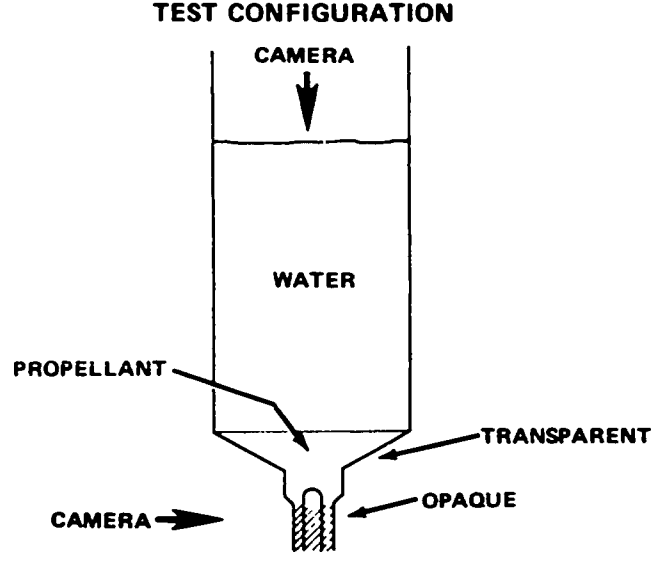

Figure 32 HIGH SPEED PHOTOGRAPHS OF IGNITION PHENOMENA IN A WIDE-ANGLE CONE TRANSPARENT PRECOMBUSTION CHAMBER

strong contrast of surface that is suggestive of opaque gases. All the water was expelled during the test, but some very dirty appearing liquid remained in the precombustion chamber.

Test number 8 produced effects similar to test 2. The formative phase energy was low and about the same as for test 2 and the appearance of the film images was similar, showing very limited evidence of opaque gases. Again, all the water was expelled except for some dirty liquid in the precombustor.

The apparatus was blown apart by test #9 and the recovered polycarbonate tube was extremely bulged at its lower end. The noise it made was much louder than usual, indicating that ignition was more nearly complete than for any other tests. These effects were consistent with both the total energy and the duration of the formative phase, which were 24 joules and 37 μsecs, respectively. The inner diameter of the precombustion chamber was opened from 0.21 to 0.25 inch for the test, resulting in the long formative phase. No pictures were obtained for this test due to camera failure.

The sequence of pictures shown in Figure 32 are of special significance. The configuration shown here is a 45 degree half-angle cone preceded by a two-step precombustor as indicated on the figure. The white medium flowing from the inner sections of the precombustion chamber into the conical segment negotiates the large angle change with no noticeable separation. The mixing vortex at the area change, as postulated in Reference 15, does not appear to be present here as the cool liquid propellant was pushed far into the conical section. The appearance of the interface is somewhat billowy which indicates that most mixing and energy interchange occurs along this surface. The shape of this interface is slightly spherical and is consistent during its travel. This apparent consistency is contrasted with the somewhat random nature of the white cloud expansion as shown in Figures 23, 24, and 26. If mixing is related to surface area of the cloud, then the randomness shown in these figures might be expected to contribute to the observed performance differences.

A second item of significance is the lack of an opaque layer at the white medium-propellant interface of the wide-angle cone test (Figure 32) while a typical 3-step precombustor test (Figure 31) exhibited the dark layer. This observation is not completely understood. It may be postulated that the dark layer consists of products of propellant decomposition, namely NO_2. The lack of the dark layer with the conical configuration probably indicates that the concentration of this constituent is low. This could be due to the large surface area change resulting from expansion into the wide angle cone which could reduce the concentration by purely geometrical means, or rapid pressure decay resulting from the sudden expansion so soon after the arc. Medium temperature reduction due to expansion would slow the rate of decomposition leading to the reduced concentration.

If NO_2 is a necessary constituent in the reaction process, then a low concentration of this ingredient could indicate poor ignition. In this regard, some correlation has been drawn between the geometrical expansion rate of the precombustion chamber and the presence of the opaque layer of NO_2. The correlation seems to indicate that large rates of expansion decrease the concentration of NO_2 leading to poor ignition. Qualitative evidence exists to support this hypothesis. The NWC 2-step precombustor, described in Ref. 3, was a configuration promoting even more rapid expansion than the wide angle cone of these tests in contrast to the rate of expansion of the 3-step precombustor. Ignition with the NWC precombustion chamber was either characterized by low pressure or a high pressure combustion after a delay period in spite of the high electrical discharge energy levels used with that configuration. The 3-step precombustor configuration was able to achieve immediate high pressure combustion with less energy. While pictures were lost during the narrow angle precombustor test of Run 9 due to camera failure, the resounding report from that run was indicative of a much stronger ignition that that of wide angle precombustor. This suggests that a relatively slow rate of expansion of the white medium may be desirable for good ignition.

3.3.4 Intermediate Combustion Chamber

For tests characterized by high pressure combustion, pressures well in excess of 100,000 psi were experienced during most Calspan tests with the PSI-type 3-step precombustion chamber. This result was not altered substantially by modest changes in precombustor/electrode geometry, power settings, ullage, and projectile shot start. It seems reasonable to expect that the initial pressure peak might be reduced by limiting the rate of combustion. If ignition occurs within the precombustion chamber, a geometric flame front constraint would reduce the combustion rate and, therefore, the initial pressure spike.

For those cases where high pressure is reached after a delay, a method for limiting the amount of cool propellant allowed to mix with the medium expelled from the precombustor appears to have merit. The medium probably does not mix completely with the liquid since times are of the order of one millisecond and velocities are quite low, of the order of 100 feet per second. Therefore, mixing must be somewhat dependent on the area of the interface and the size and shape of the cavity into which the medium flows. If this area can be reduced in a controlled manner, the amount of liquid propellant mixed with the medium will be reduced, potentially leading to a smaller quantity burned initially and a lower peak pressure.

Tests using a chamber breech seal, were conducted at BRL (Ref. 18) and the initial pressure peak was diminished substantially for a gun initiated by a pyrotechnic primer. A series of 20mm firing tests were conducted at PSI (Ref. 1) and it was observed that very few tests experienced excessive pressures in comparison to the 30mm program described in the same report. In both cases, the combustion rate was apparently reduced by geometrical means.

The results of the transparent chamber tests, described in the previous section, indicate that the expanding medium will follow the precombustor geometry quite well for relatively large expansion angles. Therefore, it was decided to conduct a series of tests with what will be called an intermediate combustion chamber. The first configuration to be tested was simply a

fourth-stepped segment separating the three-step precombustion chamber and the main gun chamber. The ramp angle connecting this intermediate chamber with the precombustor was the same as that of the wide angle transparent chamber test. The size of this intermediate chamber was made large enough to contain the entire white medium such as that shown in Figure 24. In addition, a rim of rigid urethane foam was added in order to provide a crushable cushion, a kind of shock absorber.

Two tests were conducted with this configuration. The average propellant and projectile weights for these tests were 257 gm. and 157 gm., respectively. The breech pressure generated during one test and the intermediate chamber configuration with dimensions are shown in Figure 33. This particular test experienced no delay and the measured pressure rose to less than 85,000 psi at the first peak. While the second peak is slightly over 100,000 psi, this test demonstrated that the initial pressure could be reduced substantially by geometric means in an electrically ignited LP gun.

A second test was conducted with the identical configuration. This test experienced a delay of 1.6 msec. The initial rise to about 50,000 psi at 1.6 msec was more rapid than that shown in Figure 33 but the entire pressure curve following that point, including both peaks, was nearly identical in every respect. Thus, it was demonstrated that the ignition delay can be accommodated and made to yield satisfactory results with this configuration.

A second intermediate combustion chamber configuration was tested during Run 62. This configuration was a narrow angle cone that provided a smooth transition from a two-step precombustion chamber to the full chamber diameter. In addition, the projectile afterbody consisted of a one-inch long, 1/2 inch diameter aluminum rod covered with one-inch diameter urethane foam. The respective propellant and projectile weights were 258 gm. and 135 gm. The intermediate combustion chamber configuration and the measured breech pressure are shown in Figure 34. Again the first pressure peak was about 85,000 psi and the second peak was slightly over 100,000 psi.

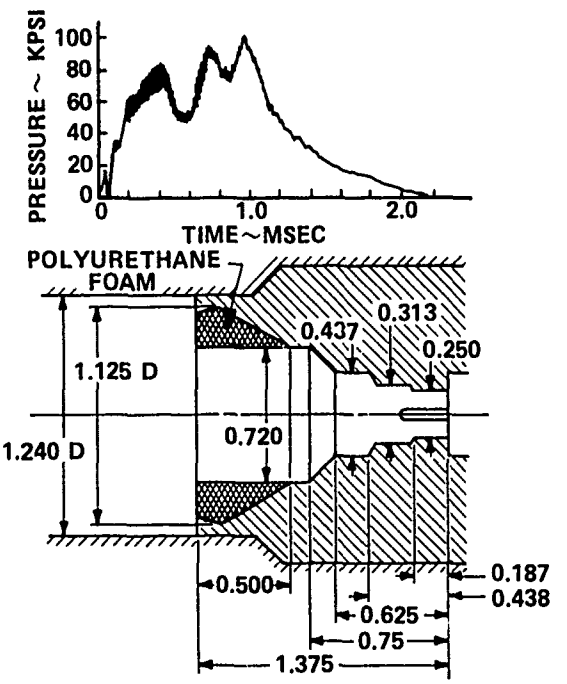

Figure 33 GUN PERFORMANCE WITH 3-STAGE STEPPED PRECOMBUSTION CHAMBER AND AN INTERMEDIATE COMBUSTION CHAMBER INCORPORATING FOAM ULLAGE

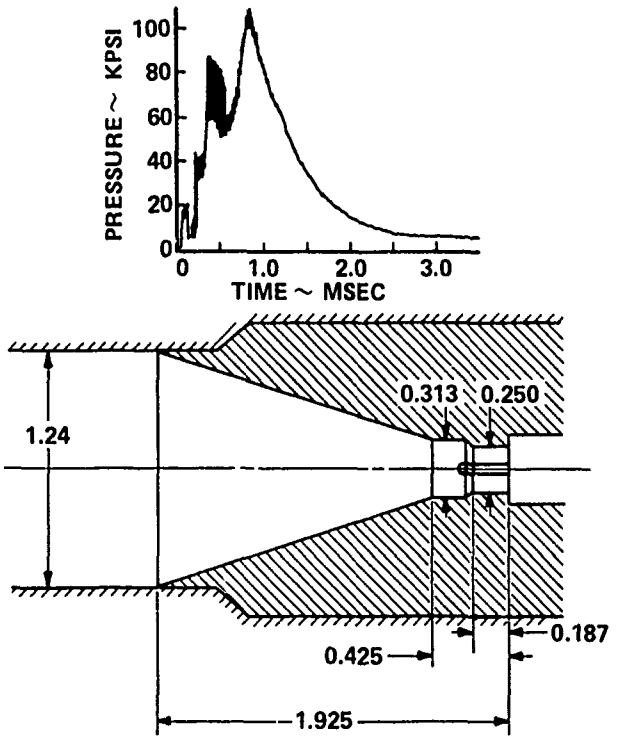

Figure 34 GUN PERFORMANCE WITH A 2-STAGE STEPPED PRECOMBUSTION CHAMBER WITH CONICAL INTERMEDIATE COMBUSTION CHAMBER

The only difference in pressure between the two intermediate chamber configurations is that the second maximum pressure in the stepped configuration contains a double peak while the conical configuration generated a single peak. This similarity in pressure histories despite the large differences in configuration is attributed to similar expansion of the white medium in both cases and reduction of the mixing area, both a result of the geometrical constraints provided by the intermediate combustion chambers.

3.3.5 Spectral and Radiation Measurements

Attempts were made to obtain spectral and radiation measurements during the latter portion of the program. Chamber windows provide an excellent opportunity for obtaining this kind of information in addition to high-speed motion pictures. The equipment used to make these measurements is described in Section 2. It is noted that a small portion of the overall effort was devoted to obtaining these measurements and the data presented here represent the first attempt.

Radiation data were obtained during Run 57. This run was a high pressure test with no combustion delay. Pictures taken during this run at 55 μsec intervals show in sequence the first light in the first picture, brilliant white media in an overexposed second picture and the mottled orange combustion characteristic in the third, fourth, and fifth pictures. The photodiode, and photomultiplier both observed this photographically recorded event. The photodiode with a wavelength response of 3500 A to 1.1 micron was used to view a spot in the center of the window. The photomultiplier with an S-11 response (3000A to 5500A) was used to view essentially the entire window area. The output from this instrumentation along with the current curve are shown in Figure 35. The photomultiplier responded sooner than the photodiode but both instruments indicated the same signal after the time of peak radiation. Part of this initial difference could be due to the different wavelength range of the two instruments but it is more likely that the photomultiplier, looking at the entire window instead of a spot at the center, responded as the medium entered the chamber while the photodiode responded when the front

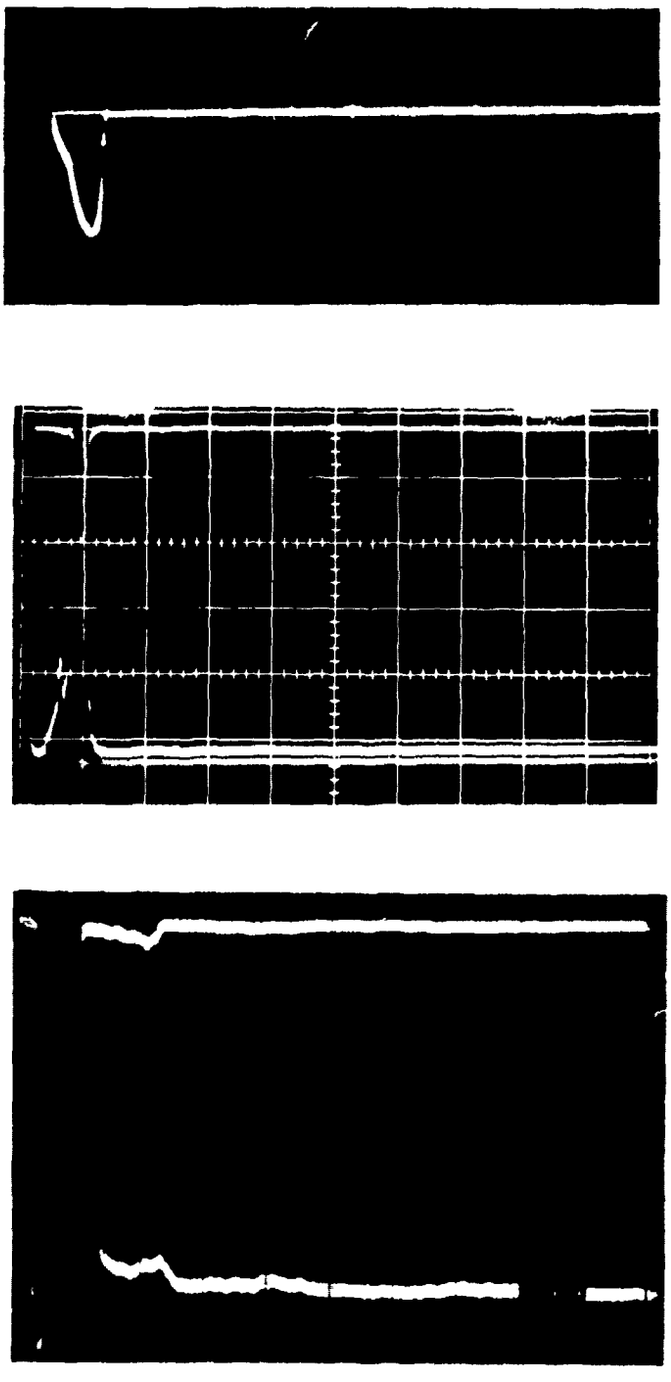

Figure 35 CORRELATION OF RADIATION DATA WITH CURRENT FOR RUN 57

reached the center of the window. It is shown that the duration of the brilliant flash is essentially equivalent to the duration of the arc, or roughly 100 μsec. Therefore, a single picture (18,000 pictures/sec) was taken after the light scattering medium had emerged from the chamber and prior to termination of the arc. The radiation sensors also measured low level radiation after the arc. Thus the radiation sensors were able to provide a continuous history of radiation to fill in the voids between pictures of this run.

Attempts at making radiation measurements were hampered severely by the presence of the opaque layer between the combusted gas and the unburned propellant. Those tests involving the intermediate combustion chamber generated virtually no radiating observables. The white cloud or the orange region of combustion were not observed at any of the window positions during those tests. Therefore, this diagnostic data may be of limited value as an indicator of flame spread or combustion in liquid propellant guns, at least those using NOS365 propellant.

A brief series of tests involving time integrated spectroscopy was conducted during this period. Spectra were measured during open cup tests with propellant and a 20% nitric acid 80% water mixture, and during a gun test with the nitric acid mixture. An attempt to complete the series with a gun test using NOS365 was unsuccessful when the photo plate fractured as a result of the overpressure experienced during the test. The spectra are presented in Figures 36, 37, and 38. The abscissa of these figures is a linear scale of wavelength, while the ordinate is a log scale of light intensity. The three spectra show basically a continuum with a few specific peaks. In particular, the three show strong absorption by the sodium doublet. Another interesting feature is an apparent pressure broadening effect in the wavelength region of 6560A. The open cup test with nitric acid, representing an unconfined configuration with little or no chemical energy addition is the case with the least pressure in the region observed. The spectrum curve reaches peak intensity in the 6560A location. The confined nitric acid and unconfined propellant with considerable chemical energy addition both represent a higher pressure process and both spectra exhibit a broadening characteristic in the region.

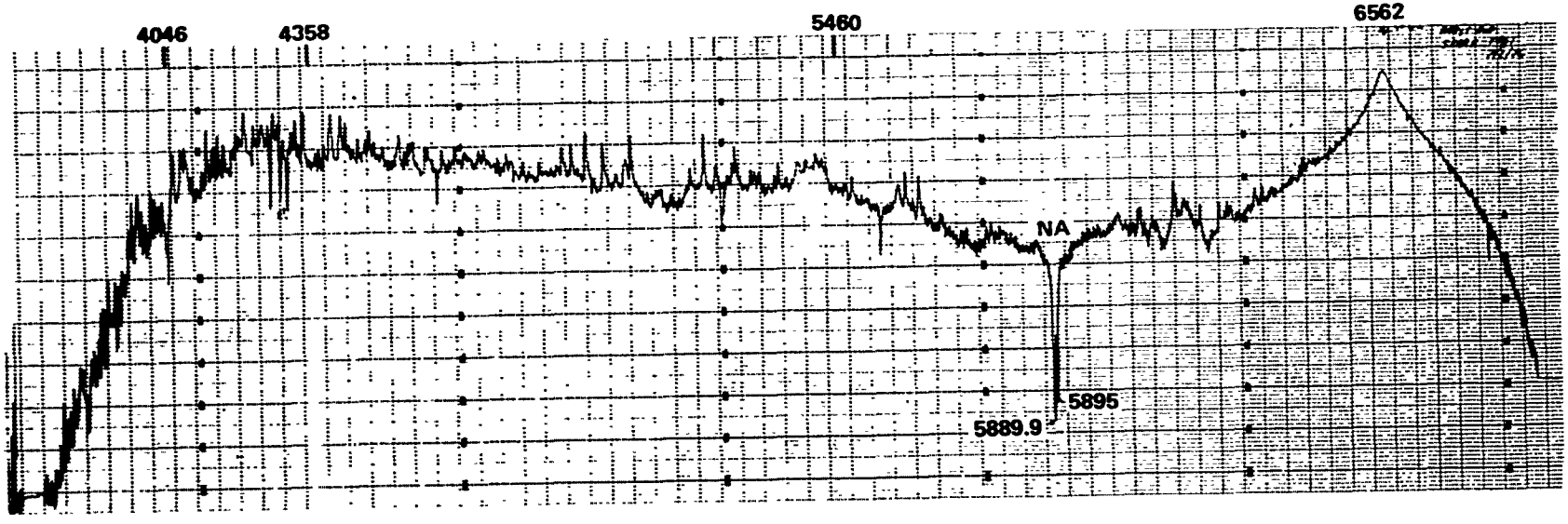

Figure 36 VISIBLE ELECTROMAGNETIC SPECTRUM TAKEN DURING AN OPEN CUP TEST WITH DILUTE NITRIC ACID

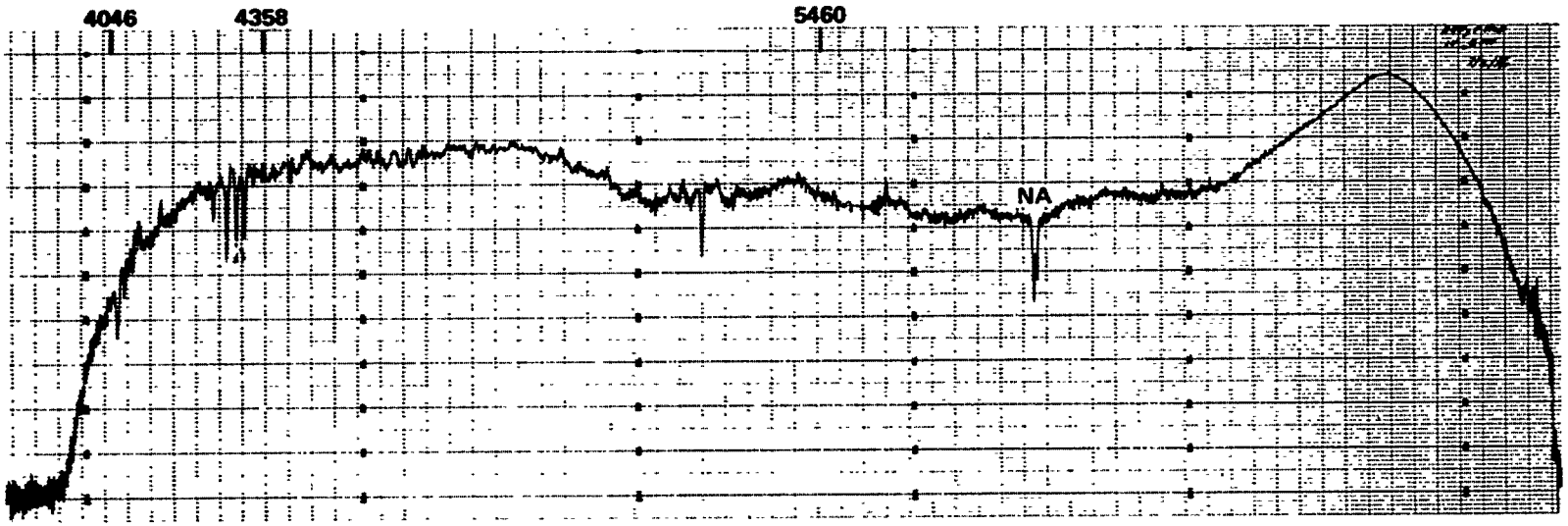

Figure 37 VISIBLE ELECTROMAGNETIC SPECTRUM TAKEN DURING A GUN TEST WITH DILUTE NITRIC ACID

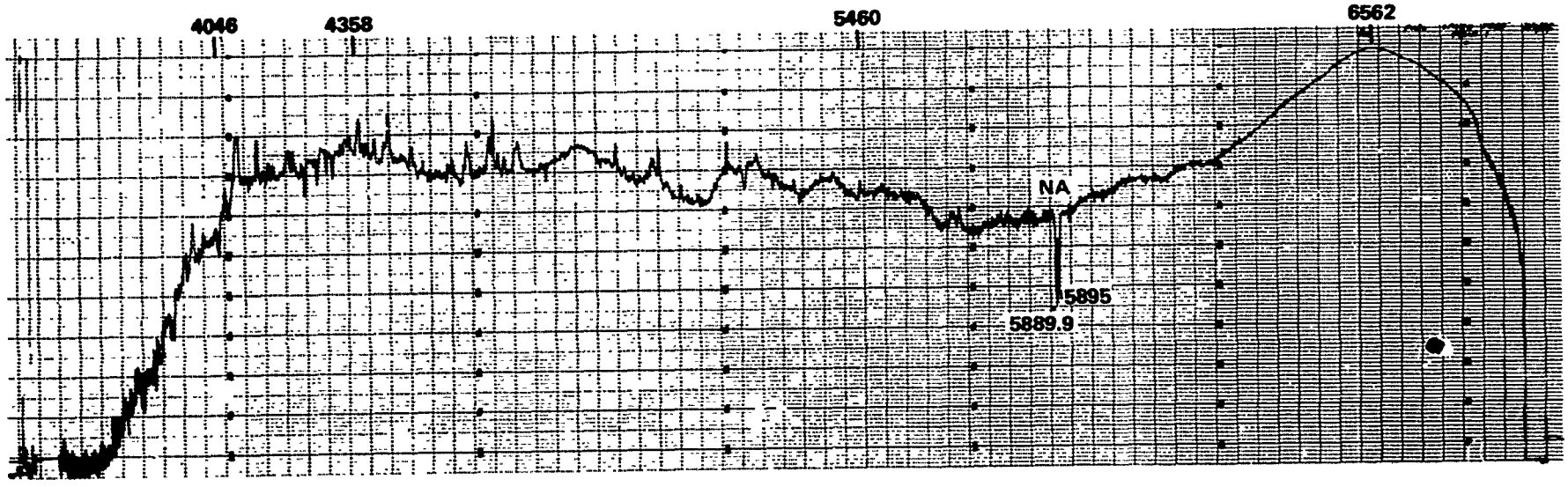

Figure 38 VISIBLE ELECTROMAGNETIC SPECTRUM TAKEN DURING AN OPEN CUP TEST WITH NOS365

This phenomenon might be calibrated as a function of ignition energy. The wide expanse of continuum radiation might be exploited beneficially to obtain temperature.

The usefulness of the spectrograph is also diminished by the presence of the opaque, non-radiating sheath at the gas-liquid interface as was the case for the radiometers. However, some test conditions do create radiating observables and for those tests the spectrograph may prove useful. The effort expended at Calspan along these lines was minimal and has primary value in laying groundwork for future experimentation.

3.4 TOTAL COMBUSTION CYCLE

3.4.1 Simultaneous Heat Transfer, Pressure, and Visual Data

3.4.1.1 Data Description

Run 62 was the most complete test of this research program in that pressures, heat flux, and motion pictures were obtained simultaneously at three locations in the chamber. The chamber used during this test is shown in Figure 3. The elements of primary significance are the large cone-shaped intermediate combustion chamber and the urethane foam-based projectile, as noted previously. The window port diameter for this test was 0.6 inch. The propellant and projectile weights for this test were 258 gm and 135 gm, respectively.

Pressures and the temperature traces generated by the heat sensors are presented in Figure 39. The locations of the pieces of instrumentation are shown with the data on the figure. The sensor locations will be referred to as breech, center and origin, the last location meaning the position nearest the barrel origin which also coincides with the initial position of the projectile base. The pressures were measured with piezoelectric transducers that have a frequency response of 500 kh and the data presented here were not filtered. This means that the presence of high frequency waves and rapid pressure rise rates are represented reasonably accurately. Heat sensors can show a temperature response to a heat input in times of the order of

50 μsec. The heat data in Figure 39 are interpreted by the slope of the curve being roughly proportional to the heating rate. Thus, a zero slope indicates zero heating and the absence of flame while a positive slope indicates the presence of convective heating which is further taken to represent a dry wall. It should be noted that the fore and aft heat sensors were not located in the same locations as the pressure transducers as shown in Figure 39. However, they will be referred to in the text as breech and projectile base sensors. The projectile exit time indicated on this figure was obtained with a muzzle breakwire.

The motion pictures taken during this test are also presented in Figure 39. The initial picture on this figure was taken 0.028 msec after discharge initiation. All pictures prior to this one were identical and showed no event. These pictures were taken at a rate of 35,600 pps as indicated by timing marks on an edge of the film. The optical setup for this test is shown in Figure 14. All three windows were provided with a backlight. The projectile base is in view at the origin window. Time correlation between the measured data and motion pictures was provided by the timing light which produced a 1 kh pulse on both the film and a pressure record. The correlation is believed to be within one picture of 28 μsec.

The breech pressure record begins with a sharp pressure spike of about 20,000 psi at time $t \approx 50\,\mu$sec. The spike is of extremely short duration and drops to an oscillatory level with an amplitude range of 5 to 10,000 psi until time $t \approx 180\,\mu$sec. Motion pictures show the emergence of what appears to be a thin opaque front during the spike that remains quite stationary during the relatively low pressure oscillatory period. The pressure spike is observed to propagate the length of the chamber at about 5000 ft/sec, the approximate acoustic velocity of the liquid. The appearance of a slit of light at the projectile base window at time $t = 112\,\mu$sec signifies the structural failure of the foam afterbody. The 0.5 inch diameter aluminum center rod is the remaining visible element of the afterbody. The projectile was observed to begin motion during this period, the motion picture at time $t = 168\,\mu$sec indicating a slight translation as shown in Figure 40.

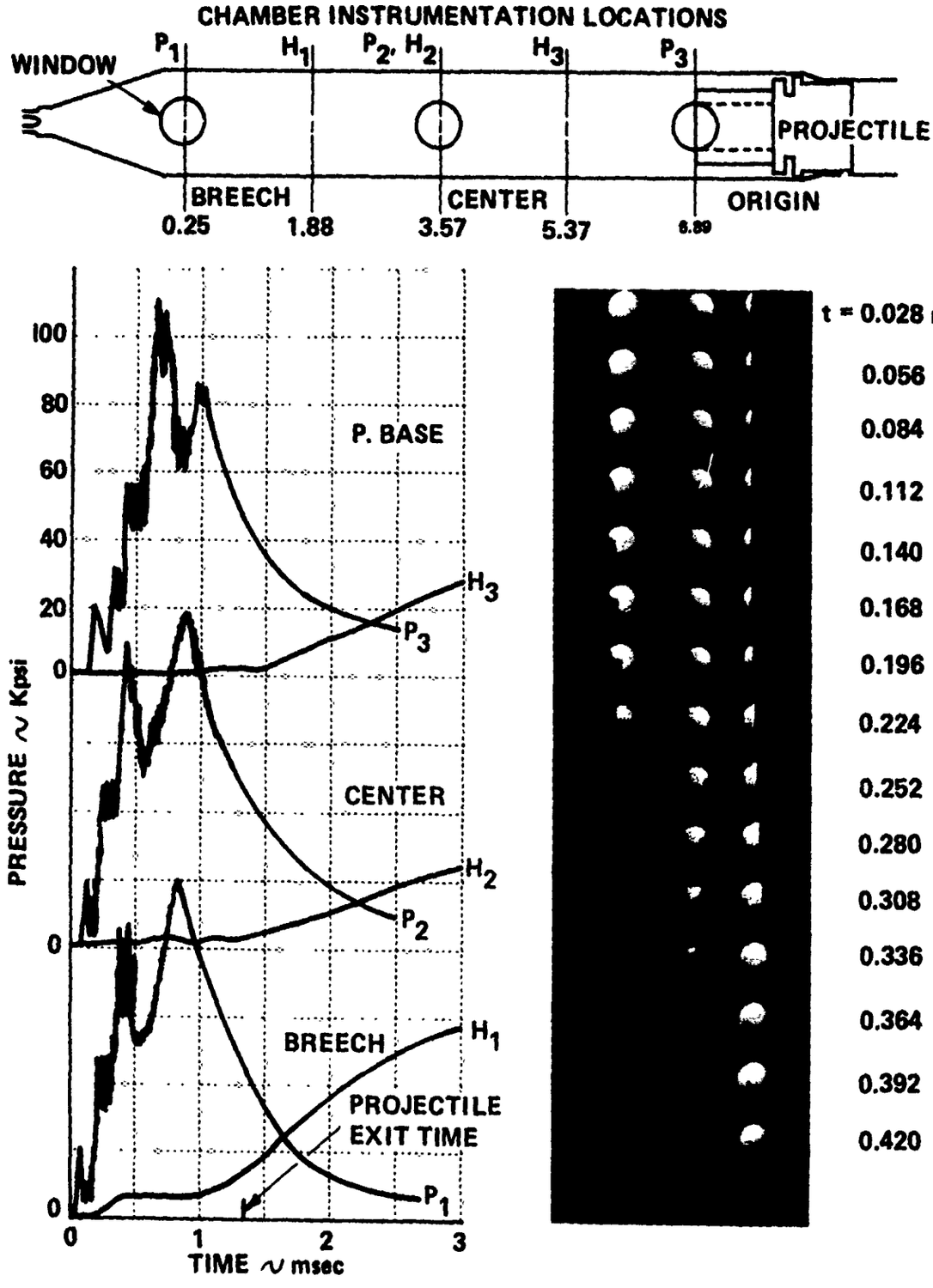

Figure 39 DIAGNOSTIC DATA FROM RUN 62

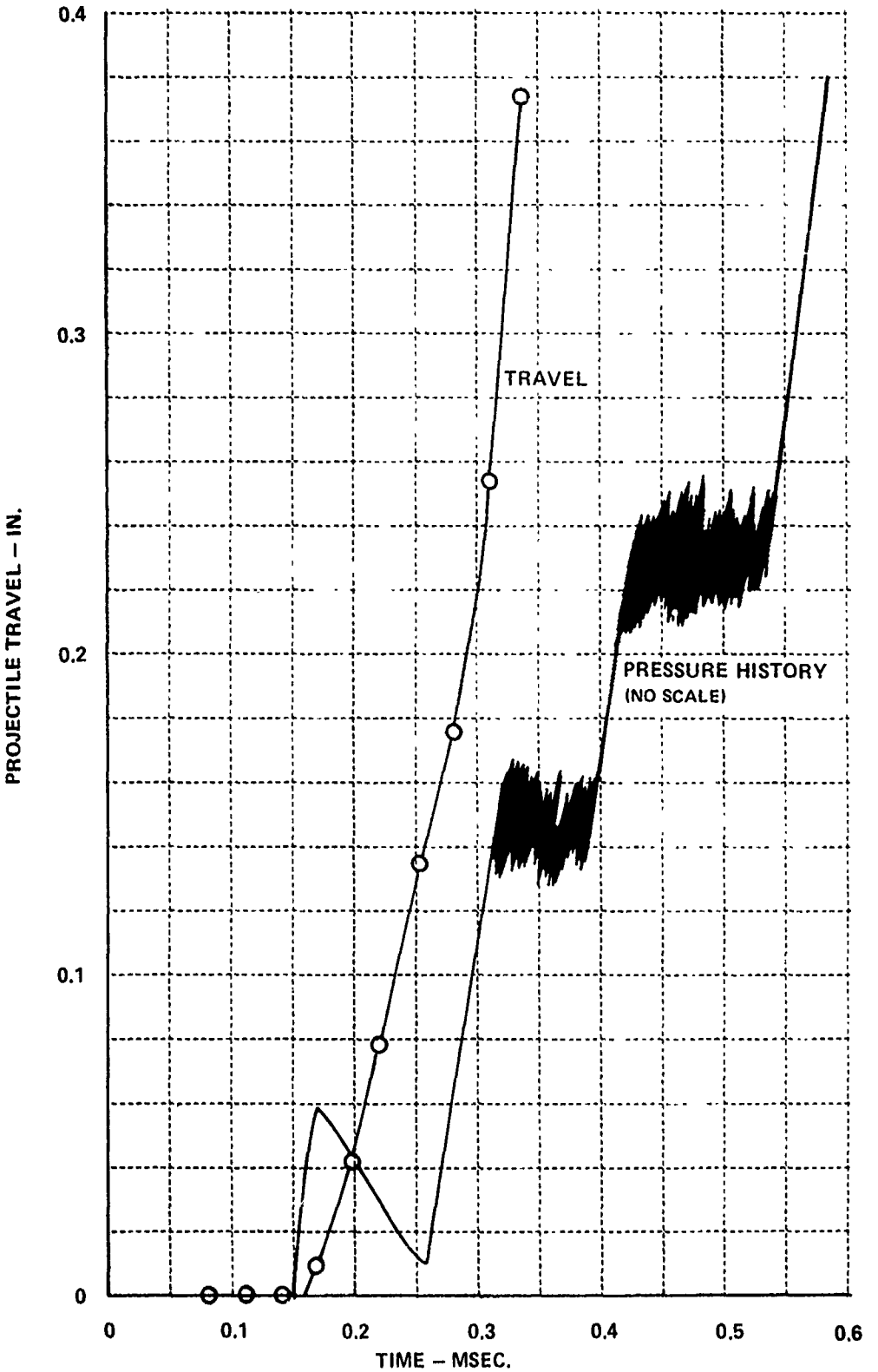

Figure 40 INITIAL PROJECTILE TRAVEL HISTORY FROM RUN 62 AS DETERMINED FROM MOTION PICTURES

A sequence characterized by abrupt pressure rise to about 50,000 psi followed by an expansion was initiated at t = 180μsec at the breech and lasted until t = 320μsec. The breech heat meter generated a sizeable signal during this period. In addition, the sequence of pictures taken through the breech window shows the emergence of a strong opaque medium from the intermediate combustion chamber. After t = 250μsec, virtually all events at the breech windows are obscured. During this period, dark opaque and rather symmetrical patterns are observed to grow at the fore and aft edges of the center window. The projectile, still under the influence of the initial pressure spike during most of this period, undergoes rather large acceleration and finally passes from view slightly after t = 336μsec (Figure 40), slightly after the pressure wave generated at the breech reached the projectile.

The breech and center pressures rose abruptly to the first peak of 85,000 psi at t = 350μsec. The projectile base pressure rose to the peak of 110,000 psi in two steps. The time at which the peak occurred was at t = 600μsec, somewhat later than that of the center and breech stations. The projectile base window looks as if it failed at about 400μsec. The breech window probably failed during the rise to the first pressure peak. No pictures of any consequence were obtained after this time. The breech heat sensor, which experienced heating during the previous breech pressure rise to 50,000 psi, continued to sense heat until the first pressure peak was reached. At the approximate time of the peak, the slope of the sensor signal suddenly became zero, indicating the removal of the heat source.

After the first pressure peak, the breech and center pressures fell to a valley of about 55000 psi and then rose to a second peak of nearly 100,000 psi. The time of occurrence of the second peak is sequentially displaced in time from the breech to projectile base locations and is followed by a monotonically decreasing curve. All heat sensors indicate sequential onset of heating, beginning with the breech, after the second pressure spike. The projectile passed from the barrel at time t $\approx$ 1.3 msec, the approximate time heating was observed from the center heat meter. The muzzle velocity from

this test was 5650 ft/sec. A breech window eventually blew out during this test. Evidence from pressure and heat sensor data indicates this occurred about the time of projectile exit.

3.4.1.2 Discussion of Combustion Data

The results of this test, Run 62, provide a wealth of information never before available. Interpretation of this data is not a straightforward task and is likely dependent to some extent on the background of the interpreter. The following discussion represents an attempt to describe LPG combustion phenomena through interpretation of data from this test.

The pressure curves from Run 62 suggest the presence of a strongly interactive hydrodynamic/comoustion process. Measured pressure data indicate that this process begins with an initial pressure wave generated in the precombustion chamber at the time of the arc. This wave is in the form of a short duration spike and is followed by a period of pressure oscillation at a much lower mean pressure than the spike. According to Reference 19, blast wave velocity decays rapidly to the acoustic velocity of the medium with increasing distance from its source. If the assumption of acoustic velocity, about 5500 ft/sec, is made for all wave travel, the time to traverse the distance between breech and projectile base transducers is about 100μsec. This elapsed time for an event to traverse the distance between pressure ports appears to correlate rather well with the arrival of this initial pressure spike at the projectile base. The propagation of this initial spike is shown in the x-t diagram of Figure 41.

It was observed that the rigid urethane foam was crushed upon arrival of this wave and that projectile motion was also initiated during this period. Both events create ullage by providing additional space inside the chamber for liquid to occupy. Early projectile motion occurs during a period where pressures are not much higher than the shot start pressure and is probably not consistent from run to run. This inconsistency is due to small differences in shot start pressure among projectiles and electrical discharge-related

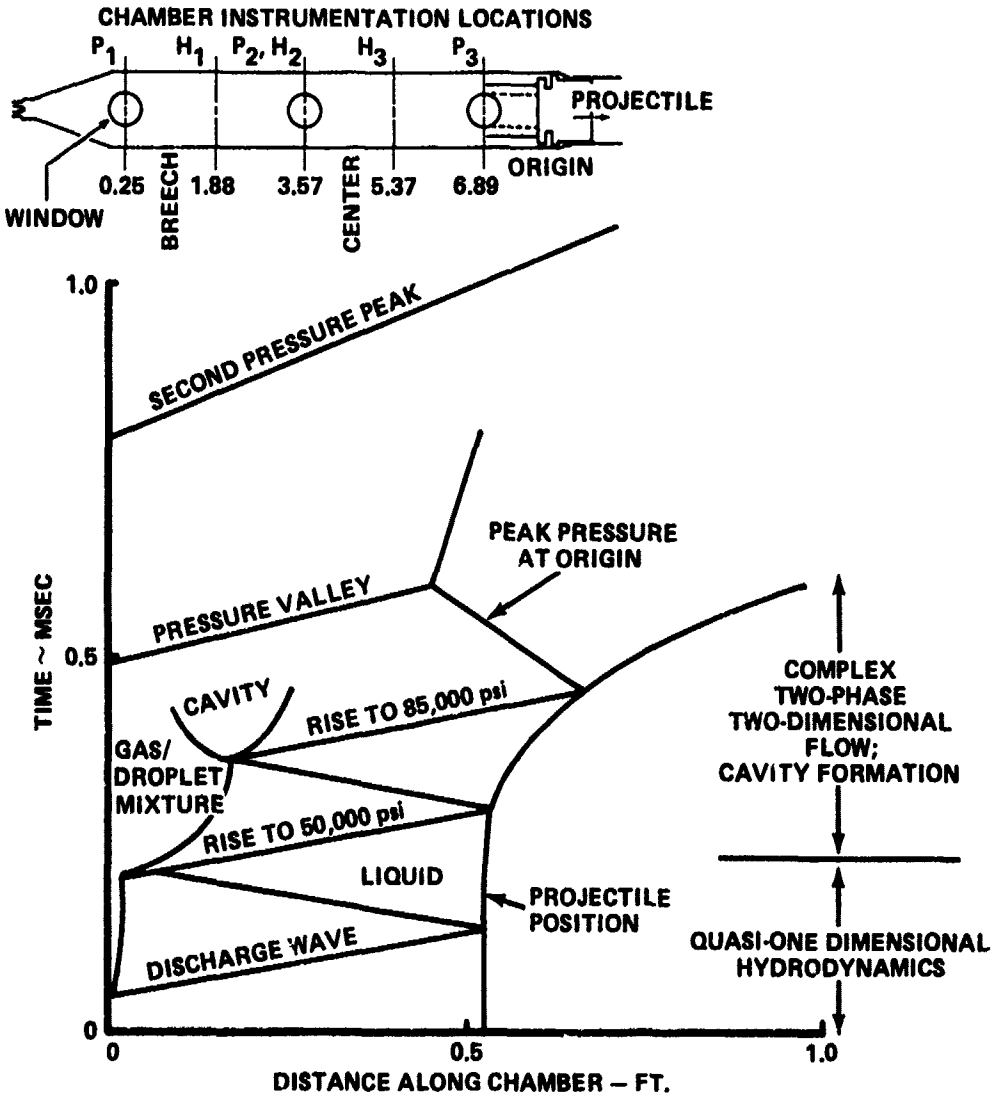

Figure 41 WAVE STRUCTURE DURING RUN 62

differences in generated pressure, and is especially prominent during tests experiencing high pressure combustion delay where travel can become significant. This signifies the need to avoid delay in high pressure combustion in order to reduce performance variability and overpressures presumed to be related to ullage.

The oscillatory low pressure period following the spike appears to be a period of incubation or mixing, similar in nature to that observed in breech motion pictures described in Section 3.3.2. The oscillations are probably due to emissions and local reflections of pressure waves resulting in part from the transition of the primary wave into a planar front from the conically expanding front in the intermediate combustion chamber. It should be noted at this point that the step change in area at the plane separating the gun chamber from the precombustion chamber during the tests discussed in Section 3.3.2 was not present here. Therefore, the vortex generated at the discontinuity, as postulated in Reference 15, is either greatly modified or nonexistent.

As shown by the diagram in Figure 41, the reflection of this primary wave, called the discharge wave, at the projectile base creates a compressive wave propagating toward the breech. The arrival time of this reflected wave at the breech nearly corresponds with the abrupt increase of breech pressure to 50,000 psi. If the average velocity of the primary and reflected waves was about 7000 ft/sec, the correlation would be exact. This correlation may be simply fortuitous, but it may also be argued that the arrival of the compressive wave may have provided the required stimulus to either initiate high pressure combustion, or to introduce mechanisms that would greatly accelerate the rate of combustion. One such mechanism that comes to mind is spallation as a compressive wave reflects from a free surface. The spalled interface would consist of droplets of partially decomposed propellant that could combust exceedingly rapidly. Such rapid combustion would be followed by a lull, as observed, as the flame front returned to its state prior to the perturbation.

The motion pictures give little indication of the existence of a Taylor cavity during this rapid rise to 50,000 psi. In fact, the transparent chamber tests (Section 3.3.3) indicate that the combustion front may be nearly planar or slightly spherical inside the cone. The heating sensed by the breech heat sensor (1.88 inches from the cone exit) indicates that the front of the interface separating gas and liquid, moved past the sensor during this period. Ullage created by the crushed projectile foam afterbody (7%) and projectile motion (1%) together with propellant compressibility at pressures of 40-50,000 psi (about 10%), the propellant burned by this time (7%) and the initial ullage (0.2%) can nearly account for the appearance of the dry wall so far into the chamber if the front is approximately planar. It is noted in passing that the chamber surface must have remained wet for some period after the luminous front has passed. This surface propellant will be heated and eventually burn, adding to the amount of combusted gas at an undetermined rate. The pressures at the center and breech locations are very similar in their rise times, probably because the combustion zone is about midway between them.

The rise to 50,000 psi at the breech is apparently felt in two stages at the origin, first by a rise to 30,000 psi as the wave travels toward the projectile and then a rise to 55,000 psi by the reflected wave. The reflected wave hits the free surface at the breech at very nearly the time the pressure there undergoes a rapid rise to 85,000 psi. This leads one to suspect a spallation type of phenomena, similar to that noted previously, as contributing to the augmented combustion rate. The wave associated with rapid rise to 85,000 psi serves to maintain the origin pressure at the 55,000 psi level (a possible expansion here before the arrival of the wave is not readily apparent because of large amplitude noise). The high pressure spike ($>$100,000 psi) measured at the origin correlates approximately with the arrival of the wave reflected from the projectile base. It should be noted that the projectile has attained a velocity of the order of 1500 ft/sec (calculated) by the time the base pressure rises to 100,000 psi. It is believed that the Taylor Cavity is formed during this period. At this point, wave analysis becomes extremely complex because of the two dimensional-two phase aspects of the problem.

The breech heat sensor (1.88 inches from the breech) gave indication of zero heat flux at about the same time the breech pressure reached 85,000 psi, which is assumed to indicate that the chamber wall was again wetted with liquid propellant. A sequence of events, illustrated in Figure 42, is proposed to explain this observation. In this figure, the first illustration is given on the basis of motion pictures of a transparent chamber test (Section 3.3.3) and those taken during Run 62. The second illustration, showing a quasi-planar front about 2 inches into the chamber, was created according to arguments put forth earlier in this section. The chamber walls are apparently dry up to the front as indicated by the signal from the heat sensor. The third illustration shows what is postulated to be the origin of the Taylor cavity at the onset of significant projectile movement. Initially, all flow is in the direction of projectile movement as gas expands in relation to travel. As the cavity deepens, gas flow over the surface strips droplets from the surface by the formation of wavelets. In addition, the arrival of the reflected wave at the free surface of the cavity at the beginning of the breech pressure rise to 85,000 psi is presumed to cause spallation at the free surface and appears to coincide with the rise. Whatever the mechanism, combustion is presumed to occur deep in the cavity. About one third of the breech end of the chamber is dry so no gas is generated there. A net outflow from the cavity into the breech region must be established in order to satisfy momentum balance requirements. It is proposed that this outflow and the adverse pressure gradient that causes it, sweep and push the annulus of liquid toward the breech so that the surface again becomes wet as shown in the fourth illustration. The pressure drops rapidly as the rate of expansion behind the projectile exceeds combustion. The readjustment in liquid leads to the fully developed Taylor cavity and velocity-augmented combustion during the period leading to the second pressure peak. The time-propagation of the pressure valley is also shown in Figure 41.

The heat meter nearest the breech begins to receive continuous heating shortly after the second pressure peak. Subsequently, the sensors at the center and near the projectile base experience this onset of heating in proper sequential order. The time of the onset of heating is shown

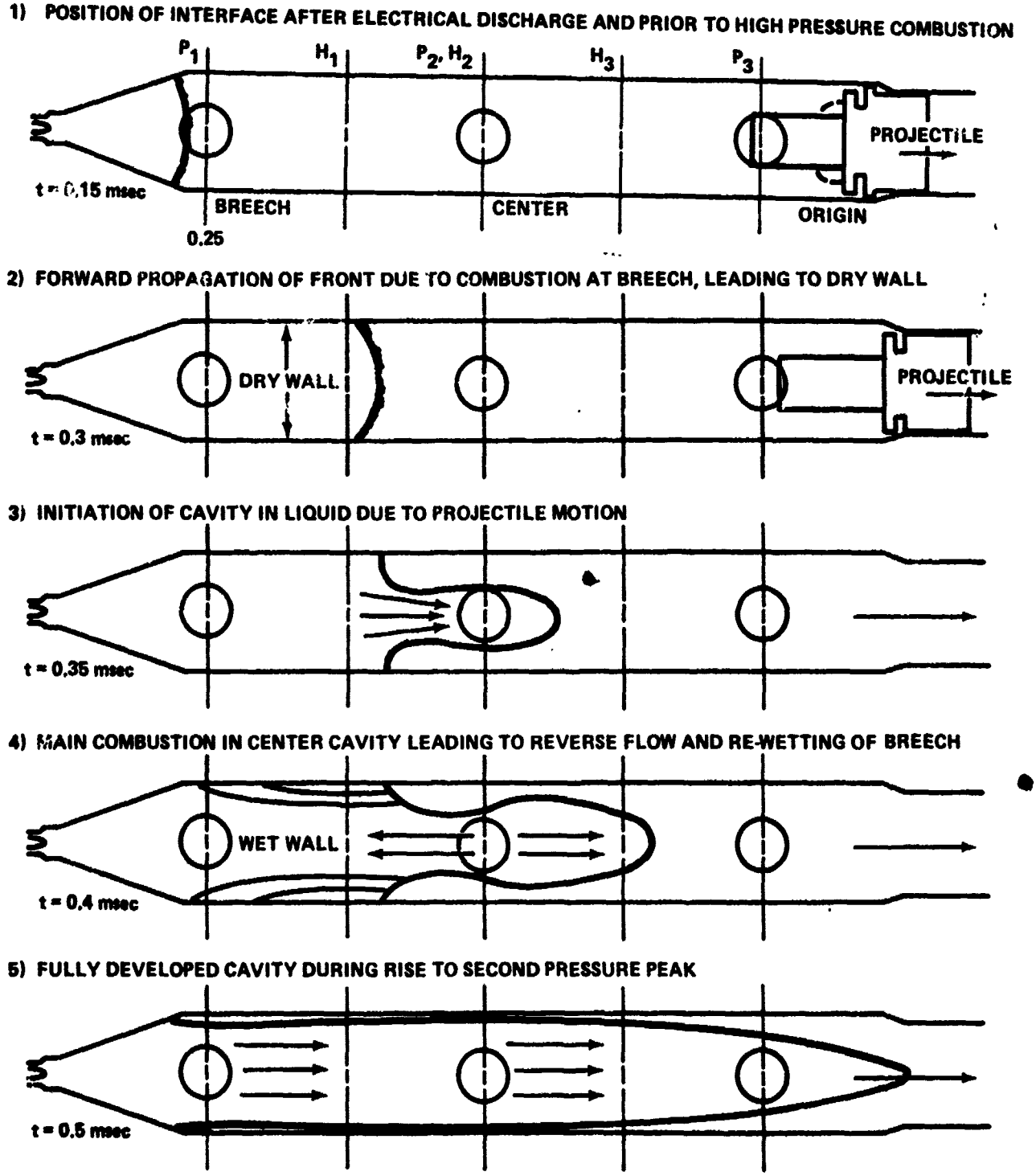

Figure 42 POSTULATED SEQUENCE OF EVENTS IN CHAMBER

plotted versus sensor location in the chamber in Figure 43. The time of the second pressure peak at the breech is also indicated on the figure. This curve indicates that the second pressure peak occurs at the time the wall becomes dry at the breech. The total burning surface area begins to undergo drastic reduction at this time and seems to correlate with the rapid drop in pressure. The sequentially later times of this second peak for the center and projectile base pressures indicate the travel time for the expansion wave originating at the breech and is plotted in Figure 41. The breakwire at the barrel muzzle indicated that the projectile passed from the barrel approximately 0.2 msec prior to apparent burnout at the forward end of the chamber. These results are significant in that they appear to verify the existence of a cavity-shaped flame front that governs the pressure history over most of the interior ballistics cycle.

3.4.1.3 Heat Transfer Results

The temperature traces generated by the heat sensors were reduced to obtain heat flux and total heat input at their respective stations. These data are presented in Table II. The computed heat flux represents the peak rate of heating experienced after the onset of heating following the second pressure peak.

The values of heat input at the center and forward positions appear to be of reasonable level. The average heat input of 23 Btu/ft^2 over the forward end of the chamber compares favorably with the lowest heat inputs measured by Calspan during a 27mm caseless gun heat transfer program, Reference 20. Heat inputs of twice this value were also measured during the same program. It appears that the extended period during which the chamber wall remains wet is a definite asset in reducing the heat transfer problem. The extent of this effect in the barrel due to the traveling charge has yet to be determined. The chamber wall temperature after 500 msec is indicative of the temperature the next charge would experience. The rate of temperature accumulation after several shots remains to be determined.

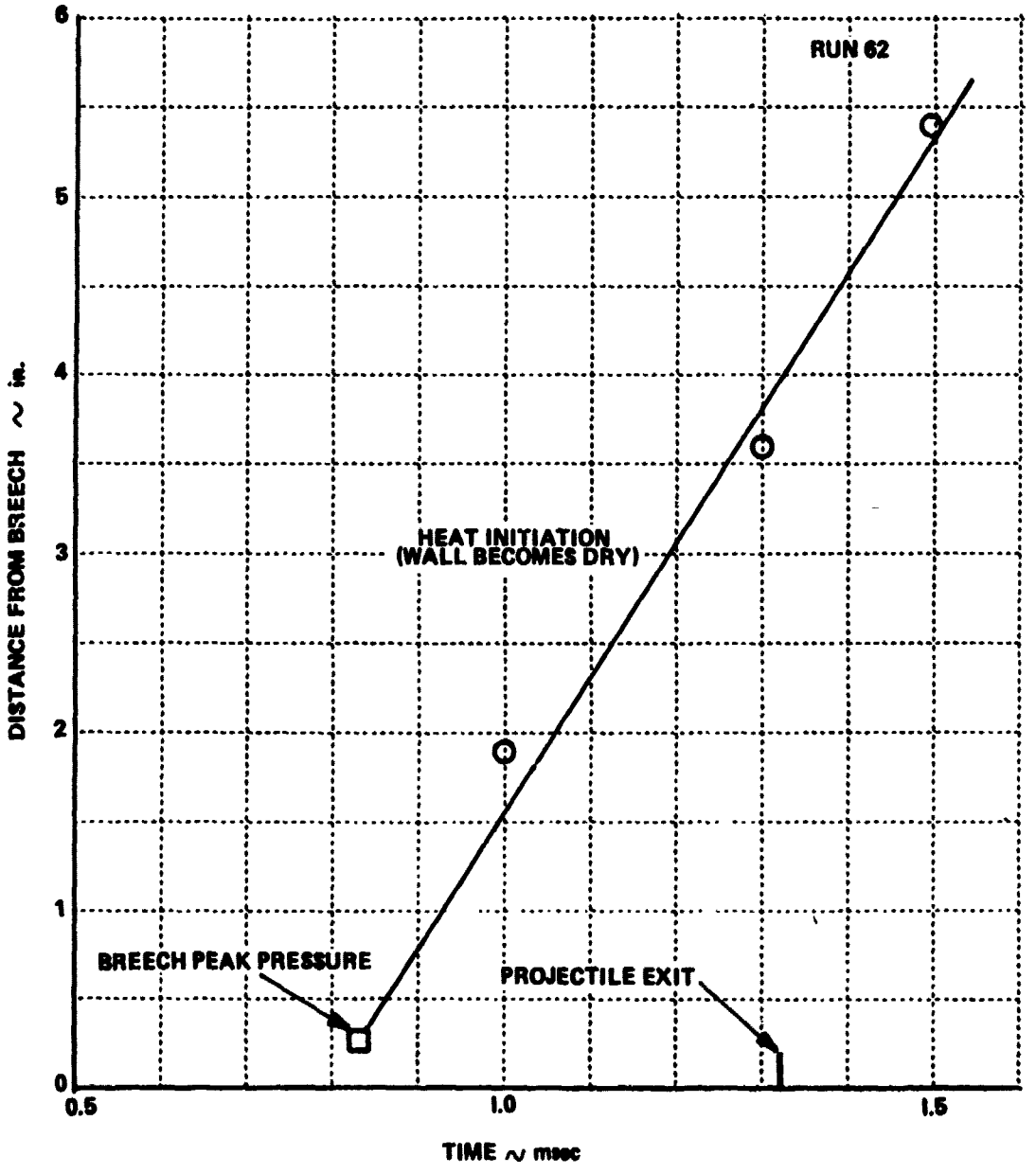

Figure 43 CORRELATION OF THE ONSET OF CHAMBER WALL HEATING WITH BREECH PEAK PRESSURE

The value of heat flux given for the breech in Table II is believed to be higher than that of the other locations because of the higher pressure present at the onset of heating. A sapphire window blew out at the breech which likely caused substantial reverse flow at the location of the breech heat meter at some time during the run. The heat flux increased substantially from the value reported in Table II 0.1 msec after the time of projectile exit and this is believed to be related to the window blowout. The total heat input measured by the sensor and surface temperature calculations were influenced by the window blowout and are not reported in the table.

3.4.2 Short Barrel Results

An interesting phenomenon was observed during tests involving the short (9 inches long) barrel. A muzzle breakwire was used during Run 55 to indicate the exact time the projectile passed from the barrel. The pressure curve from this test and the time of projectile exit are shown in Figure 44. It is interesting and significant that this exit time corresponds with the time of minimum pressure and that a general rise in pressure with several severe spikes occur after this time.

A possible explanation of this observation is that the projectile and presumed traveling charge are accelerated as a unit. When the projectile leaves the barrel, the mass being accelerated is reduced drastically. If the traveling charge actually exists, it, and the gas in the chamber, will be greatly accelerated. If it does not exist and gas blows out the barrel instead of propellant, the gas velocity in the chamber will still be increased. Therefore, the pressure increase is likely caused by augmented combustion as a result of increased velocity. This observation is but another in a series that serve to indicate the complex interactive combustion mechanisms present in liquid propellant guns.

Table II
LPG HEAT TRANSFER CHARACTERISTICS

LOCATION FROM BREECH (in)		1.88	3.57	5.37
PEAK HEAT FLUX (BTU/ft^2-sec)		14400	8600	10600
CHAMBER SURFACE TEMPERATURE RISE (ΔT - F^o)	PEAK:	–	700	860
	AFTER 500 msec:	–	26	32
TOTAL HEAT INPUT (BTU/ft^2)		–	20	25
TOTAL HEAT INPUT FROM 27mm CASELESS AMMUNITION (BTU/ft^2)		18	30	29

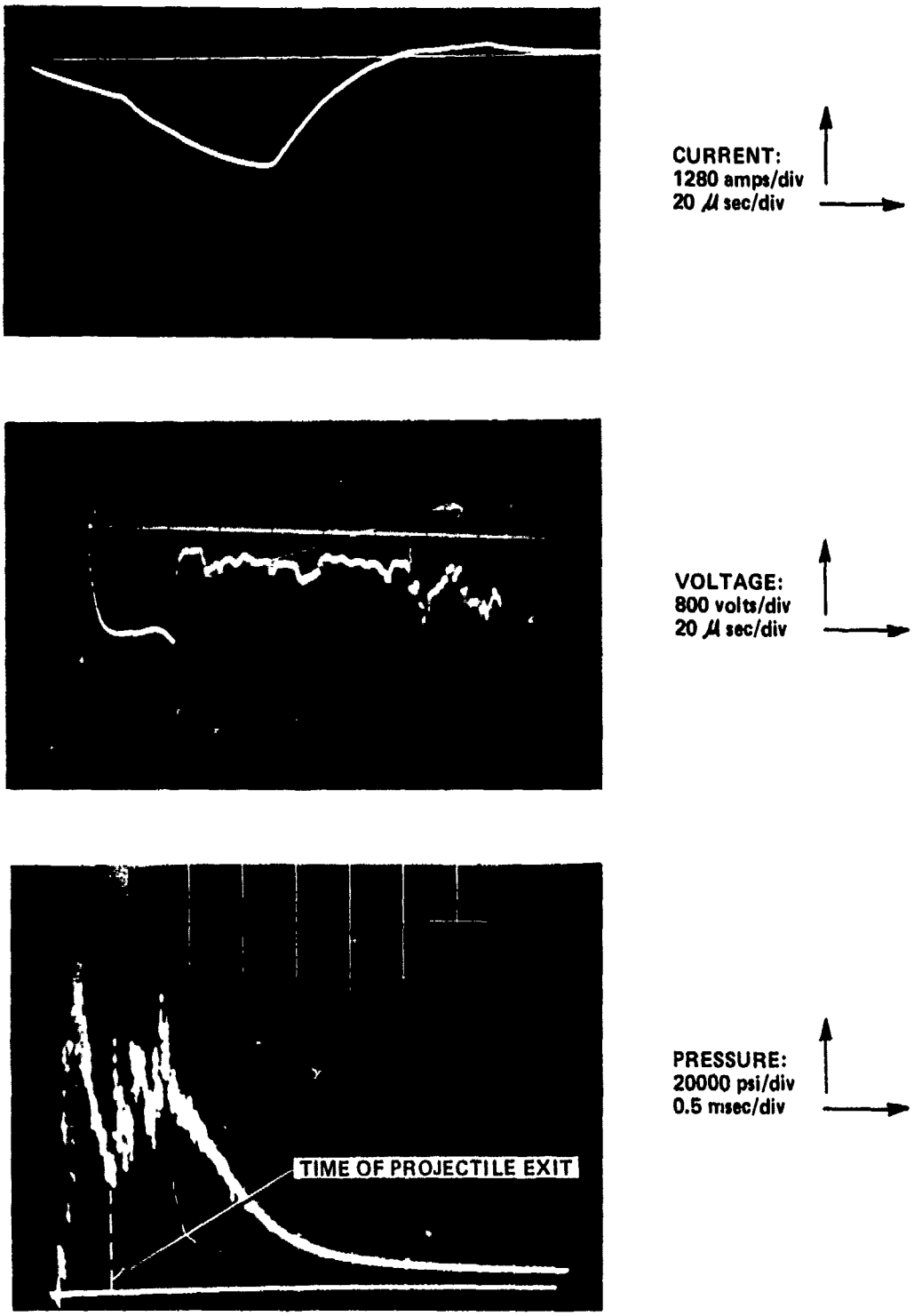

Figure 44 COMPARISON OF PRESSURE HISTORY WITH TIME OF PROJECTILE EXIT FROM 9-INCH BARREL FOR RUN 55

4.0 EPILOGUE

The LPG diagnostic experimentation program conducted at Calspan ended at a time when the rate of information generation was high and increasing. Many interesting and important phenomena have been observed. We have also demonstrated on a limited basis the ability to control ignition and combustion processes. It now remains to expand the lines of research begun during this program in order to develop LPG design criteria that will insure satisfactory gun performance. The encouraging results of the last months of this program make us feel optimistic that the LPG performance problems can be overcome with a reasonable research effort.

5.0 REFERENCES

1. "Final Technical Report for Phase I Effort on a High Performance Medium Caliber Liquid Propellant Anti-Armor Gun System (U)," Pulsepower Systems Inc., Report TR104, Contract No. N00123-73-C-1982, December 1974.

2. "Investigation of Ignition/Combustion Phenomena in a 30mm Liquid Monopropellant Gun," Calspan Corporation, First SemiAnnual Technical Report, Contract No. N00123-75-C-1520, February 1976.

3. "Investigation of Ignition/Combustion Phenomena in a 30mm Liquid Monopropellant Gun," Calspan Corporation, Second SemiAnnual Technical Report, Contract No. N00123-75-C-1520, August 1976.

4. "Investigation of Ignition/Combustion Phenomena in a 30mm Liquid Monopropellant Gun," Calspan Corporation, 14th Monthly Technical Progress Report, Contract No. N00123-75-C-1520, July 1976.

5. "Investigation of Ignition/Combustion Phenomena in a 30mm Liquid Monopropellant Gun," Calspan Corporation, 15th Monthly Technical Progress Report, Contract No. N00123-75-C-1520, August 1976.

6. "Investigation of Ignition/Combustion Phenomena in a 30mm Liquid Monopropellant Gun," Calspan Corporation, 16th Monthly Technical Progress Report, Contract No. N00123-75-C-1520, September 1976.

7. "Investigation of Ignition/Combustion Phenomena in a 30mm Liquid Monopropellant Gun," Calspan Corporation, 17th Monthly Technical Progress Report, Contract No. N00123-75-C-1520, October 1976.

8. Hickling, A., "Electrochemical Processes in Glow-Discharge at the Gas-Solution Interface," Modern Aspects of Electrochemistry, Vol. 6, Ed. by Bochris and Conway, Pub. Plenum Press, N.Y. 1971.

9. Hickling, A., and Ingram, M.D., "Contact Glow-Discharge Electrolysis," Transactions of the Faraday Society, Vol. 60, 1964. pp. 783-793.

10. Personal communication with L. Elmore, PSI, September 1975.

11. Personal communication with L. Liedtke, NWC, July 1976.

12. "Semiannual Technical Report for Phase II Effort on a High Performance Medium Caliber Liquid Propellant Anti-Armor Gun System," Pulsepower Systems Inc., Report TR110, Contract No. N00123-73-C-1982, June 1975.

13. Evans, M.W., Given, F.I., and Doran, D.G., "Ignition and Combustion Properties of Liquid Monopropellant," SRI Project No. GV-1123, Contract No. DA-04-200-ORD-320, Report AD104237, July 1956.

5.0 REFERENCES (CONT'D.)

14. Personal communications with N. Klein, BRL, March 1976.

15. "Liquid Propellant Gun Performance Analysis (U)," TRW Systems Group, Semi-Annual Technical Report, Contract No. N00123-76-C-0220, April 1976. CONFIDENTIAL.

16. Personal communications with A. Charters, NWC, November 1976.

17. Personal communication with E. Fishman, TRW Systems Group, November 1976.

18. "Liquid Monopropellant Gun - Exploratory Development Program (U)," Naval Ordnance Station, Indian Head, MD., Quarterly Report - January - March 1975, 30 May 1975.

19. Personal communications with W. Rae, Calspan Corporation, November 1976.

20. Vassallo, F.A., and Adams, D.E., "Caseless Ammunition Heat Transfer, Volume II," Calspan Report No. GI-2758-Z-1, Contract No. DAAF01-69-C-0420, Rock Island Arsenal, October 1969.